Balance on many scales:
Growth and gene expression in *Bacillus subtilis*

Niclas Nordholt

Members of the Doctoral Examination Committee

prof. dr. Bas Teusink
VU University, Amsterdam

prof. dr. Leendert Hamoen
University of Amsterdam

prof. dr. ir. Sander J. Tans
FOM Institute for Atomic and Molecular Physics, Amsterdam

dr. James Locke
University of Cambridge

dr. Rutger Hermsen
Utrecht University

dr. Frank Schreiber
Federal Institute for Materials Research and Testing, Berlin

The work presented in this thesis has been carried out at the department of Systems Bioinformatics at the VU University in Amsterdam.
I acknowledge funding from the European Union, Marie Curie ITN AMBER, 317338.

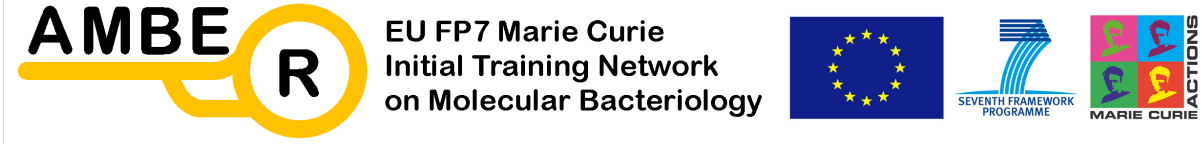

VRIJE UNIVERSITEIT

Balance on many scales: Growth and gene expression in *Bacillus subtilis*

ACADEMISCH PROEFSCHRIFT

ter verkrijging van de graad Doctor aan
de Vrije Universiteit Amsterdam,
op gezag van de rector magnificus
prof.dr. V. Subramaniam,
in het openbaar te verdedigen
ten overstaan van de promotiecommissie
van de Faculteit der Bètawetenschappen
op donderdag 18 januari 2018 om 9.45 uur
in de aula van de universiteit,
De Boelelaan 1105

door

NICLAS NORDHOLT

geboren te Wiesbaden, Duitsland

promotoren: prof.dr. F.J. Bruggeman

prof.dr. R. Kort

copromotor: dr. J.H. van Heerden

“The dream of every cell is to become two cells.”

-François Jacob

Contents

Chapter 1

Introduction

Introduction

Clonal microbial cells that grow under identical conditions show a remarkable inter-cellular variability. Individual cells exhibit differences in cell size, molecular composition and generation times. This phenotypic variability can have important consequences for cellular functioning and the ability of a cell to adapt to the environment. For instance, it can result in the formation of resilient 'persister' cells that are able to survive averse conditions, such as antibiotic treatments[111]. Bacterial persistence can lead to relapse of infectious diseases after seemingly successful therapy and facilitate the development of genetic antibiotic resistance[108]. In a biotechnological setting, the formation of non-producing subpopulations is highly undesirable, as it reduces cost-efficiency.

A complete understanding of the functioning and organisation of microbial growth and gene expression therefore encompasses an understanding of the origins and consequences of non-genetic heterogeneity. This task requires us to study microbial populations on the level of individual cells. Depending on the question that is asked, and the level of cellular organisation this question concerns, different experimental techniques and conceptual frameworks have to be employed.

Figure 1.1 poses as a graphical summary of the phenomena that we address in this thesis, and the concepts and experimental methods that we used to tackle the understanding of these phenomena, by studying individual bacterial cells. In the following sections we will address individual aspects of this figure and their significance in the creation of this work.

Single-cell measurements have revolutionised microbiology

Non-genetic heterogeneity in isogenic microbial populations can range from quantitative differences in e.g. cell size, molecule copy numbers or generation time[146,49,178] to qualitative differences in the phenotype of individual cells[205,190,95]. The discovery and understanding of these phenomena relies on the characterisation of individual cells. Among the most prevalent experimental techniques, which were also used in this work, are flow cytometry and time-lapse microscopy in combination with fluorescent proteins as a reporter for gene expression[49,27].

Flow cytometry can be used for multiparametric characterisation of thousands of individual cells per second. Besides reporting properties that relate to cell size or cytoplasmic granularity, flow cytometers are equipped with multiple lasers and detectors that allow the quantification of fluorescent dyes and reporter proteins (Figure 1.1, top right). These reporters can be utilised for instance to discriminate between viable and dead cells[94], to determine the DNA content and cell cycle stage[70] and to quantify gene expression and promoter strength in live cells[73,222] (Figure 1.1, top right). A drawback of flow cytometry, compared to other single cell methods, is the transient nature of the measurements: they only provide a 'snapshot' of the individuals of a population. While it is possible to sort cells into subpopulations based on certain properties (fluorescence assisted cell sorting, FACS), it is not possible to retrieve an individual cell from a sample and to follow that individual in time. This means that certain single cell properties, such as the age of a cell (the time that has elapsed since its birth) or single cell growth rates, can not be determined directly using flow cytometry.

Automated time-lapse fluorescence microscopy is able to overcome this limitation. Where flow cytometry adds the dimension of individuality to the measurement of bacterial populations, time-lapse microscopy adds an additional layer of depth to each single cell measurement: the dimension of time. With automated time-lapse microscopy it is possible to follow the growth of individual cells in time, from birth to division and over many generations, hundreds of cells at a time (Figure 1.1, top left). This allows us to follow the kinetics of growth and, in combination with fluorescent reporter

proteins, gene expression as function of the bacterial cell cycle. It also allows us to synchronise the cell cycles of thousands of individual cells *in silico*, which can offer insights about the bacterial cell cycle that would otherwise be obscured by the variability of the growth process of individual, asynchronously growing cells[214]. Using time-lapse microscopy in combination with automated image analysis has lead to an unprecedented wealth of data on individual cells with high spatial and temporal resolution. While flow cytometry is capable of a higher throughput of single cells, time-lapse microscopy provides a more detailed, time resolved picture of individual cells (Figure 1.1, top).

These techniques have facilitated the understanding of long-standing biological problems that were not tractable with experimental methods that asses growth on the level of the population. A few notable examples that illustrate how single-cell measurements have helped our understanding of such biological processes are given here:

The phase of zero growth ('lag-phase') that a microbial population exhibits upon inoculation into fresh growth medium or upon diauxic shift between carbon sources was long attributed to enzymatic adaptation across the population, upon completion of which growth would set on/resume homogeneously[129]. An alternative explanation for the presence of a lag-phase is, that only a fraction of the cells within the population resumes growth. Indeed, recent studies that employed flow cytometry or time-lapse microscopy, have shown that within an isogenic population, phenotypically distinct subpopulations exist that are able to transition between carbon sources due to their distinct molecular make up[190,205,95]. Sometimes this phenotypic distinction can be traced back to the variability in the expression levels of a single protein across cells[31].

Another example for non-genetic heterogeneity in microbial growth is the determination of cell fates through noisy gene expression in *Bacillus subtilis*. The competence for DNA uptake, the commitment to sporulation or switching between a chaining and a non-chaining phenotype are all the result of chance events that determine the fate of individual cells and lead to the formation of subpopulations within a population of isogenic cells[118,140,134].

In the coming sections we will provide a brief overview of the origins of non-genetic heterogeneity and its consequences on different levels of cellular organisation.

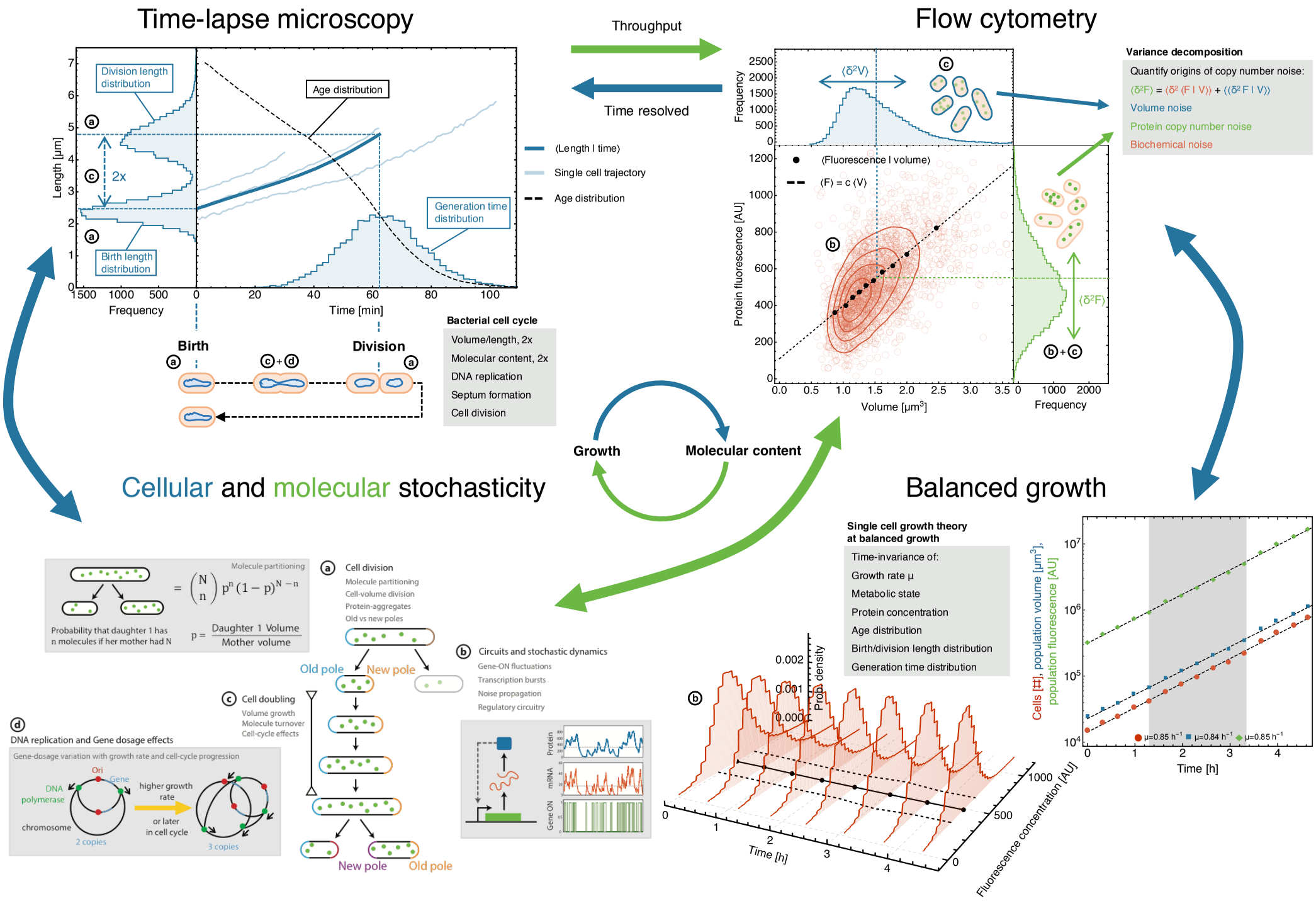
Time-lapse microscopy
Throughput
Time resolved
Flow cytometry
Division length distribution
Age distribution
Generation time distribution
Birth length distribution
2x
Length [μm]
Frequency
Time [min]
⟨Length I time⟩
Single cell trajectory
Age distribution
Bacterial cell cycle
Volume/length, 2x
Molecular content, 2x
DNA replication
Septum formation
Cell division
Birth
Division
⟨δ²V⟩
Frequency
⟨Fluorescence I volume⟩
⟨F⟩ = c ⟨V⟩
Protein fluorescence [AU]
Volume [μm³]
⟨δ²F⟩
Variance decomposition
Quantify origins of copy number noise:
⟨δ²F⟩ = ⟨δ² ⟨F I V⟩⟩ + ⟨⟨δ² F I V⟩⟩
Volume noise
Protein copy number noise
Biochemical noise
Growth
Molecular content
Cellular and molecular stochasticity
Balanced growth
Molecule partitioning
Probability that daughter 1 has n molecules if her mother had N
p = Daughter 1 Volume / Mother volume
Cell division
Molecule partitioning
Cell-volume division
Protein-aggregates
Old vs new poles
Old pole
New pole
Cell doubling
Volume growth
Molecule turnover
Cell-cycle effects
Circuits and stochastic dynamics
Gene-ON fluctuations
Transcription bursts
Noise propagation
Regulatory circuitry
Protein
mRNA
Gene ON
DNA replication and Gene dosage effects
Gene-dosage variation with growth rate and cell-cycle progression
Ori
Gene
DNA polymerase
chromosome
2 copies
higher growth rate
or later in cell cycle
3 copies
New pole
Old pole
Single cell growth theory at balanced growth
Time-invariance of:
Growth rate μ
Metabolic state
Protein concentration
Age distribution
Birth/division length distribution
Generation time distribution
Prob. density
Time [h]
Fluorescence concentration [AU]
Cells [#], population volume [μm³], population fluorescence [AU]
μ=0.85 h⁻¹
μ=0.84 h⁻¹
μ=0.85 h⁻¹
Time [h]

Figure 1.1: **Methods and concepts for studying growth and gene expression in single microbial cells.** This figure illustrates various aspects of single cell growth and gene expression, their interdependence and how they are affected by stochasticity. Different areas represent different chapters in this thesis that each addresses one of the many aspects of single-cell growth and gene expression and how these aspects can be characterised experimentally. Note that the plots in this figure are not sketches, but actual experimental data from chapters 3 and 4. **Chapter 2 (bottom left)** reviews the origins of non-genetic heterogeneity and its consequences for the ability of individual cells to adapt to dynamic changes in the environment. **Chapter 3 (top right)** addresses the relation between inter-cellular variability of gene expression levels, cell volume and growth rate, and demonstrates, how variance decomposition can be used to quantify variability that stems from different molecular and cellular processes. The influence of the bacterial cell cycle on the dynamics of growth and gene expression gets investigated in **chapter 4 (top left)**. All experiments in this thesis were conducted specifically under conditions of **balanced growth**, an important prerequisite for understanding a microorganisms physiology. The **bottom right** of this figure illustrates, how the state of balanced growth can be identified from experimental data.

Stochasticity in gene expression

The origins of the variability in cellular properties that we observe across any population of isogenic cells are diverse, but all of them relate to biochemical reactions that, together, constitute the process of gene expression, which lies at the heart of cell growth.

Gene expression is the process in which the information that is encoded in the functional unit of DNA – a gene – is transcribed into a gene product, typically messenger RNA (mRNA), which is then translated into protein, which ultimately determines the phenotype of a cell. Biochemical reactions, such as transcription or translation, form the basis of life. They are inherently stochastic, which leads to random inter- and intra-cellular fluctuations in the number of macromolecules and the timing of reactions at any given time point. Genes, mRNAs and regulatory proteins are macromolecules that are typically present in low copy numbers, which makes reactions in which they are involved sensitive to fluctuations. The timescales at which macromolecular species are produced and degraded are also an important factor in these stochastic fluctuations, as their lifetime determines whether and at what timescales fluctuations occur[168,152].

The first step in gene expression, transcription, has been identified as a prevalent source of noise in protein numbers[49]. mRNAs are typically present in low copy numbers and exhibit a relatively short life time, both factors that make mRNA levels prone to fluctuations, which can propagate to protein levels[158]. For any given gene, the steady state mRNA concentration is set by the rate of production and degradation. Production and degradation are independent processes, resulting in fluctuations of mRNA levels around their 'true' steady-state value[179]. Another source of variation is the discontinuity of mRNA synthesis. Rather than being a continuous process with a fixed rate, mRNA synthesis occurs in bursts during short times of gene activity followed by a (long) period of inactivity[227,40,32]. Burst size as well as burst frequency relative to mRNA lifetime are critical factors that determine the magnitude of noise – larger bursts and a lower frequency both result in higher levels of noise[179,41]. The consequence of this is that genes with the same mean expression level can exhibit different levels of noise[179].

At low expression levels, transcriptional noise gets propagated to the level of proteins[11,137,146]. With increasing expression levels, the noise in protein levels diminishes until it encounters a 'noise floor' at high levels of expression[196,222,83]. The mechanistic origin of this lower limit of protein noise likely lies in variations of general cellular properties that globally act upon reaction rates. Cell-cycle progression, variations in cell size, random partitioning of molecules upon cell division, translational efficiency, bursting, cellular growth rate and RNA-polymerase concentration have all been suggested to cause or at least contribute to the noise floor[76,41,81,224]. In chapter 2 we extensively review current literature on the origins of non-genetic heterogeneity and its consequences for the

ability of isogenic microbial populations to adapt to dynamic changes in the environment.

Quantification of the contribution of individual processes to the total variability of a certain property across single cells does not only require the measurement of single cells. It also requires dedicated statistical frameworks and formulations. Variance decomposition is a statistical tool that can be employed to disentangle and quantify the contributions of different sources of noise, such as growth, cell division and biochemical noise, to the total variability of, for instance, the expression levels of a protein[177] (Figure 1.1, top right). In chapter 3 we make use of this elegant approach to quantify the contributions of volume noise and biochemical noise to the total variability of protein copy numbers across a population of isogenic cells which we measured with flow cytometry.

Interdependence of microbial growth and molecular composition of a cell

From the last section we have an idea of the biochemical processes that underlie non-genetic heterogeneity. However, the relation between a cell's phenotype and fluctuations in its molecular composition is not unidirectional. The metabolic state of a microbial cell is determined by the proteins it expresses and the environment that surrounds it. In order to grow, a cell needs to meet the requirements of the environment by expressing a particular set of proteins that enable it to utilise the nutrients that are present and to cope with potential stresses that it is exposed to. The growth rate of a cell, and thus the generation time, depends on the nutrient quality and how well the cellular proteome is adapted to the environmental conditions[180,84,112]. In turn, growth and the metabolic state of the cell feed back onto the molecular composition of a cell, e.g. through dilution-by-growth as the cell's volume expands[44,89,71]. This means that there exists a reverberating relation between growth of a cell and its molecular content[180] (Figure 1.1, centre). Hence, the fluctuations that occur on the molecular level of a cell (as introduced in the last section) can propagate to higher levels of organisation, resulting in variability of the growth process itself, and vice versa[31] (Figure 1.1, bottom left). For instance, noise in the expression levels of a single protein does not only depend on factors that are intrinsic to the protein (as discussed in the previous section), but also on global, extrinsic factors that are directly related to cell growth, such as volume expansion, random partitioning of molecules upon cell division or the availability of transcriptional and translational machinery[76,71,87,181] (Figure 1.1, bottom left & top right). As a result, the growth of a single cell is a stochastic process, which makes it difficult to predict the growth trajectory of individual cells (Figure 1.1, top left).

Despite extensive studies on the interrelation between growth rate, the metabolic state of a cell and its molecular composition[180,44,13], little is known about the effects of growth rate on non-genetic heterogeneity[62,83]. In chapter 3 we characterise this relation for the expression of a single protein, using a combination of experiments (flow cytometry) and theory (variance decomposition) (Figure 1.1, top right).

Microscopic growth theory

Thinking about single cells and their behaviour requires a different perspective than classical, population based cell biology. Measuring some property at the level of a population, e.g. generation time, a fluorescence value or the activity of an enzyme in a cell extract, effectively reports the average of this property from thousands or millions of individual cells. However, single cells in isogenic populations markedly deviate from this average behaviour. These circumstances require theoretical frameworks that are able to take into account uncertainties and inter-cellular differences when studying the growth and gene expression in single cells.

Regardless of the stochasticity in the growth process of each individual cell, there are certain features that are characteristic of microorganisms that proliferate by binary fission. For instance, the average cell doubles its size and molecular content before dividing into two equal-sized daughter cells. In a population of asynchronously growing cells, this results in certain distribution of growth properties of individual cells that can be deduced from such first principles. In the 1950s -1970s a 'microscopic growth theory' was developed, which rigorously characterises the statistics of microbial growth on the basis of the probability distributions of cellular properties, such as birth size or generation time[159,149,34]. While we can not predict the state of an individual cell that we pick randomly from a population, we can use this theory to predict the probability distributions of single-cell properties from a few basic measurements on the level of the population.

This theory applies under conditions of balanced growth, a microbial state of growth that has certain characteristics that directly relate to the physiology of the organism that is studied.

The concept of balanced growth

The state of balanced growth is characterised by the time-invariance of the probability distributions of cellular properties of individual cells, such as cell age, size at birth and division, generation time and gene expression levels across a microbial population[159]. A microbial population usually achieves this state after several generations of growth under constant, non-limiting conditions[159]. The distributions themselves, their shape, variance and mean value, are a characteristic of the organism and the environment in which it is growing[149]. This means that the state of balanced growth can easily be reproduced, as long as the environmental conditions are constant. The metabolic and regulatory networks of the organism will steer the distributions of cellular properties towards the average value that matches/is tied to the environment.

When the goal is to study the architecture of these networks and the mechanisms that control growth, gene expression and the variability therein, balanced growth is an important prerequisite. It guarantees that the variability that we observe in individual cells is not due to dynamic changes in the environment, but due to the stochasticity that arises from cellular and molecular processes (Figure 1.1, bottom left). The distributions of cellular properties are directly related to the processes that generate them[149,179]. Thus, although the concept of balanced growth is defined on the level of populations, it is ultimately derived from the growth properties of a single cell. This means that we can make statements about dynamic single cell processes from 'snapshots' of a population in balanced growth without observing individual cells in time and, conversely, predict the stationary distributions of a whole population by observing the growth dynamics of a single cell lineage[177].

In experimental data, balanced growth can be identified directly from the time-invariance of the probability distributions of the above mentioned cellular properties, e.g. size at birth and division, or protein concentration (Figure 1.1, bottom right). Another, equivalent criterium is the increase of extant population properties, i.e. number of cells (or optical density), cumulative length, volume or mass of the population or protein mass, at a fixed and identical rate, the specific growth rate (Figure 1.1, bottom right). In this work, all experiments were explicitly carried out under conditions of balanced growth.

Balanced growth is an invaluable concept for studying growth and physiology of microorganisms. However, the underlying mechanisms that robustly steer cells and ensure homeostasis in virtually any cellular property are not well understood. This reflects our still lacking knowledge of the bacterial cell cycle and its regulation. In recent years, time-lapse microscopy has lead to the experimental confirmation of phenomenological principles that describe how a bacterial population is able to maintain size homeostasis under constant environmental conditions[191,29,195,79]. The mechanisms underlying

these phenomenological descriptions are largely unknown, although it seems that there is a close relation between cell size homeostasis and the regulation of the cell cycle[215]. How the metabolic state of a cell, and thus the growth rate and gene expression, change as function of the cell cycle is not well studied and could provide important insights on the mechanisms that lets microorganisms achieve the state of balanced growth. In chapter 4 we tackle this question, by characterising the dynamics of growth and gene expression along the cell cycle of thousand of individual cells, using time-lapse fluorescence microscopy.

Outline of this thesis

The advent of technology that allows the characterisation of thousand of individual cells per experiment has lead to a shift in the paradigm of cell biology away from ensemble-based concepts towards theories and concepts that embrace the individuality of single cells. In a way, today we are closer than ever to being able to meticulously study life and its molecular organisation at the level of its fundamental unit, the cell. Following a systemic approach, this thesis aims to fill gaps in the understanding of the interrelation between growth and gene expression of individual microbial cells, the inter- and intra-cellular variability therein and provide new insights into the long standing question of how microbial populations achieve a state of balanced growth. *Bacillus subtilis* is the model organism that we chose to tackle these questions experimentally.

In **chapter 2** (Figure 1.1, bottom left) we start out by extensively reviewing the effects on non-genetic heterogeneity on the ability of microbial cells to adapt to dynamic changes in their environment, with a special focus on the formation of persister cells. Persister cells are highly tolerant individuals that are able to endure periods of adverse conditions, such as antibiotic treatment, without being genetically resistant to such circumstances[111]. Switching of individual cells to the persister state can be actively induced by environmental conditions, but it also occurs spontaneously and at random under conditions of balanced growth, which poses a disadvantage for the individual that undergoes this transition.

In **chapter 3** (Figure 1.1, top right) we use a combination of theory and experiments to characterise the relation between growth rate and gene expression noise in isogenic cells. Surprisingly, this relation has not received much attention in ongoing research. Using flow cytometry, we measure the distributions of cell sizes and the expression levels of a fluorescent protein in a population of isogenic cells under conditions of balanced growth. We modulate the expression levels of the fluorescent protein by varying its synthesis rate (promoter activity) and the rate at which it is diluted (growth rate). Using variance decomposition, we demonstrate how to quantify the contributions of variations in cell volume and noise in protein concentration to the variability in protein abundance across individual cells. Strikingly, we find that the noise in both, protein abundance and concentration, is solely dependent on the mean expression level, regardless whether it is set by promoter activity or growth rate. Furthermore, the contribution of cell volume variations stays constant across conditions and protein expression noise encounters a noise floor at high expression levels.

In **chapter 4** (Figure 1.1, top left) we study the dynamics of growth and gene expression along the cell cycles of thousand of individual *B. subtilis* cells at different growth rates, using time-lapse fluorescence microscopy. As a cell progresses through the cell cycle, transient disruptive events, such as DNA replication and septum formation, could possibly affect growth and gene expression. In this chapter, we aim to gain a quantitative understanding of how growth and gene expression change dynamically along the cell cycle and what role these dynamics could possibly play in cell homeostasis at balanced growth. We find that, rather than exhibiting exponential growth at a fixed rate throughout their life, individual cells show systematic deviations from this behaviour. Specifically, a growth rate change occurs at a fixed, condition independent time prior to cell division. Moreover, despite the dynamic changes in growth rate, cells are able to maintain almost perfect

homeostasis in the expression levels of an unregulated fluorescent protein. This is achieved by a concomitant change in the protein synthesis rate, which likely relates to the metabolic state, and thus the growth rate, of each individual cell.

In **chapter 5** I place our findings in the context of recent phenomenological studies that address the problem of cell size homeostasis and balanced growth. I discuss what we can learn from phenomenological principles, when they are useful and where they fail to give us deeper insights. I speculate on the relation of the cell cycle to the metabolic state of a cell and how transient, disruptive events, such as DNA replication and cell division, can perturb a potential state of balanced single cell growth. Furthermore, I discuss the question of the evolutionary costs and benefits of non-genetic heterogeneity and gene expression noise. Finally, I propose experimental approaches that can help us to fill remaining gaps in our understanding of growth and gene expression in bacterial cells.

Chapter 2

Taking chances and making mistakes: non-genetic phenotypic heterogeneity and its consequences for surviving in dynamic environments

Coco van Boxtel*, Johan H. van Heerden*, Niclas Nordholt*, Phillipp Schmidt*, Frank J. Bruggeman

* Contributed equally to this work

Abstract

Natural selection has shaped the strategies for survival and growth of microorganisms. The success of a microorganism depends not only on slow evolutionary tuning, but also on the ability to adapt to unpredictable changes in their environment. In principle, adaptive strategies range from purely deterministic mechanisms to those that exploit the randomness intrinsic to many cellular and molecular processes. Depending on the environment and selective pressures, particular strategies can lie somewhere along this continuum. In recent years, non-genetic cell-to-cell differences has a received a lot of attention, not least because of its potential impact on the ability of microbial populations to survive in dynamic environments. Using several examples, we describe the origins of spontaneous and induced mechanisms of phenotypic adaptation. We identify some of the commonalities of these examples and consider the potential role of chance and constraints in microbial phenotypic adaptation.

Microbial biodiversity and phenotypic plasticity: one of life's many marvels

Microorganisms occupy an enormous number of niches on Earth; they are its most abundant life form. This evolutionarily success points to the remarkable flexibility and adaptability of microorganisms, not the least because their niches vary greatly. Although niches can be stable on a long time scale, many of them are characterized by highly dynamic conditions, with frequent fluctuations in environmental variables (e.g. nutrients, temperature, osmolarity etc.). Microbes are therefore forced to continuously adapt their phenotype to changing conditions, to survive and to prevent being out-competed by other species or genetic variants. The mechanisms for phenotypic adaptation are continuously tinkered by evolution, via mutation and selection. Their variety underscores the intriguing resourcefulness of microbe sub-populations in coping with environmental dynamics. Adaptation to new niches and sustaining their occupancy, therefore relies on phenotypic adaptation, on a short time-scale, and its slow evolutionary tuning, via mutations on longer time scale[100].

Our view of microorganisms, and in particular of their amazing phenotypic plasticity, is also still evolving. The classical view, which emphasises the determinacy of the phenotype from the genotype and the environment, has in the past decade been challenged by observations of partial indeterminacy, as underscored by phenotypic heterogeneity[48,163]. Single-cell studies invariably indicate that the molecular state varies between isogenic cells, even at constant conditions for sister cells, sharing the same mother cell[60]. This heterogeneity is caused by various stochastic phenomena in a cell, which can even lead to the emergence of sub-populations of cells with qualitatively different phenotypes, known as phenotypic diversification[141]. Population diversification can be a potent fitness enhancer for a population of microorganisms. For instance, to survive sudden extinction-threatening conditions, bacteria can enter a dormant, resilient physiological state to become a 'persister cell'[10]. Stochastic phenomena can also be fitness reducing. They can distort information transmission and perturb regulatory mechanisms in cells to such an extent that adaptation dynamics to a new state is affected, possibly leading to maladaptation[205].

Phenotypic heterogeneity indicates that an understanding of microbial phenotypic-adaptation requires studies of single cells. Inevitable molecular stochasticity can cause isogenic cells to adapt differently. The precise state that a cell is in, when conditions change, therefore determines its adaptation dynamics; whether it successfully adapts or not, and, if it does, how long this adaptation takes[31]. This is likely even more pronounced for eukaryotic microorganisms. Their phenotype is cell-cycle-stage dependent, which constitutes an additional 'deterministic' factor of phenotypic variability[150]. Cell-to-cell differences in adaptation dynamics forces us to revisit 'understood' classical environmental transitions studies, such as nutrient transitions, which were mostly population-based, and take into account the impact of molecular stochasticity[31,23,205,95]. Below we discuss how this new paradigm has led to surprising insights and novel systemic relations between cellular growth and stress tasks.

Elucidating how the stochasticity of specific molecular circuits influences fitness is not a simple task. This is perhaps surprising given the simplicity of the definition of microbial (geometric) fitness; which is the factor of increase in the number of viable offspring during some period of particular (dynamic) environmental conditions[167,102,53]. The complication arises from the fact that phenotypic heterogeneity in the context of fitness is still poorly understood and difficult to quantify, with many open questions that are hard to answer. Is phenotypic heterogeneity an evolved trait or is it the inevitable consequence of physicochemical constraints and limitations in molecular circuits? In other words, how much of the cell-to-cell variability we observe in phenotypic traits arises from selection of noise-generating mechanisms (e.g. because it enhances fitness under certain conditions) and how much of it is due simply to physicochemical limits in molecular circuits that cannot easily be improved by evolution (because it will result in a trade-off). What are the selective pressures that

promote heterogeneity? To what extent are the fitness consequences of phenotypic heterogeneity dependent on time-scales and sub-population sizes? First efforts to answer these questions have been undertaken[59,1,167,47,212], but it remains a challenge for modern biology to expand on them and finally give definite answers.

Natural selection enhances the occurrence of microorganisms with phenotypic adaptation mechanisms, including those that generate stochasticity, provided that they confer a fitness advantage. Such mechanisms may involve different types of molecular circuits that contribute to fitness such as signalling, metabolism, motility and stress. So even though fitness itself is one dimensional, it is a single number, a cell sets this number via a multidimensional mechanism, which resembles a 'single-objective, multi-task optimisation' problem. Similar problems occur in other disciplines such as in control engineering and finance. The resemblance is even deeper, the theories used in evolution to understand the fitness of organisms in dynamic environments have many similarities with theories used in other disciplines[167,102,18,47].

A successful fitness theory allows for descriptions of phenotypic adaptation 'strategies' at various levels of abstraction; from coarse and phenomenological descriptions to detailed molecular-mechanistic models[167,47,64]. Such a theory allows for the evaluation of adaptive strategies in terms of the fitness benefits of different molecular circuits and their fitness costs, associated with their consumption of limited biosynthetic resources[219,128] and inevitable stochastic disturbances. In our opinion, such an integrative, systemic view is ultimately required to understand the phenotypic adaptation of a bacterial species. It appears that with existing fitness theories and experimental capabilities this can indeed by achieved[115,104,102,1,18,47,59,64,212]. Much development is still required to achieve a comprehensive understanding of phenotypic adaptation, which we shall return to in the closing section of this review.

In this review, we address several aspects of the role of stochasticity in phenotypic adaptation by microorganisms; i.e. how it influences fitness, given the adaptational challenges that microbes face in their dynamic environments. We focus on phenotypic adaptation, so the process of a cell with a fixed genome that is changing its physiological behaviour. We will discuss several cases of phenotypic heterogeneity. In some examples the fitness consequences are evident while for others they are more speculative. We aim to describe many of the possible roles of non-genetic heterogeneity in the adaptation strategies of microorganisms in dynamic environments.

Pioneering single-cell work

Nowadays, we exploit fluorescence microscopes and fluorescent reporters to study the surprising behaviours of single cells. This was not possible decades ago. However, already in the 1950s many researchers started asking questions about the functioning of single cells. The questions they asked are very similar to those that are most pressing now. For instance, they realised that the behaviour of individual cells in isogenic populations could deviate from the population average. The existence of sub-populations, that they likely form via chance events, that single cells vary in molecule copy numbers and show variable birth and division length, instantaneous growth rates and generation times, were all being considered experimentally and theoretically[142,121,16,159,34,67,149,125,17]. How we study single cells now, using fluorescence microscopy and fluorescent reporters[117], saw an enormous growth after the introduction of several influential papers in the early 2000s[168,49,152,146]. Then, the focus was mostly on noise of molecular circuits, without much consideration of the cellular effects of molecular chance events. Recent work is mostly dealing with how systemic behaviour with a fitness effect varies from cell to cell. This review will be mostly concerned with the latter work.

Individuality in the responses of isogenic cells to nutrient transitions

Real-time imaging of growth and fluorescent reporter-protein expression by single cells, with fluorescence microscopy[117], has drastically changed the way we think about populations of isogenic microbial cells (Fig. 2.1)[48,152,141]. These populations turn out to be inhomogeneous, with cells behaving as 'individuals'. The molecular state of cells vary, in a dynamic, spontaneously-fluctuating manner[168,49,60] (This aspect has been reviewed earlier[152,113]). A recent insight is that populations of isogenic cells can diversify into sub-populations with distinct phenotypes[141]. Such an adaptation strategy can be analysed in terms of a framework for fitness in dynamic environments[167,64]. A diversifying response may either be an evolved strategy or purely result from molecular noise, causing variation in cellular responses. In this section, we will discuss some striking examples that are provided by nutrient transition studies (Fig. 2.1).

A chance event can determine whether a cell adapts

A surprising finding was made with the lactose operon in *E. coli*[31], a system which was thought to be well understood. Whether a single cell initiates growth on lactose turns out to depend purely on a chance event in its recent past. This insight was gained by tagging the lactose permease with a fluorescent protein and tracking its expression in single cells. At intermediate induction of the lac operon a colony consists of two different phenotypes: cells with high and low expression (see also[147]). A cell has to reach a threshold permease level in order to commit to lactose growth. Only when the expression level is high enough a positive feedback mechanism becomes active that enhances permease expression to a level required for growth. This expression threshold has to occur before the cell is aware of lactose in its environment, since it lacks sensors for it and lactose cannot pass the membrane by diffusion. At intermediate induction, the lac repressor dissociates randomly from the lac promoter and occasionally leads to a burst of transcription activity that, if it lasts long enough, can lead to the threshold level expression of permease, priming the cell for lactose growth when it is present. As a result of this the response times of *E. coli* cells to a sudden lactose addition are very broadly distributed, because it can take a long time before cells reach the threshold expression level of the permease[23]. Chance therefore decides when cells adapt. This is an example of stochastic adaptation. Evolution simulations indicate that bistability of the lac operon may not be so prominent in natural settings[206].

Responsive adaptation leads to more homogeneous responses of all cells

When cells perceive the extracellular environmental change, e.g. via a dedicated sensor, cells can respond much more homogeneously. This is illustrated by a study with the budding yeast, *S. cerevisiae*, in which the the number of transcripts of the gene *MET5* was counted in single cells. *MET5* is required for the synthesis of methionine, when it is absent from the environment[177]. By changing the sulphur source in the medium from methionine to sulphate, the dynamics of *MET5* induction could be monitored. It was observed that individual cells exhibited nearly identical response times. Although there were still differences in adaptation times (i.e. the time needed to induce gene expression) between individual cells, all cells eventually adapted. The spread in adaptation times is mostly a consequence of transcriptional noise and much less due to differences in the timing of perception. Clearly cells perceived the presence and absence of methionine with high precision. The entire population shifts uniformly to the new state within a relatively short time period (compared to the generation time). The presence of an initial variability in transcription activity is expected to have only a minor influence on cellular fitness.

The phenotypic state of a cell can cause it to maladapt

Examples exist that indicate that a sub-population of cells is not able to initiate growth on a new carbon source, or one that is suddenly increased in concentration. When yeast cells are, for instance, exposed to a glucose transition a small fraction arrests growth, because they were in a deviating metabolic state[205]. Different metabolic states are most likely caused by varying enzyme concentrations and can result in depletion of cellular ATP when the rate of upper glycolysis exceeds the rate of lower glycolysis by too much. Similar behaviour is observed with *E. coli* cells[162,95,4], although this behaviour likely originates from a different molecular mechanism.

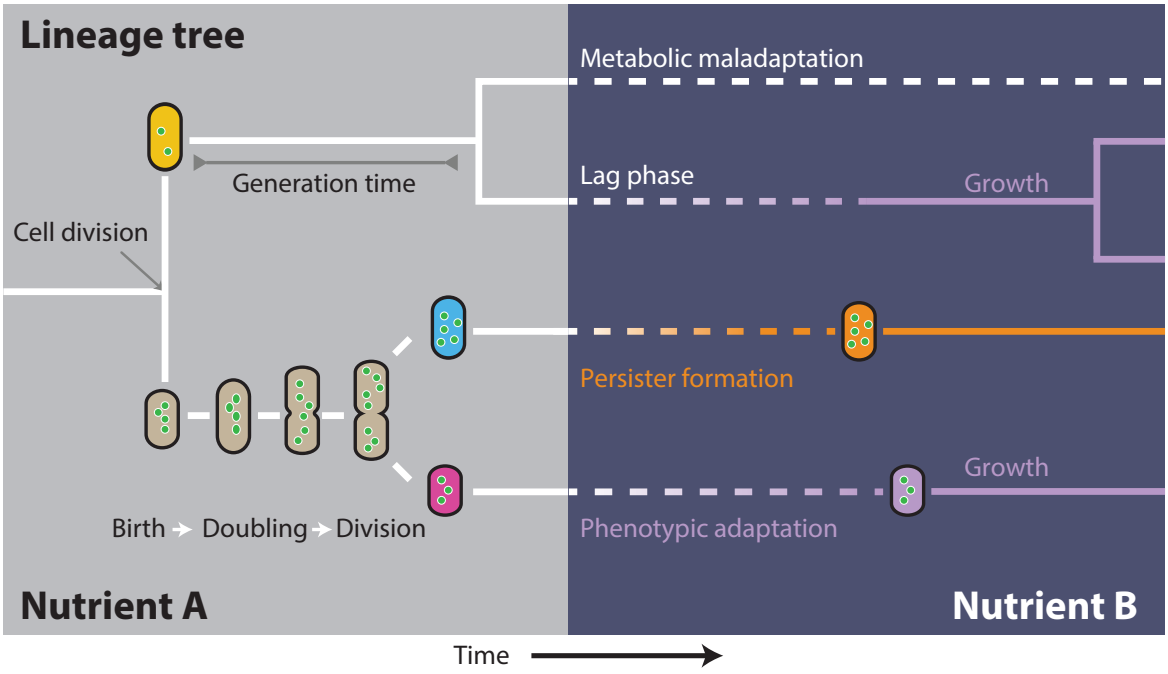

Figure 2.1: **Conceptual framework for single-cell growth and phenotypic diversification upon a sudden nutrient transition in isogenic populations.** During steady-state exponential growth of a population of isogenic cells, at constant environmental conditions, the total cell number increases exponentially. Individual cells progress asynchronously through their cell cycle. Cells vary in size, molecular composition and doubling time, due to inevitable stochastic effects, even those that are at the same cell-cycle progression and were born from the same mother[168,49,60]. When individual cells are suddenly confronted with a nutrient transition, not all of them have the capacity to adapt, even though they do have the metabolic machinery to grow on the new carbon source. This can lead to lag-phases, temporary growth arrest[190] or maladapted states[205], and even the formation of persister cells in bacteria[4,95,162].

Distinguishing generalist from specialist adaptation strategies

When discussing different phenotypes we usually distinguish sub-populations that vary greatly in growth rate, e.g. growing versus non-growing[162,95,4,205]. The situation can also be more subtle. A nice example exists where different phenotypes show varying capacities for growth[136]. In this study, yeast cells were exposed to alternating levels of glucose and maltose. Fluorescent labelling of an enzyme required for utilising maltose, combined with time-lapse microscopy allowed the tracking of different phenotypes. It was shown that the phenotypes that initiated growth on maltose grew slower when they were switched back to glucose, compared to the phenotype that never performed the switch to maltose. This means that adapting to a new environment may depend on the cell's history. Different wild yeast strains displayed differences in lag time after the switch[136,208]. It was proposed that this is due to different levels of catabolite expression and that two different strategies could be identified. A 'specialist' strain has high levels of catabolite expression, which gives it a growth rate advantage on a specific nutrient, while a generalist grows slower on specific substrates,

but switches faster and achieves higher growth rates on other substrates.

Cell-density dependent sub-population formation

Solopova et al.[190] grew *Lactococcus lactis* in the presence of two different carbon sources, glucose and cellobiose. Glucose is the preferred carbon source. Cell sense when the glucose concentration drops below some threshold (Fig. 2.2A) and initiate gene expression to prepare them for growth on alternative substrates, such as cellobiose. What Solopova et al.[190] found was that cell density determined the fraction of cells that successfully make the transition from glucose to cellobiose growth. Specifically, the higher the cell density, the lower the fraction of cells that resume growth on cellobiose. The explanation for this finding likely lies in the time required for individual cells to prepare for a transition from a substrate like glucose to another, such as cellobiose. Implementing the physiological changes required for growth on cellobiose (e.g. expression of new metabolic genes) takes time, and any differences between individual cells, at the moment that low glucose is sensed, will result in some cells needing more or less time than others to prepare (Fig. 2.2B). The time available to all cells, is determined by how quickly the remaining glucose disappears from the environment. At high cell densities, this will happen very quickly and only a small fraction of cells will manage to make the necessary changes for growth on cellobiose before glucose is depleted; cells that fail to do so, will be stuck in a physiological state that is incompatible with cellobiose consumption. If, on the other hand, cell densities are low when the threshold is sensed, the rate at which glucose disappears will be slow and most cells will have sufficient time to prepare for the new condition.

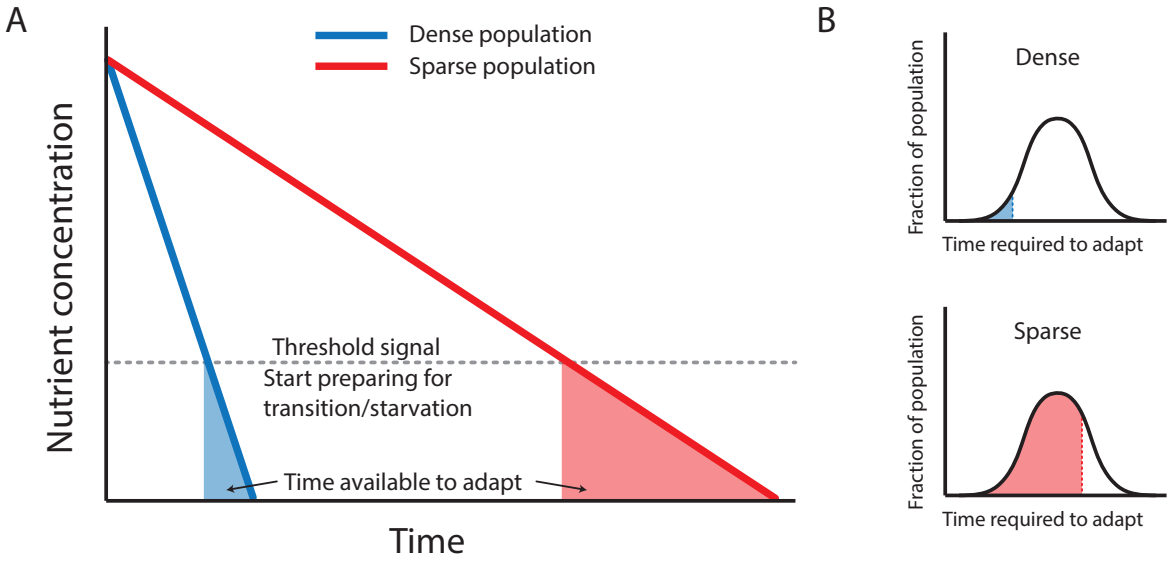

Figure 2.2: **The ability of individual cells to successfully transition from one nutrient state to another is dependent on population density.**(A) The rate at which a nutrient such as glucose disappears from the environment is determined by the cell density. Shown are two scenarios, where a very dense (blue line) and a very sparse (red line) population consume a nutrient. In both cases, low nutrient levels are detected at some threshold concentration, at which point cells have to prepare for nutrient depletion. (B) The time needed to prepare for a new condition, will differ for individual cells (this can be described by a distribution), depending on their exact state at the time a threshold signal is detected. If the nutrient abruptly runs out, as in the case of a very dense population, only a small fraction of cells will be prepared for the new condition. When the population density is low, the time window will be large and most cells will adapt in time.

Chance events that can impact the fate of a cell

The previous examples of phenotypic adaptation indicate that chance events co-determine the fate of single cells upon an environmental change. The types of chance events found so far can be categorised into four classes: i. molecular origins, ii. cellular and systemic effects, iii. cell-cycle stage and DNA-replication dependences, and iv. history effects (Fig. 2.3).

Molecular stochasticity

Biochemical reactions are inherently stochastic, which leads to fluctuations in concentrations of macromolecules[153]. At large numbers of reactant molecules the behaviour of biochemical reactions is predictable, because fluctuations in copy numbers are negligible (Box 1). Stochasticity in molecule copy numbers can make systems inherently nondeterministic when those numbers are low. Transcription factors and mRNAs are typically present at such low numbers. The lifetimes of these molecules determine the rate and duration of fluctuations[168,152]. While fast fluctuations typically average out during one cell cycle, slow fluctuations that exist on time scales equal or longer than the cell cycle can provide a 'molecular memory'[157,185,140,122]. The size of a fluctuation in the copy number of a molecule is set by the size of the imbalance between the synthesis and degradation rate of a molecule, and how quickly the system dissipates the fluctuation[153]. The fluctuation size can be quantified as the relative width (dispersion) of the probability distribution that describes the copy number of a molecule in each cell and is called noise. Noise can propagate in networks[158], and get amplified or attenuated along the way, leading to systemic phenotypic variations in populations of clonal cells. In box 1, we briefly summarise the great variety of molecule stochasticity effect that have been discovered.

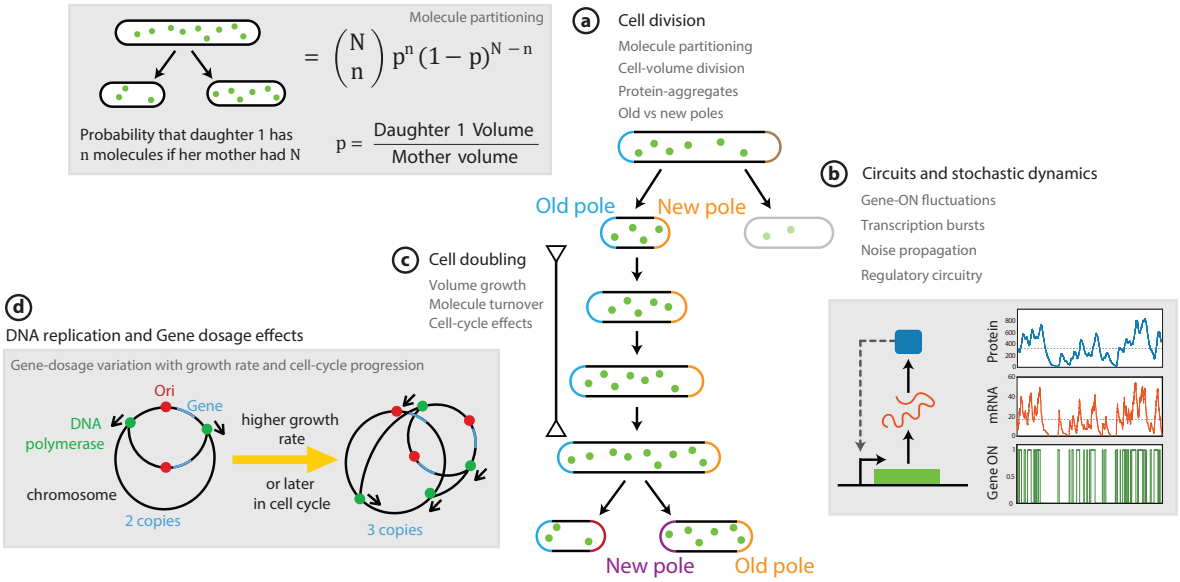

Figure 2.3: **Overview of molecular and cellular stochastic processes.** Numerous mechanisms contribute to the cell-to-cell variability of cellular characteristics during steady-state, exponential growth. (a) Molecule partitioning can be described by a simple model based on the ratio of daughter and mother volumes. Protein aggregation at the poles can lead to distinctive protein concentrations in daughter cells and determines pole age. (b) Gene expression consists of multiple stochastic processes. Transcription occurs in bursts and this noise can propagate to the protein level. Network motifs can further modulate the effect of noise. (c) Cell doubling, dilution by growth and cell cycle progression influence the physiological state of the cell. (d) The position of the gene on the chromosome and the number of chromosomes determine the level of gene dosage effects.

Chance events at cell division

In symmetrically dividing bacteria, such as *E. coli* and *B. subtilis*, division produces, on average, two equally sized new-born daughter cells. While mechanisms exist that ensure the equal partitioning of DNA content[199], other molecules are partitioned in a more random manner such as random diffusion in the cytosol or based on cellular localisation (like membrane or pole proteins[75,76]).

Freely diffusing molecules are inherited in approximately equal concentrations by the daughters, even if they differ in birth volumes, provided their copy numbers are high. The noise (variance divided by the mean squared) in the number of proteins that a daughter with birth volume V_1 received from her mother, with N molecules and volume V, equals $\frac{1}{N}\left(\frac{V}{V_1}-1\right)$, which quickly becomes negligible for large N. Differences in the size of the two daughters will lead to differences in their absolute molecule numbers, which can diversify their behaviour.

An interesting example of non-diffusive partitioning is that of RNA-polymerase (RNAP). Bakshi et al.[8] showed that $\approx 82\%$ of RNAP is bound to DNA; the remainder concerns two pools, which are in equilibrium with the bound pool. RNAP abundance therefore correlates strongly with DNA content (and not with cell volume). Volume differences between two daughter cells will therefore result in RNAP concentration differences, with higher concentrations of RNAP in the smallest daughter. Yang et al.[224], showed that cell-to-cell variability in the RNAP concentration leads to heterogeneous protein-expression across cells.

The partitioning of molecules during division, be it through active or passive processes, nearly always has a chance component. For molecules present at low numbers, partitioning errors can be large in the absence of mechanisms that coordinate segregation[76,75]. Eukaryotic cells, like yeasts, contain a variety of specialised organelles, including mitochondria, vacuoles and lysosomes, that are present at much lower numbers than most proteins and metabolites. Cells can partition those low abundant structures more evenly, using dedicated actin-dependent transport processes[114,22]. Even if segregation involves such coordinated mechanisms, Huh and Paulsson[76] showed that accurate partitioning of this class of low abundant organelles and molecules is extremely difficult to achieve and that cell-to-cell variability is almost inevitable. This conclusion is experimentally supported by the finding that cell-to-cell variability in mitochondrial content likely arises from errors in partitioning during cell division[42].

Asymmetric partitioning of molecules or organelles also has a biological function. For example, yeast differentially enriches particular proteins in mother and daughter cells, using an active sorting mechanism[223]; a process that has been linked to ageing in these cells. Mother cells age because they retain damaged, or life-span limiting, proteins such that their daughters start with a younger, 'reset' physiology. Levy et al.[110] found that replicative ageing influences cell-to-cell variability in protein expression: the abundance of a protein involved in trehalose biosynthesis, TSL1, correlated with the number of divisions a cell has undergone and that this, in turn, correlated with its survival chance upon sudden heat stress. Others have shown age related asymmetry in mitochondrial function[74]. These findings suggest a general functional role of asymmetry in partitioning as a means of rejuvenation, but more importantly underscores the fact that cells of different chronological ages differ physiologically.

Age-related asymmetric protein partitioning has also been described in *E. coli*[192,116,216,164]. *E. coli* cells are rod shaped, with two poles. Upon division, each daughter cell receives an old and a new pole. A cell's age can be quantified by the number of times its old pole has been inherited. In the case of *E. coli*, cell age correlates with growth rate and older cells appear to accumulate protein aggregates[192,116,216]. Beyond growth rate effects, the consequences of age-dependent protein aggregation in bacteria remains unclear, but the finding that in *Mycobacterium smegmatis* cell age and antibiotic susceptibility correlate (albeit weakly)[213], suggest a possible role in physiological

heterogeneity.

DNA replication and gene dosage

Symmetrically-dividing cells double their molecular content from birth to division at steady-state, exponential growth (i.e. balanced growth). While the abundance of most molecules increases in proportion with cell volume, gene copy number (i.e. gene dosage) is an exception, due to the discrete nature of DNA replication[12]. Since cells generally grow asynchronously – some have just been born, while others are halfway through their cell cycle or are about to divide – DNA content and gene copy number varies between cells at different stages of the cell cycle. This can cause cell-to-cell variability in their molecular constitution if the production rates of proteins are sensitive to changes in gene dosage[214].

In bacteria, the circular genome is copied in a bi-directional linear manner; starting from the origin of replication (oriC) towards the terminus (terC). This is a more or less continuous process[214], although periods without active replication are observed under slow growth. DNA replication leads to a sudden discrete increase in gene copy-number. In bacteria, this change in gene dosage propagates to protein content[12,214] and the chromosomal position of a gene determines the concentration dynamics of the associated protein[214]. In eukaryotes, where replication occurs exclusively during the S-phase of the cell cycle, gene-dosage dependent effects appear to be suppressed by some mechanism, likely involving chromatin modifications[12].

Cell-cycle effects in eukaryotes

The eukaryotic cell cycle comprises distinct stages, consisting of growth (G1 and G2), DNA synthesis (S), mitosis and cytokinesis (M). Cell-cycle progression is achieved by a complex protein network that imposes checkpoints to ensure orderly transitions from one stage to the next. In *S. cerevisiae*, studies have shown that progression through these stages is accompanied by global rearrangements in almost all cellular processes and that structured cell-cycle-dependent changes occur across many layers of organisation, including the transcriptome[170,188,124] and the metabolome[58,131], as well as in protein localisation[201] and organelle morphology[201].

Distinct cell-cycle stages (growth, DNA synthesis, mitosis and cytokinesis), at which metabolism is different,[150] enhance the cell-to-cell variability in an asynchronously growing population of cells. Individual cells will be in different physiological states according to their position in the cell-cycle. In yeast, cell-cycle dependent gene-expression variation exceeds variability due to stochastic fluctuations in gene expression, even for noisy promoters[228].

Molecular memory and history effects

Cell-to-cell variability is not only influenced by spontaneous fluctuations inside a cell, but also by its history, including that of its (immediate) ancestors[122,168]. The molecular composition of a newborn cell is determined by that of its mother at division. The inheritance of molecules from their ancestor cell gives microorganisms a 'molecular memory' that can confer a fitness advantage[31,104,122]. Once again, the *lac* operon in *E. coli* has proven to be an excellent model to demonstrate this effect. *E. coli* cells that passed the expression threshold of *lac* permease (*lacY*) in the past were more likely to commit to phenotype switching upon reinduction after several generations of growth in the absence of *lacY* induction[31,104]. In the absence of an inducer, no new *lacY* proteins are produced; the existing proteins dilute by volume growth and are partitioned into daughter cells. Due to the long lifetime of *lacY*, in comparison with the generation time, the *lacY* levels decrease only slowly

over several generations. Cells that have been repeatedly induced will commit faster to growth on lactose than cells whose ancestors did not express *lacY* in their recent history.

A similar history dependence has been observed during cell fate decisions by *B. subtilis*. Cells are primed for differentiation to a new phenotypic state several generations before they actually commit to it[109,134]. Alternatively, they can maintain a phenotypic state for a pre-determined period of time[140].

The phenomenon of molecular memory is not isolated to bacteria. Recent studies indicate that the ability of yeast cells to respond to nutrient changes depends on past nutrient availability, several generations earlier. This was found during repeated switches between glucose and galactose[193]. The underling mechanism involved the inheritance of cytoplasmic proteins and particular chromatin modifications[193].

With this universal mechanism of 'passive transmission' of stable molecules from mother to daughter in mind, it is not difficult to envision that cell-cycle and environment-independent (long-term) oscillations in gene expression or metabolism will have an effect on phenotypic heterogeneity[150,30,197,135]. While these oscillations can introduce synchrony amongst cells of an extant population[30,197], cells born in different phases of the oscillations will show variations in their molecular makeup and likely react differently to environmental cues due to their distinct phenotypic state.

Box 1: Molecular stochasticity
Quantification of stochasticity: the noise measure Noise measures the magnitude of cell-to-cell variability. For an isogenic population it quantifies the dispersion (relative width) of the distribution of measured cellular characteristics as $\frac{var}{m^2}$ with var as variance and m as mean of those measured values. Since variances of independent events are additive, variance is used rather than standard deviation. To get an idea: a system with constant synthesis and first-order degradation, i.e. $\xrightarrow{k_s} X \xrightarrow{k_d n_X}$, gives as steady-state noise for the number of protein X, n_X: $\frac{m}{var^2} = \frac{1}{m} = \frac{k_d}{k_s}$, indicating that noise is high when molecule copy numbers are low. The noise measure we refer to in the text is defined at a particular moment in time (called static noise).
Transcription stochasticity and bursts The copy numbers of transcription factors, genes and mRNA are generally low in microbial cells, transcription stochasticity is therefore significant. Since mRNAs are synthesised when the promoter is in its 'ON state', two time scales exit in mRNA dynamics; waiting times for consecutive mRNA synthesis events and for OFF to ON transition events. When this time scale separation is pronounced, the gene is defined as 'bursty': then during the ON state mRNA is produced and degraded and during the OFF state it is only degraded, leading to much greater noise than when mRNA would be produced at a constant rate.
Promoter design Promoter design influences noise in mRNA and protein numbers[73,186,21,182,222]. Different designs affect the sizes and frequencies of transcription bursts, due to, for instance, fluctuations in TF (un)binding and DNA looping[65,78]. In yeast, the precise sequence and structural properties of the TATA-box influence noise[73,21,103].
Chromatin effects in higher eukaryotes As chromatin reorganisation is a slow step involved in gene activity switching, tightly packed regions of the chromosome exhibit more noisy expression[137]. Genes under the control of nucleosome-free promoters are expected to exhibit lower (Poissonian) noise[171,179].
Noise in protein copy numbers and network design The extent to which fluctuations in mRNA levels are propagated to protein levels, and thus potentially lead to phenotypic diversification, is largely determined by mRNA translation efficiency and the ribosome binding site[146] or particular mRNA codons[63]. While fluctuations in mRNA levels are typically fast, and average out during the cell cycle, fluctuations in protein levels are slower and can persist over several generations[168]. The number of transcription binding sites in the promoter region also affects noise[198,182]. The noise in transcription factor numbers can propagate to the expression of their target genes[158]. Regulatory motifs, for example a negative feedback, can attenuate noise or shift it to different components of the regulatory network[7,24,15,189]. The noise characteristics of a gene sometimes reflect the dynamics of its modulators[130].

Persister cells: a case study for the fitness consequences of chance events

The previous sections considered examples of phenotypic diversification upon changes in nutrient availability. In the context of nutrient shifts, it is often not clear whether sub-populations emerge as part of a fitness-enhancing strategy or whether a fraction of the population maladapts. While theoretical arguments are often offered to support claims that phenotypic heterogeneity improves

the adaptive flexibility (which is implied to be fitness enhancing) of cell populations, experimental demonstrations are limited in scope and difficult to generalize. In the paragraphs that follow, we consider the phenomenon of bacterial persistence, which is an example of non-genetic phenotypic heterogeneity that confers a fitness enhancement.

The role of stochasticity in persister cell formation

Isogenic populations of bacteria can contain sub-populations of cells that are slow-growing and generally highly tolerant to antibiotics and other stresses (Fig. 2.4); these cells are called persisters[111,209]. Their formation appears to be a survival mechanism that protects the population from extinction, when sudden harsh conditions occur. Most often, but not exclusively, these antibiotic tolerant sub-populations are formed via a mechanism called stochastic-phenotype-switching[120,10]. This is a spontaneous process that occurs even during exponential growth and is a prime example of stochastic adaptation[141]. Due to continuous switching a sub-population of persister cells is always maintained. Persisters can, however, also be formed via responsive adaptation; i.e. in response to particular environmental conditions such as stresses[148], nutrient transitions[4,162,95] and at the onset of the stationary phase, when at least one nutrient is depleted[144].

That persister cells are slow-growing does not fully explain why they are less susceptible to antibiotics, not even to antibiotics that directly influence growth processes; since a faster growth rate can sometimes also reduce susceptibility[61]. Persistence is therefore explained by a distinct physiological state[162]. The physiology of persistent cells, so their degree of tolerance and the duration of their persistent state, is dependent on whether they have been formed during a nutrient transition, removal or depletion[57]. For example, persister cells formed during a nutrient transition show a different response to antibiotics than tolerant cells formed upon a removal of a nutrient[162]. The size of these persister sub-populations can vary greatly with conditions[120,10,4,162,95], ranging from about 1 in a million under conditions of fast, steady-state exponential growth[10], to almost the entire population switching to this state in response to certain nutrient transitions[95]. While the molecular details of the mechanisms behind persister formation differ, stochasticity plays a central role.

Stochasticity and persister formation during steady-state exponential growth

The role of stochasticity in persister formation is best understood during steady-state, exponential growth[120,10]. The 'alarmone' molecule (p)ppGpp plays a central role herein. It is a key control molecule in *E. coli* that tunes the bacterium's physiology as a function of growth rate[119]. When it is high in concentration, (p)ppGpp inhibits growth processes and activates general stress and stationary-phase systems. At fast exponential growth, i.e. on rich or mineral media supplemented with glucose, the concentration of (p)ppGpp is generally low. However, when (p)ppGpp-fluctuations occur in a cell under these conditions, concentrations can spontaneously rise to a threshold level and induce a non-growing state. A self-perpetuating positive feedback mechanism then 'locks' this cell in the persister state, via the activation of toxin/antitoxin systems (TA)[120,51]. In this manner, growing and non-growing cells can stably co-exist in an environment that supports fast growth. Thus, at exponential growth, cells switch into the persister phenotype by chance; their conversion back is also likely a chance event, but this is less well understood.

TA-systems play a central role in the spontaneous formation of persisters during exponential growth and in the adaptive response to stress conditions. The design of TA-systems allows for the co-existence of a non-growing fraction in an exponentially growing population. The HipA toxin and HipB antitoxin for example, are both constitutively expressed, generally in a balanced manner. When the ratio of HipA toxin to HipB antitoxin exceeds a certain threshold, be it through a random

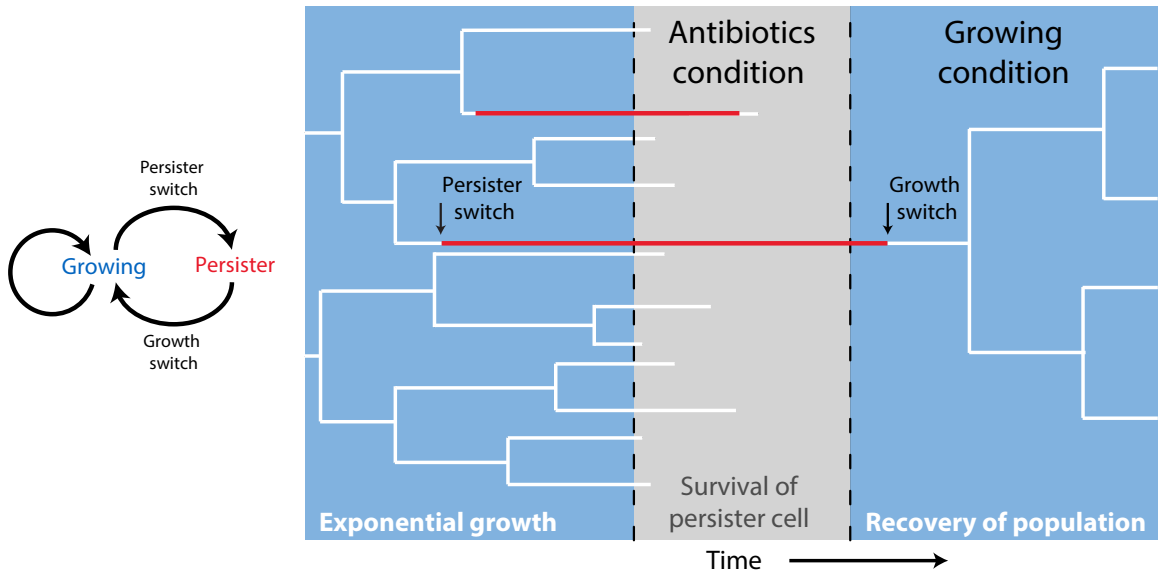

Figure 2.4: **The fitness advantage of spontaneous formation of persister cells during steady-state exponential growth.** Persister cells can form spontaneously under constant conditions of steady-state exponential-growth, conferring a fitness advantage when a sudden extinction-threatening condition occurs, such as an antibiotic[10,120]. Normally growing cells, or persisters that switch back to a growing state, will likely succumb to the effects of the antibiotic.

or regulatory event, persistent cells are formed[169]. Evolutionary tuning of transcriptional regulation, protein stability or toxin/antitoxin interactions[176] could therefore affect the probability of whether a particular cell exceeds the threshold. In turn, changes in the fraction of persisters and their lifetimes, can be fitness increasing or decreasing, depending on the environmental dynamics. As a consequence, the probability for spontaneous persister formation itself is expected to be evolvable. In fact, antibiotic resistant strains are known to sometimes carry *hipAB* mutations[93], and experiments have indeed shown that evolution can shape system properties to match the antibiotic treatment pattern[55].

Stochasticity and persister formation during nutrient transitions

Nutrient transitions can lead to the appearance of phenotypically distinct sub-populations[205,95,190] (see previous section), often distinguishable as growing and non- (or slow) growing fractions. Heinemann and colleagues[95,162] found that non-growing sub-populations of *E. coli*, which appear after transitions from glucose to gluconeogenic substrates (e.g. acetate or fumarate), exhibited increased antibiotic tolerance with characteristics similar to the persister phenotype. They found elevated levels of (p)ppGpp and activation of TA systems upon a nutrient shift, indicating that the mechanism of persister formation during exponential growth and upon nutrient transitions are related. Tolerant cells formed upon nutrient removal are however more susceptible to an antibiotic treatment than those formed during a nutrient transition, as their low catabolic capacity cannot match the ATP-maintenance requirements. They do have in common that the RpoS-mediated generalised stress response is activated, likely triggered by elevated levels of (p)ppGpp. Radzikowski *et al.*[162] concluded that persister formation is induced by a strong deviation from metabolic homoeostasis upon a change in nutrient availability, such that synthesis of new proteins required for new catabolic activity cannot be realised. Instead, cells take a less 'risky' strategy and invest into stress response and cellular maintenance, which is apparently less costly and leaves the metabolic state of the cells intact. The metabolic origin of this persistence state was underscored by demonstrating that persister cells quickly resuscitated upon re-addition of glucose.

How persister formation relates to a trade-off between instantaneous and long-term fitness

An increase in the heterogeneity of key molecules in stress response systems (e.g. TA-system) can improve single-cell fitness and as a consequence, population survival. Even though several aspects of the cellular stress response indicate that it is optimised for speed, such as the constitutive expression of toxin/antitoxin systems to ensure rapid growth arrest when needed, there is still an adaptation time. Sudden extinction-threatening conditions are therefore likely beyond the capacity of responsive systems. Here, the continuous formation of persister cells, via stochastic, reversible phenotype switching provides a solution, as a sub-population of stress-tolerant cells renders the population always prepared for sudden adverse conditions. However, this readiness comes with a trade-off. It reduces the instantaneous fitness of the population; the non- or slow-growing sub-population of persister cells will only make a small contribution to the generation of new cells. Evolution therefore plays an important role here: via tuning of the switching kinetics this trade-off can be optimised[59,101,115,104,200,47].

Other examples of phenotypic heterogeneity with fitness consequences

Persister sub-population formation provides an example of how molecular stochasticity can be fitness enhancing. A major challenge in single-cell studies is to figure out whether, and under which conditions, phenotypic heterogeneity has fitness consequences. Clearly demonstrating that it impacts fitness is not trivial. A few other examples exist, however, that show how heterogeneity affects a population's adaptive capacity. These examples include the ability to invade a new niche, better preparation for changes in a current niche, and the ability to deal with extinction-threatening conditions.

A clear model that illustrates how noisy expression can expand or open up new niches was given by Ackermann *et al*[2]. They showed how the heterogeneous expression of virulence factors by *Salmonella typhimurium* leads to two distinct sub-populations: one that ultimately sacrifices itself so that the other can invade a new environment. In this scenario, a phenomenon called self-destructive cooperation involves a small phenotypically distinct sub-population that, through expression of a particular virulence factor, can trigger an inflammatory response in the gut. This results in both the elimination of intestinal microflora and the sub-population itself, but in doing so removes competitors and allows the remaining *S. typhimurium* population to invade.

An example of phenotypic heterogeneity leading to better preparedness in changing environments is provided by the finding that the galactose regulatory pathway is activated in a fraction of the cell population of *S. cerevisiae*, hours before glucose is fully consumed[208]. This strategy reflects the trade-off between the cost of being prepared, in terms of growth rate and unnecessary enzyme expression, and the ability to make a fast switch as a population. In contrast to the previous example, this does not necessarily involve any change of niche. However, once there is competition for resources with other species within the same niche, making a fast switch has a clear fitness advantage.

Heterogeneous gene expression can also affect fitness negatively, as demonstrated by Deris *et al*.[45] in a study on antibiotic resistant *E. coli* strains. They show how molecular fluctuations underlie a bistability, via global feedback between growth and gene expression, producing sub-populations with reduced expression of proteins that protect against antibiotic action. In this case, an isogenic population of antibiotic resistant individuals diversify into growing (resistant) and non-growing (sensitive) sub-populations for a range of drug concentrations. This is a clearly an example where chance leads to phenotypic heterogeneity that reduces, rather than enhances, the fitness of a population.

Most likely the best understood example of how molecular noise can improve cellular fitness by improving the functioning of a molecular circuit is bacterial chemotaxis. This is one of the few systems in molecular biology for which we have a mechanistic understanding of its functional systemic properties (i.e. tumble-bias and adaptation time) and we can study how these properties affect *E. coli*'s fitness[54,212]. The functional properties of the chemotactic circuit are very sensitive to the concentration of its proteins, which fluctuate. For instance, the tumble bias is a determinant of the distance that *E. coli* travels and protein fluctuations cause isogenic cells to vary in their travelled distances[212]. This cell-varying foraging behaviour is advantageous when conditions change, e.g. from a steep to a shallow nutrient gradient. Noise in tumble bias then ensures that some cells search for food in small areas while others cover longer distances. In this case, phenotypic heterogeneity enhances the fitness of the genotype.

That fluctuations in phenotypic behaviour can be fitness enhancing and evolvable is illustrated by Beaumont et al[14]. They showed that subjecting *Pseudomonas fluorescens* to a switching environment led to the evolution of a bet-hedging genotype, which switched randomly between phenotypes.

Emerging concepts in the study of phenotypic adaptation

We have discussed examples of adaptation strategies of microorganisms when they are confronted with particular environmental dynamics. We emphasised the fitness effects of chance events. Some species adapt purely by chance, via stochastic phenotypic diversification[141], in order to prepare for future conditions. In this strategy, the size and lifetimes of the resulting sub-populations co-determine fitness[59,18,47]. Adaptation is more deterministic when sensing-response mechanisms are used. In these strategies, phenotypic diversification is undesired. Noise still plays a role in the variability in the magnitude and timing of the response[178]. Which adaptation strategy is best can be decided through an analysis of its fitness effects, in experiments[1,115,104] and theory[102,167,218,203,212,102]. We consider this an important research direction that may ultimately lead to a comprehensive theory of microbial phenotypic adaptation mechanisms and strategies.

The evaluation of the fitness of a particular adaptation strategy involves at least two descriptions. One is systemic, and ideally involves measuring the one-dimensional fitness value, by challenging a microbial population with specific changing conditions[1,115,104,10,205,190]. The other is the characterisation of the molecular mechanisms for adaptation, including the stochasticity of its dynamics in single cells, to assess cell-to-cell variability in adaptivity, including maladaptation and phenotypic diversification[120,205,1]. With theory and experimental studies of carefully-chosen mutant strains, the fitness effects of the strategy can be assessed.

Figuring out the fitness contribution of stochasticity to an adaptation strategy is a complex problem. It dates back to earlier studies in population genetics[25] and several innovative studies have recently been carried out that address this using a combination of experiments and theory[222,1,115,104,190]. One complicating aspect is that stochasticity is an inevitable consequence of molecular and cellular processes[153,168] and that it is therefore often questionable to what extent its magnitude has evolved[226]. And, even if stochasticity is fitness contributing, this will likely be so only in particular environments, and we generally do not know the evolutionary history of microorganisms. Exploratory theory and simulations[59,18,47,167,101] can then help in sharpening our thoughts and intuitions, and suggest informative experiments that could further reveal the surprisingly diverse roles of stochasticity in microbial fitness[1,115,104,10,205,190].

Several constraints that shape phenotypic adaptation by microorganisms have recently been identified. Firstly, the allocation of finite biosynthetic resources has proven to be an important limit that constrains the protein expression profile of microorganisms[87,180,77]. The molecular circuits in a cell that are responsible for different tasks, such as catabolism, anabolism and stress-systems, com-

pete for limited biosynthetic and cellular resources, such as transcription and translation machinery, cytoplasmic and membrane space[219,128]. Since many reaction rates depend linearly on enzyme concentrations, higher enzyme concentrations are generally advantageous for cellular processes, enforcing resource competition[19]. A second emerging constraint is that cells turn out to have limited phenotypic plasticity and sensing capabilities. Cells simply do not have all the circuits required for growth and survival in particular environments encoded on their genome; they may simply lack certain metabolic pathways. Nonetheless, the metabolic plasticity of some microorganisms is truly amazing. *E. coli* for instance, is expected to grow on hundreds of carbon sources[165]. Even though it has this latent capacity, it lacks sensors for the majority of the nutrients it can in principle grow on; *E. coli* i.e. does not have hundreds of carbon sensors[92]. This could partially explain why *E. coli* shows a limited capacity to restore growth when carbon sources are suddenly changed, where some cells fail to initiate growth[95]. On the other hand, some cells are capable of switching, indicating that metabolism does have the capacity to restore growth on new carbon sources, but this is dependent on a cell-state dependent mechanism that is partially understood[162]. Limited membrane capacity[128] and the reduction of growth rate, when protein are produced that are not directly needed,[180] may drive microorganisms towards reducing their sensing capacities. Finally, many constraints exist that prevent a cell from tracking its environment. Molecular noise in sensing, transcription and translation circuitry is an obvious effect that causes isogenic cells to grow differently in the same environment[85]. Another reason why perfect environmental tracking is impossible, is that protein synthesis is costly[180]. In short-lived environmental states the benefits from newly expressed proteins can not be reaped to recover the investment costs of biosynthetic resources, leading to a net fitness loss[104]. The lag time, associated with cellular responses, limits the number of offspring cells can make during a transition to a new condition, especially when it is of a short duration[104]. Sometimes responding fast, or even anticipating some environmental transitions[141], can have big fitness advantages.

Concluding remarks

During the last decade it has become clear that non-genetic heterogeneity pervades all aspects of biology. It has prompted a re-evaluation of the way we think about many cellular phenomena, including our views on microbial fitness and adaptation. In this review, we discussed many mechanisms that are now known, or thought, to generate non-genetic variability. However, their biological role is not always fully understood. For example, despite numerous studies on molecular and cellular stochasticity (both experimental and theoretical) only a handful have managed to demonstrate clear effects on fitness. It is often unclear how much of the observed cell-to-cell molecular variability serves a biological function, and how much of it simply reflects the robustness (or lack thereof) of the underlying molecular circuits. Related to this unknown is an important practical question: to what extent can these cellular stochastic phenomena be artificially manipulated? While, non-genetic phenotypic heterogeneity is fascinating from an evolutionary perspective, randomness and unpredictability is often undesirable in biotechnological or biomedical settings, where it can significantly impact culture performance or treatment efficacies. If it is simply biochemical limitations that cause much of the variability we observe, then it may be difficult to override or steer. On the other hand, if a noise source has been tuned by selective pressures, it seems reasonable to expect that engineered alterations are possible. In this regard, theoretical approaches, combined with synthetic molecular biology, will be pivotal in untangling the complex relationship that exists between stochastic molecular and cellular processes and the phenotypic characteristics of individual cells.

Chapter 3

Effects of growth rate and promoter activity on single-cell protein expression

Niclas Nordholt, Johan H. van Heerden, Remco Kort, Frank J. Bruggeman

Abstract

Protein expression in a single cell depends on its global physiological state. Moreover, genetically-identical cells exhibit variability (noise) in protein expression, arising from the stochastic nature of biochemical processes, cell growth and division. While it is well understood how cellular growth rate influences mean protein expression, little is known about the relationship between growth rate and noise in protein expression. Here we quantify this relationship in *Bacillus subtilis* by a novel combination of experiments and theory. We measure the effects of promoter activity and growth rate on the expression of a fluorescent protein in single cells. We disentangle the observed protein expression noise into protein-specific and systemic contributions, using theory and variance decomposition. We find that noise in protein expression depends solely on mean expression levels, regardless of whether expression is set by promoter activity or growth rate, and that noise increases linearly with growth rate. Our results can aid studies of (synthetic) gene circuits of single cells and their condition dependence.

Introduction

The phenotypic state of a cell is largely determined by its repertoire of expressed proteins. Protein concentration, and its variation across isogenic cells, is dependent on various systemic and protein-specific factors. Protein expression depends for instance on the availability of transcriptional and translational machinery, which is growth-rate dependent and considered part of a 'global-feedback' mechanism[44,180,84,134,87,89,112]. In addition, it depends on protein-specific properties such as regulatory promoter-sequences, the quality of the ribosome binding site and the stability of transcripts and proteins[98,63].

Global feedback on protein expression also has important consequences for the physiology of single cells[181]. Fluctuations in global regulatory mechanisms can for instance lead to phenotypic diversification of populations of isogenic cells[207]. They can cause the co-existence of a stress-sensitive, growing subpopulation and a stress-resistant, hardly-growing subpopulation of 'persister' cells[120]. Fluctuations in protein concentration and the growth rate of single cells turn out to have a reverberating relation[85]. Stochasticity is therefore an important aspect of protein expression and the phenotype of a single cell.

Single, isogenic cells vary in protein expression[49,146] because of systemic and protein-specific stochastic processes[194,69,152,177]. Since cell volume and protein content double during the cell cycle, the average number of (constitutively) expressed transcripts and proteins scales with cell volume during balanced cell growth[81]. Spontaneous fluctuations in reaction rates (e.g. transcription and translation), asymmetric division and uneven protein partitioning during cell division cause individual cells to deviate from this average behaviour[168,76,177]. Copy-number and volume scaling causes the heterogeneity in protein copy number, across isogenic cells, to be higher than the heterogeneity in protein concentration[177,81].

Many noise sources are systemic and contribute to extrinsic noise[69,194]. Intrinsic noise, in contrast, refers to protein and gene-specific noise sources such as promoter activity, noise propagation from transcriptional regulators, and degradation of transcripts and proteins[146,168,158]. Net protein-expression fluctuations result from extrinsic and intrinsic factors, making noise of protein-expression time and cell-state dependent[60,178,168]. Understanding protein expression in single cells therefore requires methods for quantification of the contributions of independent noise factors[168,194,49,69,177].

The relationship between protein expression noise and the mean protein expression level, in populations of isogenic cells, turns out be very similar across microbial species and growth conditions. Protein expression noise, defined by the ratio of the variance of protein expression and its squared mean value, decreases with the mean expression level until a constant noise floor is reached[196,137,222]. This noise floor is generally attributed to systemic, extrinsic noise, but its origins are not fully understood. Data suggest that fluctuations in the concentrations of transcription and translation machinery, or translational burst size, may be involved[224,9,41]. This noise-vs-mean scaling is found regardless of whether protein expression is quantified as total fluorescence per cell, molecule copy number or concentration[196,137,222].

Growth rate is an important determinant of protein expression in single cells, influencing intrinsic as well as extrinsic factors. While we understand its influence on the mean protein concentration[71,89], via protein dilution, which is species independent, its influences on the stochasticity of protein expression is however much less explored. A complicating phenomenon is that many microbial cells adjust their transcription and translation machinery with growth rate[89], and the extent to which this compensates for protein dilution and influences protein expression noise is not well understood, and likely species dependent.

In this study, we exploited a titratable, constitutively-expressed, fluorescent reporter protein to

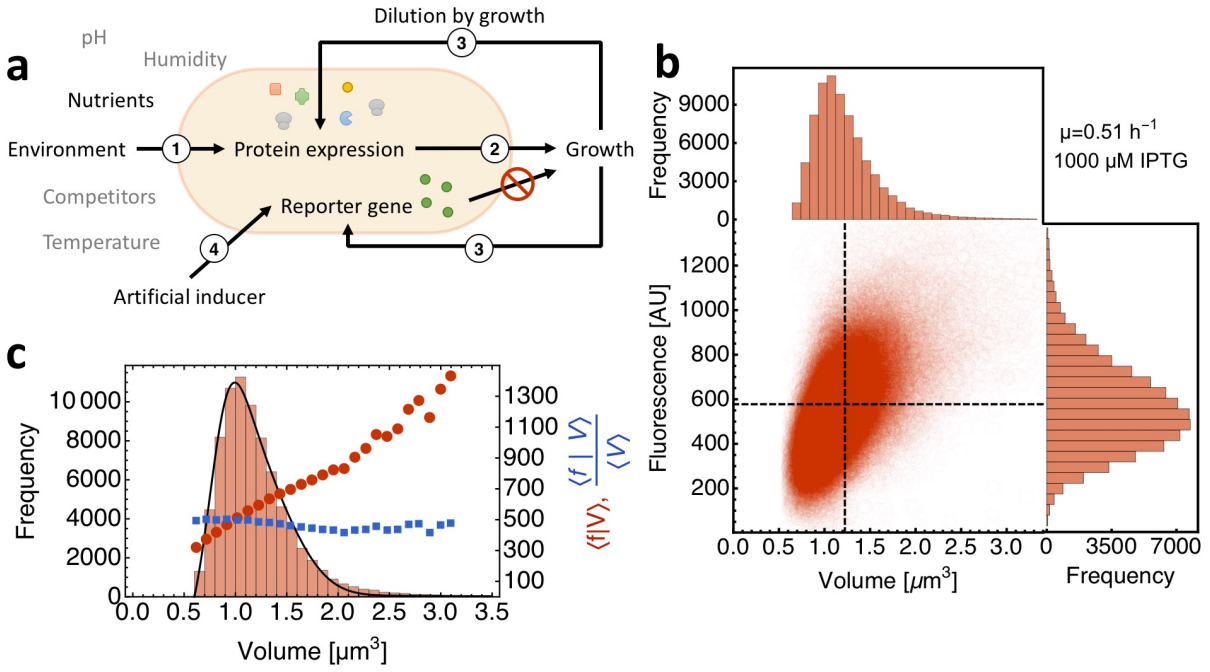

Figure 3.1: **Quantification of the independent effects of growth rate and promoter activity on single-cell protein expression. a.** Protein expression in a single cell is set by various factors indicated by the numbered arrows. The environment and cellular control circuits influence protein expression via their influences on transcriptional and translational rates (1). If the protein contributes to growth it exerts an effect on growth rate (2). The resulting physiological state of the cell feeds back onto protein expression (3) via for instance dilution by volume-growth. Usage of a non-catalytic protein allows for the quantification of growth feedback on protein expression (4). **b.** Flow cytometric quantification of single-cell protein expression. For each cell, we measured its total fluorescence and its scatter values, from which we inferred its volume using a cross-calibration of the Coulter counter and the flow cytometer (Figure S13, details can be found in the 'Materials and methods'). These data give rise to a distribution of total cell fluorescence, cell volumes and fluorescence concentration, which is analysed in this paper. **c.** Relationship between the volume, fluorescence and fluorescence concentration of a cell. During balanced growth, cell fluorescence is proportional to volume (red), such that the fluorescence concentration (blue) remains constant across the population and over time. The black line is a fit according to the equation derived by Collins & Richmond[34] to describe the extant volume distribution of exponentially growing cells.

investigate the role of growth rate and promoter activity on protein expression and its cell-to-cell variability, using the bacterium *Bacillus subtilis* as our model organism. Such a protein is very suitable for studying effects of growth rate on protein expression in single cells, as it does not have a catalytic activity that influences growth rate. It serves as a reporter for growth rate effects on protein expression if the promoter activity is monitored at constant transcription inducer concentration and variable growth rates. A comparison of protein expression in single cells at constant growth rate and at variable transcription inducer concentrations shows the effects of promoter activity.

We analyse single-cell fluorescence data, obtained with flow cytometry, within a theoretical framework of protein expression under conditions of balanced growth. In balanced growth, attributes of a whole population such as population volume, biomass and total protein increase at the same rate; as a consequence, the distributions of properties of individual cells, such as cell size and protein concentration, become time invariant[52]. Combining theory and noise decomposition, we disentangle the protein expression noise that we observed in our experiments into contributions from extrinsic, systemic and intrinsic, protein-specific sources. The theory we present is not limited to bacteria, but is applicable to any organism that exhibits balanced cell growth.

Results

Influences of promoter activity and growth rate on single-cell protein expression

In order to separate influences of growth rate and promoter activity on protein expression, we introduced the gene encoding green fluorescent protein (GFP), under control of the synthetic isopropyl -D-thiogalactoside (IPTG) inducible hyper-spank promoter,[225,161] into the genome of *B. subtilis*. Since the fluorescent reporter protein does not exert any catalytic activity that impacts cell physiology, it does not influence growth rate, as long as its protein burden remains negligible. Our data show no evidence for a burden (Figure S1, in the Supplementary Information). Therefore, we have effectively cut the bidirectional influence between the expression of catalytic protein and growth rate; such that only the unidirectional relation from growth rate to protein expression remains (Figure 3.1a).

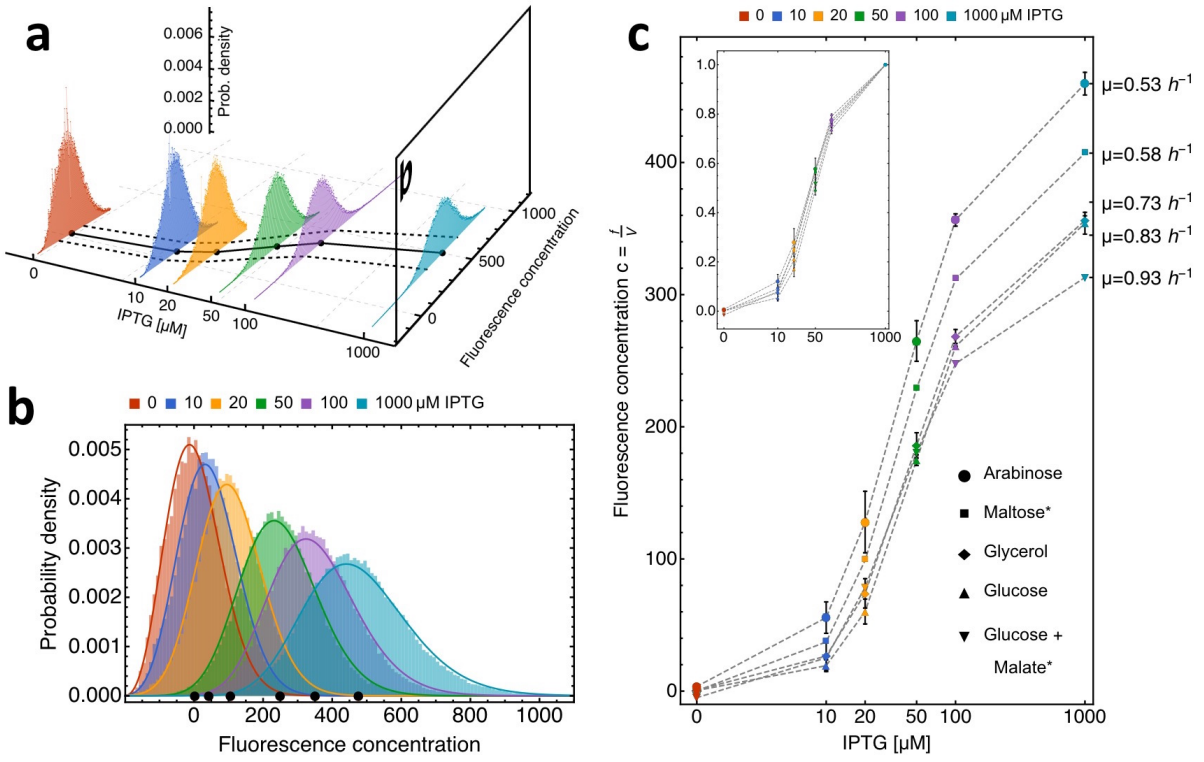

Figure 3.2: **Protein expression is increased by enhanced promoter activity and reduced by enhanced growth rates. a.** The distribution of GFP-fluorescence concentration across a population of isogenic *B. subtilis* cells, during growth on arabinose (growth rate $\mu \approx 0.5\ h^{-1}$), as function of the IPTG concentration. The dots indicate mean expression, the line corresponds to the dose-response curve and the dashed lines indicate the mean $\pm$ std, indicating cell-to-cell variability. **b.** The distribution of GFP-fluorescence concentration across a population of isogenic *B. subtilis* cells, during growth on arabinose at different IPTG concentration, indicated by the colour of the distributions. Black dots indicate mean values, as in Figure a. Distributions are fitted with gamma distributions (solid lines). **c.** The mean GFP fluorescence concentration as function of the IPTG concentration at 5 different growth rates, achieved with different carbon sources added to the growth medium. All data points represent the average of two biological replicates, with the exception of maltose and glucose+malate (*), which represent single experiments. Error bars show the standard error of the mean (SEM) of biological replicates. The growth rates indicated on the right side represent the average growth rate for growth on the respective carbon source. The inset shows fluorescence concentration normalised to full induction as function of IPTG, indicating that growth rate influences all protein expression values in the same manner.

With the genetically-engineered strain we quantified protein expression at balanced growth and modulated growth rate and promoter activity in an independent manner. The growth rate was varied by changing the carbon source in the growth medium. Promoter activity was varied with the IPTG concentration (note: in the text we use promoter activity and IPTG concentration as interchangeable

terms). We used flow cytometry to quantify population growth rate, cell volume and the total fluorescence per cell.

Fluorescence per cell and cell volume each follow a positively skewed distribution as described earlier[34,196] (Figures 3.1b and c). Total fluorescence increases in proportion to cell volume (Figure 3.1b). Fluorescence concentration is independent of cell size (Figure 3.1c). Both relations are in agreement with the notion that cells grow balanced[52]. (In the inset of Figure 3.2c, we normalise the induction curves to their maximal values; they nearly overlap, but not fully, we return to this effect below when we discuss the relation between protein synthesis rate and growth rate.) Other indications of balanced growth are that the number of cells, population volume and fluorescence increased at the same rate for several generation times (Figures S2-S9, in the Supplementary Information). As a result, protein expression (fluorescence concentration) achieved a steady state, for a period longer than several generation times (Figure S10, in the Supplementary Information). All data that we analyse below correspond to this period of balanced growth.

The influences of growth rate and promoter activity on protein expression are shown in the plots of Figure 3.2. As a representative example, data for growth on arabinose (Figures 3.2a and b) show that mean protein expression, expressed in fluorescence concentration, increases with the IPTG concentration and that individual cells show variable protein expression. The measured distributions of fluorescence concentration (Figure 3.2b) and fluorescence per cell (see Figure S11, in the Supplementary Information) fit well to gamma distributions, which is in agreement with earlier findings.[146,27,56,33] The relation between protein expression and the IPTG concentration is sigmoidal for all carbon sources (Figure 3.2c) and protein expression is reduced at higher growth rates. The promoter we used proved very sensitive in a range from 10 to 50 μM IPTG. Within the range of IPTG concentrations used, we observed a maximal induction of 8- to 17-fold, depending on the growth rate. Half-maximal induction was reached around 50 to 70 μM IPTG in all cases. In the absence of IPTG, we did not detect (leaky) expression from the inserted promoter. With increasing induction the fluorescence concentration distributions get wider (Figure 3.2 b); we discuss this effect below. Additionally, our data show that the mean cell volume increased with the cellular growth rate (see Figure S1), which is in agreement with earlier findings[195].

We note that the simultaneous measurement of the volume (calculated from scatter, see Materials and methods) and fluorescence values per cell allows us to quantify protein expression either in total units fluorescence per cell or in fluorescence concentration per cell. These two different units we shall exploit in the decomposition of protein expression noise.

Enhanced protein dilution by volume-growth at higher growth rate reduces the mean protein concentration

Our data show that both the growth rate and the IPTG concentration influence protein expression during balanced growth (Figure 3.2c). The effect of growth rate becomes apparent when one compares protein expression at fixed IPTG concentrations. A higher growth rate reduces protein expression. To understand this effect it is instructive to consider the balance for the protein concentration,

$$\frac{dc}{dt} = k(i,\mu) - \mu c, \tag{3.1}$$

with c as the protein concentration, μ as the growth-rate and k as the protein synthesis rate, which is dependent on the IPTG concentration, i, and possibly also on growth rate – hence the notation $k(i,\mu)$. Here we consider dilution by volume-growth as the only process that reduces the protein concentration. This is warranted because the GFP which we used is highly stable and not subject to proteolysis[156].

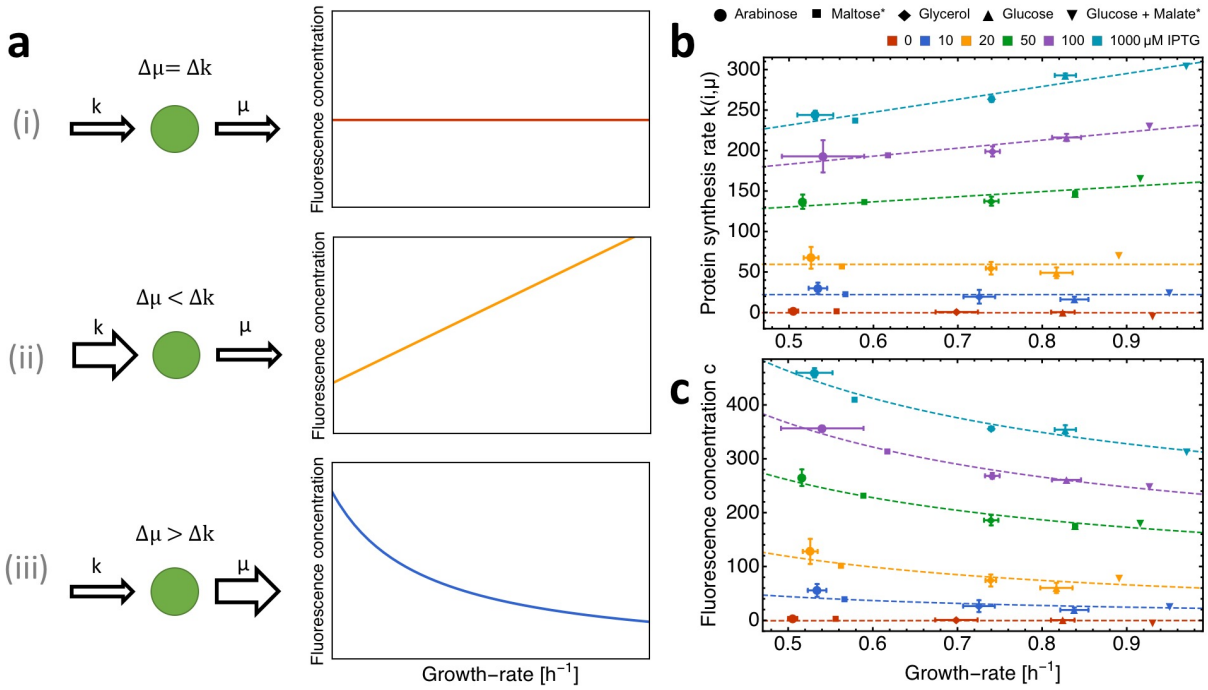

Figure 3.3: **Reduced protein expression by dilution by growth is partially compensated for by enhanced protein synthesis rate at higher growth rates. a.** Three scenarios can be distinguished for the response of protein synthesis rate to an enhanced growth rate: i. perfect compensation, ii. overcompensation and iii. undercompensation. **b.** Protein synthesis rate k is invariant to growth rate at low IPTG concentrations and increases linearly with growth rate at intermediate to high IPTG concentrations. **c.** The change in protein concentration as function of growth rate is dominated by dilution by growth. At IPTG concentrations above 50 μM, an increased protein synthesis rate partially compensates dilution by growth. Dashed lines, model predictions from equation 3.1 using fitted linear functions for k. Data points are either single experiments or the average of two biological replicates. Error bars show the standard error of the mean (SEM) of biological replicates. All individual experimental data points can be found in Figure S15 in the Supplementary Information.

The protein synthesis rate k corresponds to the effective rate of all processes from transcription to the mature protein, many of these are known to increase, to varying degrees, with growth rate[89,44]. Since we carry out all experiments at balanced growth, the protein concentration is at steady state: $\frac{dc}{dt} = 0$. We can therefore calculate the protein synthesis rate, by rearranging equation 3.1, from the product of the growth rate and fluorescence concentration value.

We distinguish three scenarios of the scaling of the protein concentration with growth (Figure 3.3a): i. perfect compensation (k changes in proportion to μ), ii. overcompensation (k changes exceed those of growth rate), and iii. undercompensation (k changes are smaller than those of growth rate).

Figure 3.3b shows the relation between the inferred protein synthesis rate k and the growth rate. While at low induction levels k is invariant to growth rate, k increased with growth rate at IPTG concentrations above 50 μM (Figure 3.3b). For an 87% increase in growth rate, we observed an increase of around 20% in protein synthesis rate at full induction.

With the $k(i, \mu)$ values from figure 3.3b (using the dashed, fit-lines) we can calculate the relation between the fluorescence concentration and growth rate (dashed line in figure 3.3c). The resulting relation agrees very well with the measured data. Figure 3.3c indicates that fluorescence concentration generally decreases with growth rate, indicating that changes in k are smaller than those of growth rate (Figure 3.3a, scenario iii). At induction levels above 50 μM, the increase in protein synthesis with growth rate alleviates dilution by growth (figure 3.3b), but cannot fully compensate for it, resulting in a net decrease in fluorescence concentration.

We therefore conclude that the relation between mean protein expression (in fluorescence concentration units) with growth rate indicates the undercompensation scenario (mode iii in figure 3.3a).

Effects of promoter activity and growth rate on protein expression noise are indistinguishable

We quantified the cell-to-cell variability in protein expression, in order to understand how growth rate and promoter activity influence it. To do so, we used the noise measure[152,49,146]. It is defined as the variance in protein expression over the squared mean protein expression. It equals the squared coefficient of variation, and quantifies the relative width of the distribution of protein expression across cells. Larger values indicate higher cell-to-cell variability in protein expression. The advantage of using the noise measure, rather than the coefficient of variation, is that variance of independent random variables is additive, which we will exploit below.

We denote the variance and mean of a random variable X, with values x, by $\langle \delta^2 x \rangle_X$ and $\langle x \rangle_X$, respectively; the subscript denotes that we averaged over all values of X. The noise value can be calculated from the ratio $\frac{\langle \delta^2 x \rangle_X}{\langle x \rangle_X^2}$. In Figure 3.4a, we plot the relation between the noise in the total cell fluorescence as function of the mean total cell fluorescence values, across growth conditions and promoter activities (i.e. IPTG concentrations), as indicated by different symbols and colours, respectively. Regardless of whether protein expression was changed by growth rate or promoter activities, all data points fall on an invariant noise-vs-mean relation. This characteristic relation holds also for protein concentration (Figure 3.4c).

In order to understand how systemic and gene-specific effects contribute to protein expression noise, we decompose the noise in independent terms. We shall the denote the mean and variance of X values at a particular constant value y of another random variable Y as $\langle x|y \rangle_X$ and $\langle \delta^2 x|y \rangle_X$, respectively. It can now be shown (see SI) that the total variance in X equals the sum of two variance contributions: $\langle \langle \delta^2 x|y \rangle_X \rangle_Y$ and $\langle \delta^2 \langle x|y \rangle_X \rangle_Y$. The term $\langle \langle \delta^2 x|y \rangle_X \rangle_Y$ equals the total 'intrinsic' contribution. It quantifies the changes in X values that occur independently of changes

in Y values, i.e. changes in x at constant Y values. The total 'extrinsic' contribution $\langle \delta^2 \langle x|y \rangle_X \rangle_Y$ quantifies the changes in X values due to changes in Y values. In the equations below we omit the subscript notation to simplify the notation. For a visual representation of the law of total variance that we exploit here see Fig. S12 in the Supplementary Information.

In Figure 3.4b, we decompose the noise in total cell fluorescence into its intrinsic and extrinsic components. The extrinsic component quantifies the variation in fluorescence due to the variation in cell volume, since at balanced growth the fluorescence of a cell is proportional to its volume (see Supplementary Information and Figure 3.1c), which is captured by the relation $\langle f|V \rangle = \langle c \rangle V$, with $\langle c \rangle$ as the mean fluorescence concentration per cell. A consequence is that the noise in total cell fluorescence, generated by a fluorescent protein that is constitutively expressed, equals

$$\frac{\langle \delta^2 f \rangle}{\langle f \rangle^2} = \underbrace{\frac{\langle \langle \delta^2 f|V \rangle \rangle}{\langle f \rangle^2}}_{\text{Intrinsic noise}} + \underbrace{\frac{\langle \delta^2 \langle f|V \rangle \rangle}{\langle f \rangle^2}}_{\substack{\text{Volume noise} \\ = \langle \delta^2 V \rangle / \langle V \rangle^2}} \tag{3.2}$$

The derivation of this equation can be found in the Supplementary Information.

We note that our interpretation of extrinsic and intrinsic noise is different from that of others (e.g.[49,194,69]). The mathematical procedure is the same, but we condition the protein expression values on cell volume data (which was also done in Kempe, et al.[81]); most other current work does not do this. We choose for this approach, because we are interested in the origins of noise in protein concentration, whether is either due to variation in cell volume (a systemic, extrinsic effect) or due to variation in protein copy numbers (a gene specific, intrinsic effect). This means that our intrinsic and extrinsic noise values cannot be directly compared to those obtained by, for instance, Elowitz et al.[49].

Our intrinsic noise term captures variations in protein expression that cause deviations from the balanced-growth relation $\langle f|V \rangle = \langle c \rangle V$. Those are stochastic fluctuations that have biochemical and cellular origins. It includes noise sources such as asynchronous activities of biochemical synthesising and degradation reactions, propagation of reaction noise by fluctuating effector molecules and uneven partitioning of molecules during cell division. The intrinsic noise term decreased with the mean total cell fluorescence (Figure 3.4b) until a noise floor is reached at high mean concentrations[196,222]. This noise floor is thought to arise from sources of noise that do not directly scale with volume, such as fluctuations in the concentration of transcription and translation machinery[224,41]. The reduction of intrinsic noise with the mean fluorescence level follows $\frac{\langle \langle \delta^2 f|V \rangle \rangle}{\langle f \rangle^2} = \frac{a}{\langle f \rangle} + b$ (those are the dashed lines in figure 3.4b). In principle, transcription or translation bursts can occur, contributing to the a or b values, but we cannot decide from our data whether this is the case; this would require knowledge of the true total-cell protein copy number rather than total-cell protein fluorescence.

The extrinsic noise term equals volume noise at balanced growth (see the Supplementary Information). It is determined by cellular heterogeneity in volume. It results from differences in cell cycle progression (cells double their volume on average during a cell cycle), asymmetric division of mother cells, variability in interdivision times, noise in cellular growth rate as function of the cell cycle and other processes. The extrinsic noise term is independent of the mean total cell fluorescence (Figure 3.4b), indicating that cell volume noise is hardly changing across growth conditions and promoter activity. This is likely explained by the constant variation in cell volume from birth to division (a factor 2), a constant noise of mother and daughter volumes, and a constant dependency of mean cell volume on cell-age (cell-cycle progression)[81].

According to us, intrinsic noise in fluorescence concentration is an informative measure about functional heterogeneity in isogenic cells. Since cells with the same protein concentration will experience the same biochemical influence of this protein. Those cells are therefore identical

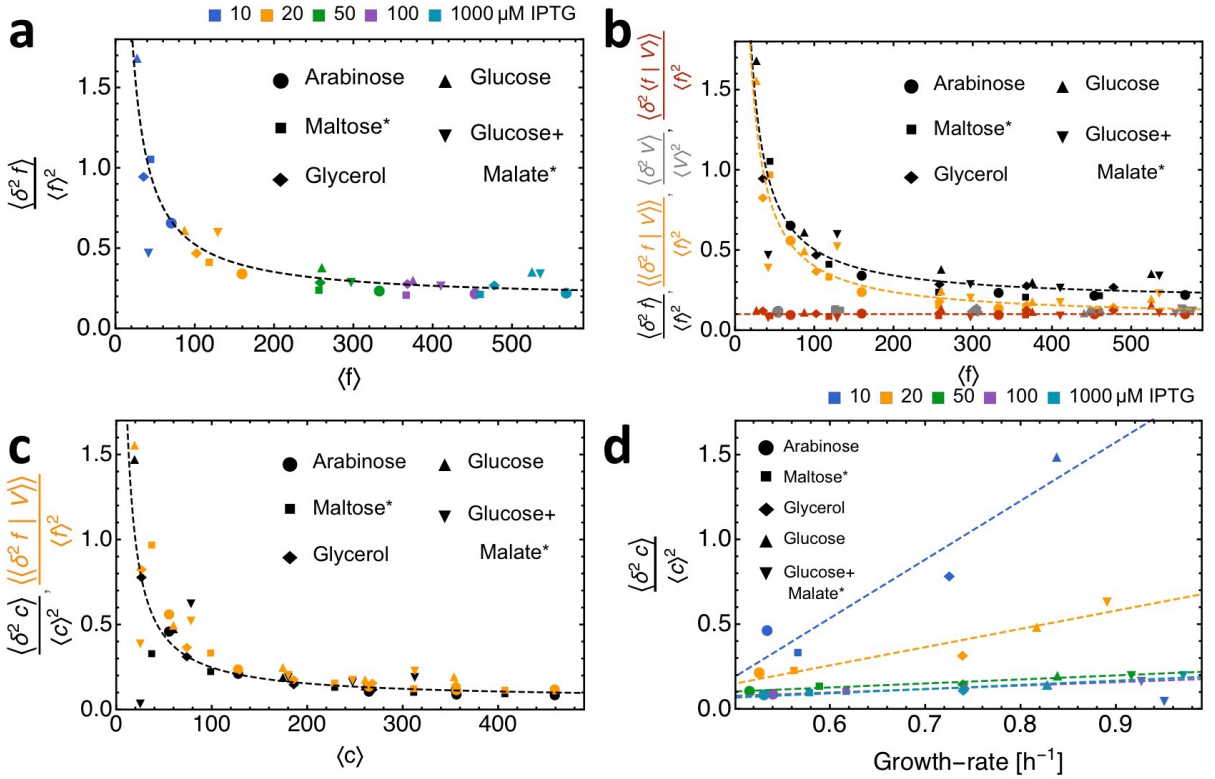

Figure 3.4: **Effects of promoter activity and growth rate on noise are indistinguishable and fall on an invariant relation between noise and mean of protein expression. a.** Noise in total cell fluorescence as function of mean total cell fluorescence across growth rates and promoter activities. **b.** Decomposition of noise in total cell fluorescence into its intrinsic, 'biochemical' contribution, $\frac{\langle\langle \delta^2 f|V\rangle\rangle}{\langle f\rangle^2}$, and its extrinsic, 'volume-variation' contribution, $\frac{\langle \delta^2\langle f|V\rangle\rangle}{\langle f\rangle^2}$. At balanced growth $\frac{\langle \delta^2\langle f|V\rangle\rangle}{\langle f\rangle^2} = \frac{\langle \delta^2 V\rangle}{\langle V\rangle^2}$, indicating that fluorescence variation scales with volume variation per cell, which is indeed evident from our experimental data. **c.** Noise in fluorescence concentration per cell is shown as function of the mean concentration. At balanced growth, the following equality holds $\frac{\langle \delta^2 c\rangle}{\langle c\rangle^2} = \frac{\langle\langle \delta^2 c|V\rangle\rangle}{\langle c\rangle^2} = \frac{\langle\langle \delta^2 f|V\rangle\rangle}{\langle f\rangle^2}$, which indicates that protein expression noise due to biochemical origins is directly captured by noise in fluorescence concentration. (a-c) Dashed lines are fits of the form $\frac{\langle \delta^2 x\rangle}{\langle x\rangle^2} = \frac{a}{\langle x\rangle} + b$. **d.** Dependence of noise in fluorescence concentration on the cellular growth rate at different magnitudes of promoter activity. The changes in fluorescence concentration noise can be explained by the decreasing mean expression, through dilution by volume-growth. Dashed lines are linear fits to guide the eye. For each carbon source, data points from 10 to 1000 μM IPTG are shown. Carbon sources with asterisks indicate single experiments, all other data points are the average of two biological replicates. Plots with all individual replicates are shown in Figure S16, in the Supplementary Information.

with respect to the functional, or physiological, consequences of this protein. Noise in protein concentration is therefore very informative about the functional noise across isogenic cells.

At balanced growth, noise in fluorescence concentration, intrinsic noise in total cell fluorescence and fluorescence concentration are all identical in value (see Supplementary Information).

$$\frac{\langle \delta^2 c \rangle}{\langle c \rangle^2} = \frac{\langle \langle \delta^2 c | V \rangle \rangle}{\langle c \rangle^2} = \frac{\langle \langle \delta^2 f | V \rangle \rangle}{\langle f \rangle^2} := \text{ functional noise in protein expression} \tag{3.3}$$

The relation between noise in fluorescence concentration and the mean fluorescence concentration is shown in Figure 3.4c. Regardless of how the mean protein expression was varied, via the growth rate or promoter activity, its relation to the noise in protein expression remains unaffected, most noticeably at high mean expression values. At low mean expression levels (low induction levels) we find deviations from the relation. One likely explanation for this is that at low induction levels, noise in transcript copy numbers propagates to protein copy numbers[152]. At low induction levels, a higher growth rate increases the noise because: i. a higher rate of division reduces mean transcript levels and increase transcript noise and ii. more frequent transcript partitioning at cell division also increases transcript noise. The effect of growth rate on protein expression noise diminishes at higher induction levels because noise propagation from transcription to translation decreases.

To identify the relation between functional noise in protein expression and cellular growth rate, we plot fluorescence concentration versus growth rate (Figure 3.4d). The individual lines relate noise values at constant promoter activity and therefore indicate the effect of growth rate. We see that noise increases linearly with growth rate, regardless of promoter activity. This is explained by the effect of an enhanced growth rate on the mean protein expression, as this is decreased via enhanced concentration dilution by volume-growth. At low induction levels the deviation from the linear relation is largest because of the effects discussed in the previous paragraph.

Discussion

The magnitude of protein expression in a single cell depends on promoter activity and cellular growth rate, which are both environment-dependent. The growth rate effect is systemic and affects all cellular proteins, whereas promoter activity effects are protein specific. Promoter activity directly tunes transcription rate, resulting in an altered protein synthesis rate. Growth rate has two opposing effects on protein expression. It can reduce it, via protein dilution due to cell volume-growth, and it can increase expression, as the translation machinery often increases in abundance with growth rate. The net outcomes of promoter activity and growth rate variation on protein expression are therefore not self evident. Their joint effect on cell-to-cell variation in protein expression is even harder to predict. In this paper, we performed experiments to quantify those effects.

We found that promoter activity had the expected effect on protein expression, with a sigmoidal dependence of protein expression on the concentration of the promoter-activity regulator, IPTG. We quantified the dual effect of growth rate on protein expression, i.e. its effect on protein synthesis and degradation, by measuring mean protein expression and cellular growth rate and their product equals protein synthesis rate (when growth is balanced). Mean protein expression decreased as function of growth rate, indicating that protein dilution dominates over growth-rate effects on protein synthesis. Conversely, protein accumulates at lower growth rates, indicating a mechanism of 'passive regulation', which was shown recently for the sporulation response in *B. subtilis*[134]. At high expression levels we found that protein synthesis increased with growth rate, which partially compensates for protein dilution.

A striking result is that the relation between the noise and mean of protein expression is nearly independent of how protein expression was changed and regardless of which unit for protein

expression is taken, total fluorescence per cell or fluorescence concentration per cell (Figure 3.4a and c). At low mean expression levels we observe deviations from this relation; likely due to propagation of transcription and cell-division noise. Promoter activity and growth rate effects therefore fall predominantly on the same noise-vs-mean relation. In addition, noise decreases with mean expression levels and extrapolating the relation suggests the existence of a noise floor at expression levels that are higher than those we measured, which is in agreement with other studies[222,137,196]. Our data, obtained with a single fluorescent protein, are therefore in agreement with other, broader studies.

Various studies have found that protein expression noise decreases as function of the mean expression level until a noise floor is hit[222,137,196]; see Sanchez & Golding for a recent review.[173] This 'universal' noise-vs-mean relation has been found for a large set of genes. Part of its underlying mechanism must therefore be gene/promoter-sequence independent, often referred to systemic, extrinsic noise.[173] Our data follows the universal relation (Figure 3.4b and c). We find it both for total cell fluorescence and fluorescence concentration, which indicates that protein expression noise, when corrected for cell-volume variation (an extrinsic noise component), retains a noise floor. Other extrinsic noise terms, such as fluctuations in transcription and translational machinery, also play a role in the setting the noise floor. This contributes for about 50% in our data (compare Figure 3.4b and c, at the maximal fluorescence and concentration values).

A novel insight from our work is that the effects of growth rate and promoter activity on the mean and noise of protein expression are indistinguishable. From the relation between mean and noise that we observe in figure 3.4a we can speculate that in bacteria, noise in constitutive protein expression increases with growth rate because it causes a reduction of mean expression by way of increasing protein dilution by volume-growth. As the noise-vs-mean relation appears universal (see above), we expect the growth rate effect to be universal as well. This statement is not limited to constitutive proteins, since also proteins that have a growth-rate dependent promoter-activity will have fallen on the noise-vs-mean relation. Regulated genes are, however, expected to have elevated noise levels, due to noise propagation from noisy regulators which can be present at low copy numbers. More experimental studies are required to test our expectations.

We illustrate that the units of protein expression, whether expressed in total fluorescence per cell or fluorescence concentration per cell, matter for the quantification of functional noise – noise that has a phenotypic consequence. Noise in concentration captures functional noise[81]. Since noise in total cell fluorescence contains a contribution from the variation of cell volume, its correction for volume noise reveals functional noise, which is illustrated by equation 3.2 (valid in balanced growth). Our experimental data are in accordance with those equalities (Figure 3.4c). Besides indicating how functional noise can be obtained from single-cell fluorescence data, it also provides a consistency check of the fluorescence and cell-volume data.

The consequences of this work are two-fold. From a fundamental perspective this paper indicates that cellular regulation of protein expression, via promoter activity or growth rate influences, impacts protein expression noise via their effect on mean protein expression. As a result, noise of protein expression decreases with growth rate because it reduces mean protein expression. This effect could facilitate phenotypic diversification even under optimal conditions, where growth rates are high. From a practical point of view, our work has consequences for the design of synthetic circuits composed out of multiple proteins. Synthetic circuit function is likely to be condition dependent, due to cellular growth rate effects.

Methods

Strains and medium composition

For growth experiments, prototrophic *Bacillus subtilis* strain BSB1[138] was cultivated in a defined morphilinopropanesulphonic acid (MOPS) - buffered minimal medium (MM) containing: 40 mM MOPS (adjusted to pH 7.4), 2 mM potassium phosphate (pH 7.0), 15 mM $(NH_4)_2SO_4$, 811 μM $MgSO_4$, 80 nM $MnCl_2$, 5 μM $FeCl_3$, 10 nM $ZnCl_2$, 30 nM $CoCl_2$ and 10 nM $CuSO_4$[160]. The medium was supplemented with different carbon sources to the following final concentrations: 5 mM glucose, 10 mM glycerol, 6 mM arabinose, 2.5 mM maltose, 3.75 mM malate and 2.5 mM glucose. From a 1 M stock solution of isopropyl β-D-1-thiogalactopyranoside (IPTG) an appropriate amount was added to the medium to reach a final concentration of 0, 10, 20, 50, 100 or 1000 μM.

Escherichia coli strain JM109 (Promega) was used for cloning and amplification of plasmids. For cloning, *E. coli* and *Bacillus subtilis* were grown in LB + 0.5% w/v glucose supplemented with the appropriate antibiotic in the following concentrations: ampicillin, 100 μg/ml; spectinomycin 150 μg/ml. For LB plates, 1.5% w/v agar were added prior to autoclaving.
Plasmid pDR111-N015-superfolderGFP was constructed by amplifying the coding sequence of superfolderGFP (sfGFP) by PCR with primers N015 (ggtggtgctagcaggaggtgatccagtatgtctaaaggtgaagaactg) and N017 (ggtggtgcatgcttatttgtagagctcatccat), digestion of the product and backbone pDR111[126] (*bla amyE' spc*^{R} $P_{hyperspank}$ *lacI 'amyE*; kind gift from David Rudner) with NheI and SphI and subsequent ligation. After transformation of chemocompetent *Escherichia coli* JM109 (Promega) and plasmid isolation, the identity of pDR111-N015-sfGFP was confirmed by sequencing. *Bacillus subtilis* strain B15 (BSB1 *spc*^{R} $P_{hyper-spank}$*-sfGFP lacI::amyE*) was constructed as following: pDR111-N015-sfGFP was linearised with SacII, added to a BSB1 culture grown in MM+glucose until starvation phase, and incubated for one hour before addition of fresh MM and plating on LB+glucose+spc for selection. Genomic insertion into *amyE* was confirmed by amylase deficiency, PCR and sequencing. The *amyE* locus is situated at $\approx$ 28 degrees on the genome. We address the influence of the maturation time of the used fluorescent protein in the SI.

Growth experiments

Cells were inoculated directly from single-use 15% glycerol stocks into 50 ml Greiner tubes with 5 ml MM supplemented with IPTG and grown at 37 degrees Celcius and 200 rpm. After 10 to 15 generations, the cultures reached an OD between 0.01 and 0.2 and were diluted in 250 ml Erlenmeyer flasks with 50 ml fresh, pre-warmed MM with IPTG to an OD of 0.0001 to 0.0003 and growth was monitored at least twice per generation. At each time-point, 500 μl of culture were sampled into 2 ml eppendorf tubes and immediately subjected to flow cytometry. For each experiment, the wild type BSB1 culture was taken along under the same conditions as the B15 cultures to correct for autofluorescence and control for effects of IPTG or GFP expression on cell growth.

Balanced growth criterium

In each experiment, we monitored population volume, fluorescence and cell count for several hours and calculated the specific growth rate for each of these properties (Figures S2-S9). In balanced growth, extensive attributes such as population volume and fluorescence as well as cell number increase exponentially at the same rate, resulting in concentration homeostasis of GFP[52]. For all analyses, we defined a region of at least 1.5 generation times in which fluorescence concentration was most stable (Figure S10, in the Supplementary Information).

Flow cytometry

For all experiments, a BD Accuri C6 Flow Cytometer with the manufacturers software was used to acquire counts, fluorescence and light scattering properties of single cells in 20 μl of culture. The

software settings were as following: Fluidics, slow; Threshold, 15000 on FSC-H; Run with limits, 20 μl. Undiluted cultures were used up to a cell count of no more than 5000 events per second at which point the samples were diluted 1:10 in pre-warmed MM of the same batch. Fresh MM without cells was used as a background control. After each experiment, all data were exported in FCS format and analysed using MATHEMATICA, version 10 (Wolfram Research, Champaign, IL, USA).

Cross-calibration of forward scatter area and cell volume

Forward scatter correlates with volume[210]. Comparing the distributions of volume and forward scatter area (FSC-A) of a population of cells indicates a linear relationship between those two properties. To calculate volume from FSC-A, we performed calibration experiments with all 5 carbon sources, using a Beckman Coulter Multisizer 3 Coulter counter for volume determination. Per carbon source, BSB1 cells were grown as described in section 4. After propagation, cells were grown for 5 to 6 hours when samples were taken and subjected directly to flow cytometry or, after 1:200 dilution in 10 ml ISOTON diluent (Beckman Coulter), measured on the Multisizer 3. Dilutions for the Multisizer 3 were done in triplicates and run with identical settings. Bins were centred and counts per bin were averaged over the triplicates. As a sanity check and to control for dilution artefacts, we calculated the number of cells per μl from both data sets (Figure S13, in the Supplementary Information). To convert FSC-A to volume, we computed every other percentile in a range from the 2nd to the 98th of both, the volume and FSC-A distributions and fitted a linear function through them (Figure S13, in the Supplementary Information). The linear function was used to convert FSC-A to volume.

Data analysis

Data analysis was carried out in MATHEMATICA, version 10 (Wolfram Research, Champaign, IL, USA), using custom scripts. As a pre-filtering step, all events with an FSC-H $\leq$ 18000 and an FSC-A $\geq$ 150000 were discarded. The first filter was applied to exclude small particles such as cell debris, the second filter to exclude chains of cells and other measurement artefacts. From each file, the beginning time of acquisition was extracted and for each event, FSC-A was converted to volume [μm^3] and exported along with the GFP fluorescence channel area value (FL1-A; excitation 488 nm, emission 533 nm).

Calculation of cellular growth-rate

Growth-rates were calculated based on cell counts at each time point. Particle counts from medium-only samples were subtracted at each time point to correct for background, such as salt precipitate, in the medium. The background was low in all samples and didn't affect the calculated growth rate. The first and last time point of each experiment were excluded from analysis. Using the MATHEMATICA function LinearModelFit, a linear fit through the Log-transformed data was computed. The slope of this fit gives the specific growth rate μ in units [h^{-1}]. There were no differences in growth rate between BSB1 and B15 under the same conditions (Figure S13, in the Supplementary Information).

Correction for autofluorescence strength

Autofluorescence can contribute a significant amount to total fluorescence and mask actual GFP signals. Autofluorescence correlates with cell size under identical conditions (data not shown), so we chose a correction method based on cell size. All corrections described here were carried out for all individual carbon sources, IPTG concentrations and time points, using BSB1 wild type cultures that were taken along during all experiments.

Cells were binned by volume into fixed bins of width 0.2 μm^3 and the mean FL1-A was calculated for BSB1 wild type samples. This mean value was then subtracted from all single events in the

corresponding bin of the B15 sample. Bins with less than 20 cells in either of the samples were excluded from further analysis.

Correction for autofluorescence variance

The variance in background fluorescence can contribute significantly to variance in total fluorescence at low induction levels (Figure S14, in the Supplementary Information). This leads to a distortion of the noise measure at low mean fluorescence, such that an apparent scaling of noise with the variance over the mean squared can be observed (Figure S14, in the Supplementary Information). Correcting for this background variance reveals the inverse proportionality of noise to the mean that has been observed before [196,153,222].

To estimate the variance in background fluorescence, we corrected the BSB1 wild-type samples for autofluorescence as described above, effectively shifting their mean to 0. We then calculated the volume-conditional variances in fluorescence and fluorescence concentration (see section on noise in the Supplementary Information) at each time point and IPTG concentration in balanced growth and removed data points with the highest and lowest variance for each sample. In the following we make use of the law of total variance (refer to noise section in the Supplementary Information for details). For each carbon source, the mean variance of all time points and IPTG concentrations was used as an estimate for variance of background fluorescence $\langle \delta^2 f_{bg} \rangle = \langle \langle \delta^2 f_{bg} | V \rangle_f \rangle_V + \langle \delta^2 \langle f_{bg} | V \rangle_f \rangle_V$ or fluorescence concentration $\langle \delta^2 c_{bg} \rangle = \langle \langle \delta^2 c_{bg} | V \rangle_c \rangle_V + \langle \delta^2 \langle c_{bg} | V \rangle_c \rangle_V$. The variance in fluorescence or fluorescence concentration resulting from GFP was then simply calculated by subtracting $\langle \delta^2 f_{bg} \rangle$ and $\langle \delta^2 c_{bg} \rangle$ from $\langle \delta^2 f_{total} \rangle$ and $\langle \delta^2 c_{total} \rangle$, respectively.
For all subsequent analyses, the average of all time points from the region in which fluorescence concentration was stable in time was used (these points are shown in Figure S10).

Data availability

The datasets generated during the current study are available from the corresponding author on reasonable request.

Acknowledgements

J.v.H. and F.J.B. acknowledge funding by NWO-VIDI Project 864.11.011. N.N., R.K. and F.J.B. received funding from the European Union, Marie Curie ITN AMBER, 317338. We would like to thank C. van Boxtel for practical assistance with the cross calibration of the Coulter counter and the flow cytometer.

Author contributions statement

N.N., J.v.H., R.K. and F.J.B. conceived the experiments. N.N. and J.v.H. conducted the experiments. N.N., J.v.H. and F.J.B. analysed the results. All authors reviewed the manuscript.

Additional information

Competing financial interests

The authors declare no competing financial interests.

Appendix

Effects of fluorescent protein maturation time

To estimate the effect of fluorescent protein maturation time, we consider the following model,

$$\dot{n} = k_p - k_m n - \mu n \tag{3.4}$$
$$\dot{f} = k_m n - \mu f \tag{3.5}$$

with f and n as the fluorescent and nonfluorescent protein concentration, k_p as the protein synthesis rate, k_m as the rate constant for maturation and μ as growth rate. This system will reach a steady state with a fluorescent protein fraction $\phi = \frac{f}{n+f} = \frac{k_m}{k_m+\mu}$. The superfolder fluorescent protein which we used has a maturation time of about 10 minutes such that $k_m = 0.1\ min^{-1} = 6\ hr^{-1}$. Given the measured range of growth rates, 0.5-0.9 hr^{-1}, we obtain a range of steady state fractions of $0.87 \leq \phi \leq 0.92$. So we underoverestimate the actual concentration of the fluorescent protein by $\approx 10\%$.

Noise theory at balanced cell growth

Concentrations of constitutively expressed proteins remain constant during balanced growth

The rate of change in the concentration c of a molecule with copy number n in a cell with volume V equals

$$\frac{d}{dt}c = \frac{d}{dt}\frac{n}{V} = \frac{1}{V}\frac{d}{dt}n - \frac{n}{V^2}\frac{d}{dt}V \tag{3.6}$$

When this concentration is constant over time, the cell grows with a constant growth rate, as is indicated by the following relation,

$$\frac{1}{n}\frac{d}{dt}n = \frac{1}{V}\frac{d}{dt}V := \text{ exponential growth rate, } \mu \tag{3.7}$$

A protein that is therefore constitutively expressed (such that dn/dt is constant) shall at balanced growth, when $d\ln V/dt$ has become fixed for a duration longer than several generation times, display a constant concentration. Our experimental data indeed shows that this condition is met at balanced growth (see figure S10).
A consequence of this balanced growth condition is that at every cell volume the following relation holds, which is indeed in agreement with our experimental data,

$$\langle f|V\rangle = \langle c\rangle V \text{ and } \langle f\rangle = \langle c\rangle\langle V\rangle \tag{3.8}$$

with f as the total fluorescence per cell, which is proportional to the copy number of the fluorescent proteins that it contains.

Short introduction to variance decomposition

We shall first derive the variance decomposition equation. We consider two random variables X and Y, e.g. protein copy number and cell volume, that take on values denoted by x and y (both running from zero to infinity, in principle, and x's are discrete and the y's are continuous). We denote an average of a random variable X as $\langle x\rangle_X$ and its variance as $\langle\delta^2 x\rangle_X$ (the variance equals the mean squared deviation); the subscript denotes that we took an average over X's values, this is useful notation when we consider conditional means, which is what we do next.
We denote the average of a random variable y at a constant value of another (random) variable x – the mean of Y conditioned on a particular value of X – as $\langle y|x\rangle_Y$ and its variance as $\langle\delta^2 y|x\rangle_Y$.

We can rewrite the variance of Y in terms of two contributions using 'variance decomposition', giving rise to the 'law of total variance':

$$\begin{aligned}\langle\delta^2 y\rangle &= \langle y^2\rangle_Y - \langle y\rangle_Y^2 \\ &= \langle\langle y^2|x\rangle_Y\rangle_X - \langle\langle y|x\rangle_Y\rangle_X^2 \\ &= \langle\langle\delta^2 y|x\rangle_Y + \langle y|x\rangle_Y^2\rangle_X - \langle\langle y|x\rangle_Y\rangle_X^2 \\ &= \langle\langle\delta^2 y|x\rangle_Y\rangle_X + \langle\langle y|x\rangle_Y^2\rangle_X - \langle\langle y|x\rangle_Y\rangle_X^2 \\ &= \langle\langle\delta^2 y|x\rangle_Y\rangle_X + \langle\delta^2\langle y|x\rangle_Y\rangle_X. \end{aligned} \tag{3.9}$$

The first term in this equation is the intrinsic contribution and the second term equals the extrinsic contribution. The first term is called intrinsic because it concerns the total variation in Y values when X is constant, so those occurring independent of X; those are intrinsic to Y. Those changes in Y that are due to changes in X can captured by the second terms, those are extrinsic to Y.
Another way to think about variance decomposition is to consider the following relation, which states that y is a function of x plus a noise term that depends on x (visualised in Figure S12),

$$y(x) = f(x) + \epsilon\sigma(x) = \langle y|x\rangle + \underbrace{\epsilon\sqrt{\langle\delta^2 y|x\rangle}}_{\text{noise}},\ \epsilon \sim N(0,1), \tag{3.10}$$

with σ as a standard deviation and $N(0,1)$ as a normal distribution with mean 0 and standard deviation 1. We can determine the total variance in y from,

$$\begin{aligned}\langle\delta^2 y(x)\rangle = \langle\delta^2 y\rangle &= \langle\delta^2\langle y|x\rangle + \epsilon\sigma(x)\rangle \\ &= \langle\delta^2\langle y|x\rangle\rangle + \langle\delta^2\epsilon\sigma(x)\rangle \end{aligned} \tag{3.11}$$

The last term can be simplified further

$$\begin{aligned}\langle\delta^2\epsilon\sigma(x)\rangle &= \langle(\epsilon\sigma(x))^2\rangle - \langle\epsilon\sigma(x)\rangle^2 = \langle(\epsilon\sigma(x))^2\rangle - \langle\delta\epsilon\delta\sigma(x)\rangle - \langle\epsilon\rangle\langle\sigma(x)\rangle \\ &= \langle(\epsilon\sigma(x))^2\rangle = \langle\epsilon^2\sigma(x)^2\rangle \\ &= \langle\delta\epsilon^2\delta\sigma^2(x)\rangle + \langle\epsilon^2\rangle\langle\sigma^2(x)\rangle \\ &= 0 + (\langle\delta^2\epsilon\rangle + \langle\epsilon\rangle^2)\langle\sigma^2(x)\rangle \\ &= \langle\delta^2\epsilon\rangle\langle\sigma^2(x)\rangle = \langle\sigma^2(x)\rangle \\ &= \langle\langle\delta^2 y|x\rangle\rangle \end{aligned} \tag{3.12}$$

Therefore, equation 3.11 becomes,

$$\langle\delta^2 y\rangle = \langle\delta^2\langle y|x\rangle\rangle + \langle\langle\delta^2 y|x\rangle\rangle, \tag{3.13}$$

which is also the equation for variance decomposition (or the law of total variance).

Variance decomposition of noise in total cell fluorescence

The noise in total cell fluorescence is defined by the ratio of its variance and its squared mean value, i.e.

$$\frac{\langle\delta^2 f\rangle}{\langle f\rangle^2} \tag{3.14}$$

We can determine the role of heterogeneity in cell volume, e.g. due to cell growth, for instance to be able to assess noise in protein concentration later, using variance decomposition (the subscript indicates the random variable for which the mean or variance is calculated):

$$\frac{\langle\delta^2 f\rangle}{\langle f\rangle^2} = \frac{\langle\langle\delta^2 f|V\rangle_f\rangle_V}{\langle f\rangle^2} + \frac{\langle\delta^2\langle f|V\rangle_f\rangle_V}{\langle f\rangle^2} \tag{3.15}$$

Since $\langle f|V\rangle = \langle c\rangle V$ we can simplify $\langle\delta^2\langle f|V\rangle\rangle$ into

$$\langle\delta^2\langle f|V\rangle_f\rangle_V = \langle\delta^2\langle c\rangle V\rangle_V = \langle c\rangle^2\langle\delta^2 V\rangle_V \tag{3.16}$$

and since $\langle f\rangle = \langle c\rangle\langle V\rangle$ we can rewrite the noise term $\frac{\langle\delta^2\langle f|V\rangle\rangle}{\langle f\rangle^2}$ as

$$\frac{\langle\delta^2\langle f|V\rangle_f\rangle_V}{\langle f\rangle^2} = \frac{\langle\delta^2 V\rangle}{\langle V\rangle^2}, \tag{3.17}$$

which shows that the noise in total cell fluorescence due to cell growth equals the noise in cell volume. This is due to the fact that total cell fluorescence varies across cells with different volume, which is due to the different cell cycle progression stages of those cells and because the copy number of a constitutively expressed protein scales with cell volume at balanced growth.
Deviations from the dependency between fluorescence per cell, f, and cell volume, V, also occurring at balanced growth, also contribute to noise in total cell fluorescence. Those are quantified by the term,

$$\frac{\langle\langle\delta^2 f|V\rangle_f\rangle_V}{\langle f\rangle^2}, \tag{3.18}$$

which captures all remaining noise sources: biochemical reactions (e.g. transcription, translation, noise propagation in reaction networks), asymmetric cell division, uneven protein partitioning, etc.[177]. Variance decomposition can also be used to decompose this term further, as was shown in Schwabe & Bruggeman[177]. Note that only in the simplest cases, the Poisson relation holds that $\frac{\langle\langle\delta^2 f|V\rangle_f\rangle_V}{\langle f\rangle^2} \propto \frac{1}{\langle f\rangle}$.

Simplifying relations for noise in total cell fluorescence at balanced growth

Variance decomposition, with respect to cell volume, leads to the following equation for the noise in fluorescence concentration,

$$\frac{\langle\delta^2 c\rangle}{\langle c\rangle^2} = \frac{\langle\langle\delta^2 c|V\rangle_c\rangle_V}{\langle c\rangle^2} + \frac{\langle\delta^2\langle c|V\rangle_c\rangle_V}{\langle c\rangle^2}. \tag{3.19}$$

At balanced growth the simplification holds that

$$\langle c|V\rangle = \frac{\langle f|V\rangle}{V} = \frac{\langle c\rangle V}{V} = \langle c\rangle \;\Rightarrow\; \langle\delta^2\langle c|V\rangle_c\rangle_V = 0, \tag{3.20}$$

therefore, at balanced growth,

$$\frac{\langle\delta^2 c\rangle}{\langle c\rangle^2} = \frac{\langle\langle\delta^2 c|V\rangle_c\rangle_V}{\langle c\rangle^2}. \tag{3.21}$$

Noise in fluorescence concentration and its variance decomposition at balanced growth

The noise in a ratio of random variables, such as the concentration f/V, can be approximated by

$$\begin{aligned}\frac{\langle\delta^2 c\rangle}{\langle c\rangle^2} &= \frac{\langle\delta^2\frac{f}{V}\rangle}{\langle\frac{f}{V}\rangle^2} \approx \frac{\langle\delta^2 f\rangle}{\langle f\rangle^2} - 2\frac{\langle\delta f\delta V\rangle}{\langle f\rangle\langle V\rangle} + \frac{\langle\delta^2 V\rangle}{\langle V\rangle^2} \\ &= \frac{\langle\langle\delta^2 f|V\rangle_f\rangle_V}{\langle f\rangle^2} - 2\frac{\langle\delta f\delta V\rangle}{\langle f\rangle\langle V\rangle} + 2\frac{\langle\delta^2 V\rangle}{\langle V\rangle^2}\end{aligned} \tag{3.22}$$

The covariance between total cell fluorescence and cell volume $\langle\delta f\delta V\rangle$ can be simplified into, using $f|V = \langle c\rangle V + \epsilon(V)$ with $\epsilon(V) \sim N(0, \sqrt{\langle\delta^2 f|V\rangle})$,

$$\begin{aligned}\langle\delta f\delta V\rangle &= \langle(f - \langle f\rangle)(V - \langle V\rangle)\rangle = \langle(\langle c\rangle V + \epsilon(V) - \langle c\rangle\langle V\rangle)(V - \langle V\rangle)\rangle \\ &= \langle\langle c\rangle V^2 - \langle c\rangle V\langle V\rangle + \epsilon(V)V - \epsilon(V)\langle V\rangle - \langle c\rangle\langle V\rangle V + \langle c\rangle\langle V\rangle^2\rangle \\ &= \langle c\rangle\langle V^2\rangle - \langle c\rangle\langle V\rangle^2 + \langle\epsilon(V)V\rangle - \langle\epsilon(V)\rangle\langle V\rangle - \langle c\rangle\langle V\rangle^2 + \langle c\rangle\langle V\rangle^2 \\ &= \langle c\rangle\langle\delta^2 V\rangle + \langle\delta\epsilon(V)\delta V\rangle\end{aligned} \tag{3.23}$$

such that

$$\frac{\langle \delta f \delta V \rangle}{\langle f \rangle \langle V \rangle} = \frac{\langle c \rangle \langle \delta^2 V \rangle + \langle \delta \epsilon(V) \delta V \rangle}{\langle c \rangle \langle V \rangle^2} = \frac{\langle \delta^2 V \rangle}{\langle V \rangle^2} + \frac{\langle \delta \epsilon(V) \delta V \rangle}{\langle c \rangle \langle V \rangle^2}. \tag{3.24}$$

This simplifies equation 3.22 into

$$\frac{\langle \delta^2 c \rangle}{\langle c \rangle^2} = \frac{\langle \langle \delta^2 f | V \rangle_f \rangle_V}{\langle f \rangle^2} - 2 \frac{\langle \delta \epsilon(V) \delta V \rangle}{\langle c \rangle \langle V \rangle^2}. \tag{3.25}$$

A relation between noise in total cell fluorescence and fluorescence concentration

Therefore, if the noise in fluorescence at a fixed volume, $\epsilon(V)$, is volume independent, such that $\langle \delta \epsilon(V) \delta V \rangle = 0$, we obtain

$$\frac{\langle \delta^2 c \rangle}{\langle c \rangle^2} = \frac{\langle \langle \delta^2 f | V \rangle_f \rangle_V}{\langle f \rangle^2} = \frac{\langle \langle \delta^2 c | V \rangle_c \rangle_V}{\langle c \rangle^2} := \text{ protein-expression noise.} \tag{3.26}$$

This equation indicates why it is advantageous to focus on noise in fluorescence concentration, rather than on noise in total cell fluorescence, as it only captures the noise effects due to the biochemistry of the circuit and cellular processes such as asymmetric division and uneven protein partitioning. It is therefore independent of the heterogeneity in protein expression due to the fact that total cell fluorescence scales with volume, due to cell growth. The latter effect is captured by $\frac{\langle \delta^2 \langle f | V \rangle_f \rangle_V}{\langle f \rangle^2}$ and equals $\frac{\langle \delta^2 V \rangle}{\langle V \rangle^2}$ at balanced growth.

Supplementary figures

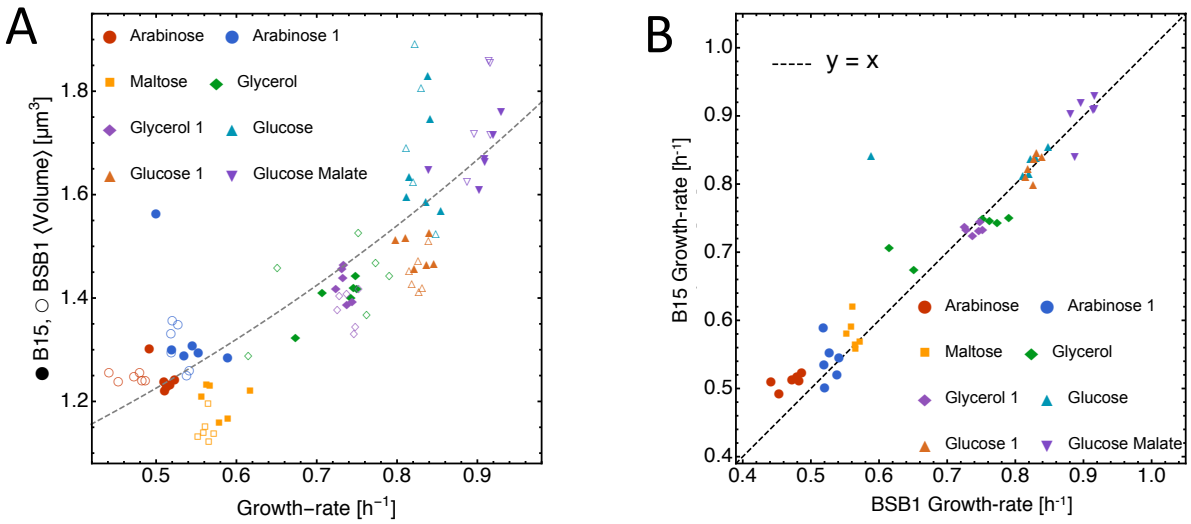

Figure S1: **Average cell volume increases with growth rate. Protein burden from GFP expression is negligible. A.** Average cell volume increases as function of growth rate. For each experiment, volumes were averaged over the range of balanced growth. Each data point represents a different IPTG concentration under a certain growth condition. Symbol shape indicates carbon source as indicated in the legend with numbers denoting biological replicates. Filled symbols, *B. subtilis* B15 with titratable GFP inserted in the *amyE* locus. Empty symbols, *B. subtilis* BSB1 wild-type. **B.** Growth rate of BSB1 wild-type and B15 GFP expressing mutant are plotted against each other. A decrease in growth rate due to protein burden from expressing GFP was not detected.

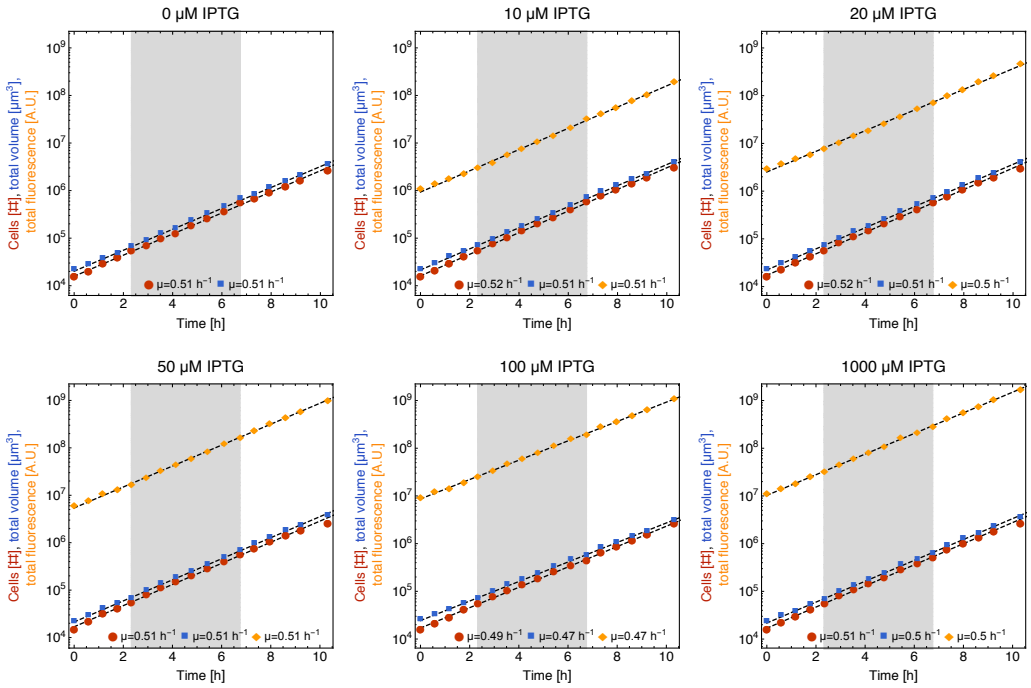

Figure S2: **Balanced growth of *B. subtilis* B15 on arabinose, sample A at different IPTG concentrations.** Population volume and -fluorescence increase at the same rate as cell numbers, indicating balanced growth. The dashed lines indicate linear fits whose slope equals the specific growth rate that is indicated at the bottom of the plot for each property (number of cells, population volume and - fluorescence). The grey background marks the region in which fluorescence concentration was most stable. Data points from this region where used for all analyses in this study. Capital letters (A,B) indicate biological replicates.

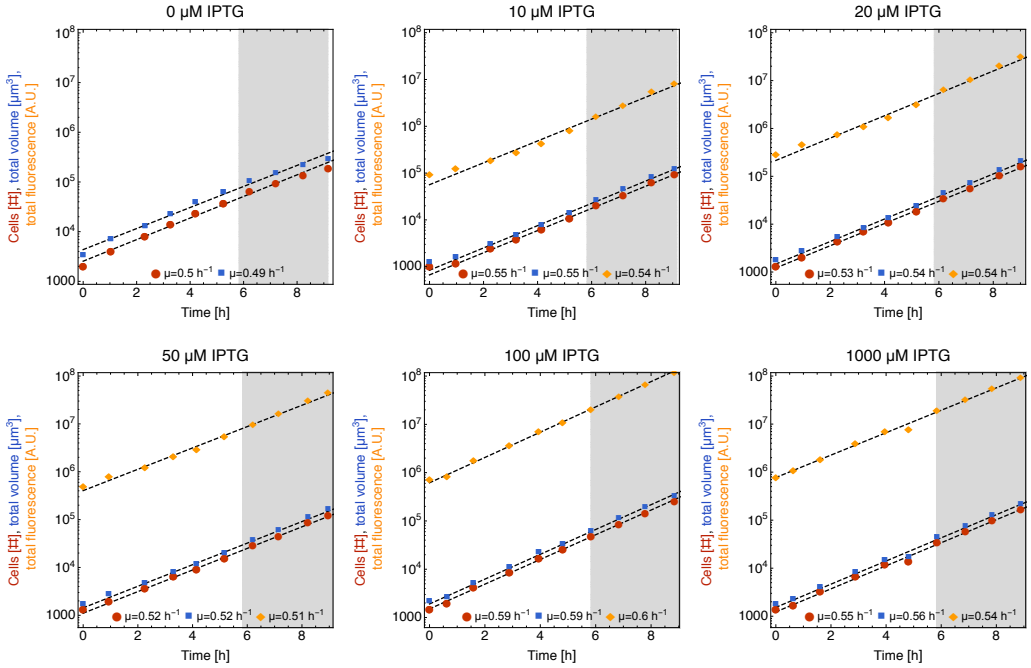

Figure S3: **Balanced growth of *B. subtilis* B15 on arabinose, sample B at different IPTG concentrations.** See figure S11 for further detail.

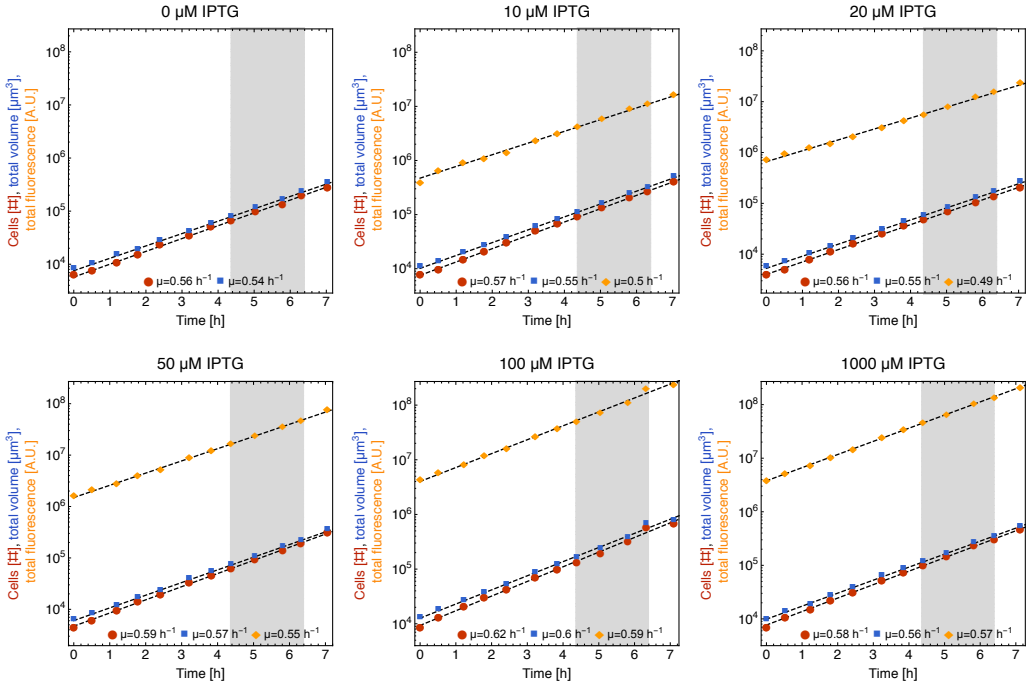

Figure S4: **Balanced growth of *B. subtilis* B15 on maltose at different IPTG concentrations.** See figure S11 for further detail.

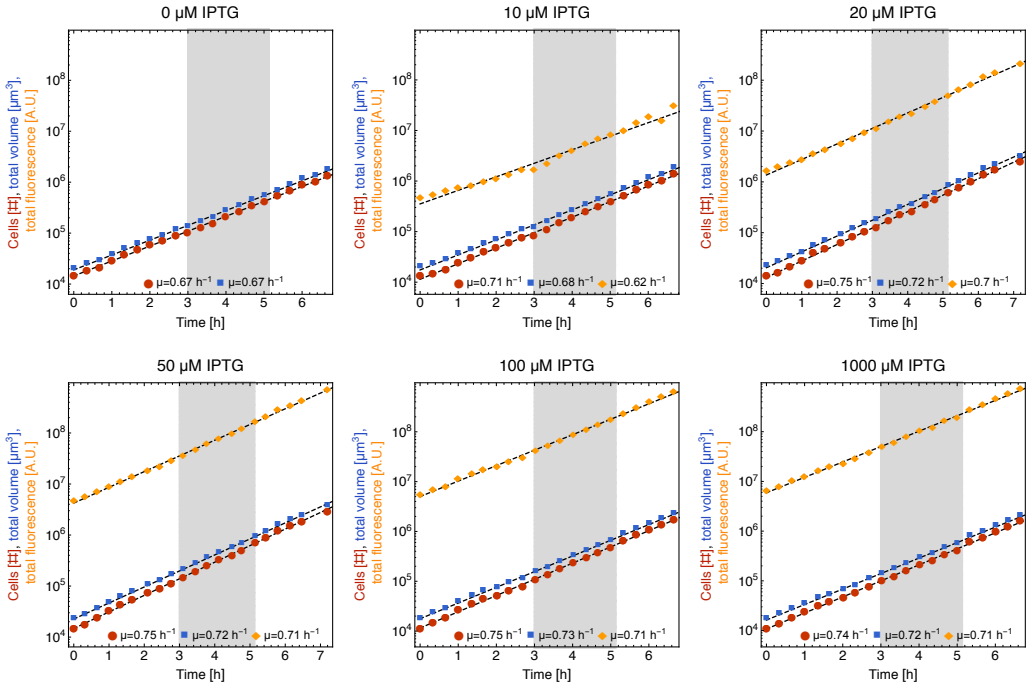

Figure S5: **Balanced growth of *B. subtilis* B15 on glycerol, sample A at different IPTG concentrations.** See figure S11 for further detail.

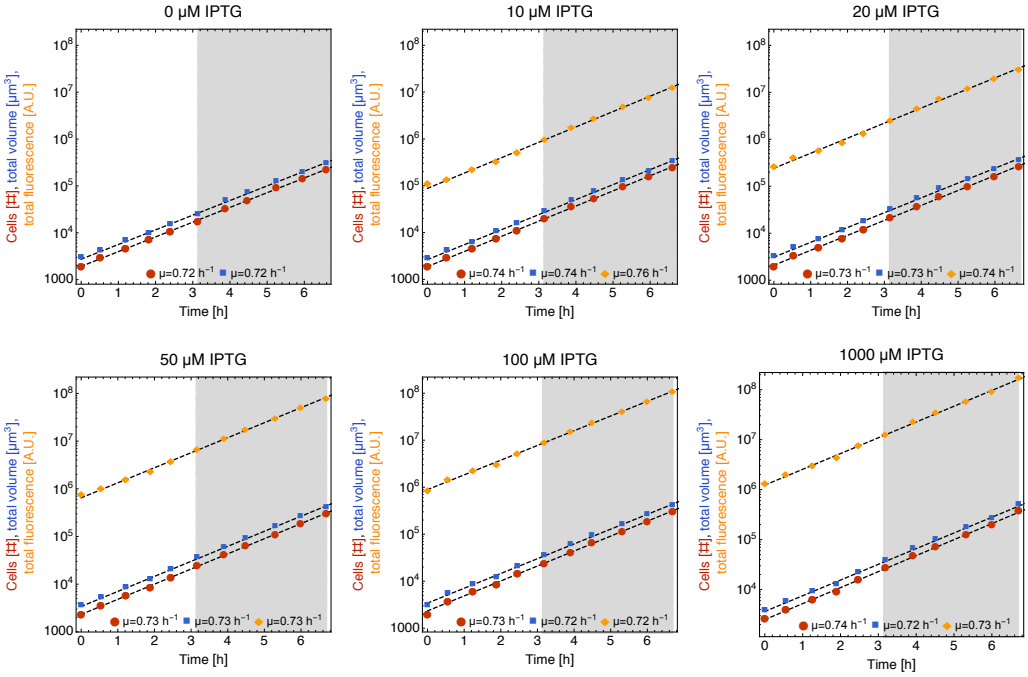

Figure S6: **Balanced growth of *B. subtilis* B15 on glycerol, sample B at different IPTG concentrations.** See figure S11 for further detail.

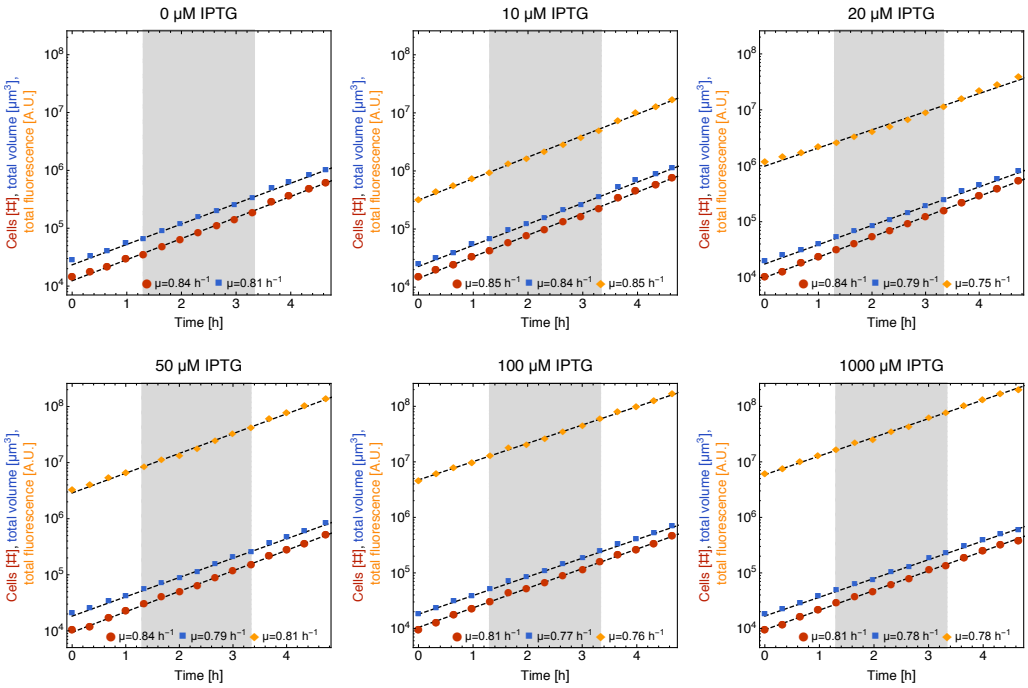

Figure S7: **Balanced growth of *B. subtilis* B15 on glucose, sample A at different IPTG concentrations.** See figure S11 for further detail.

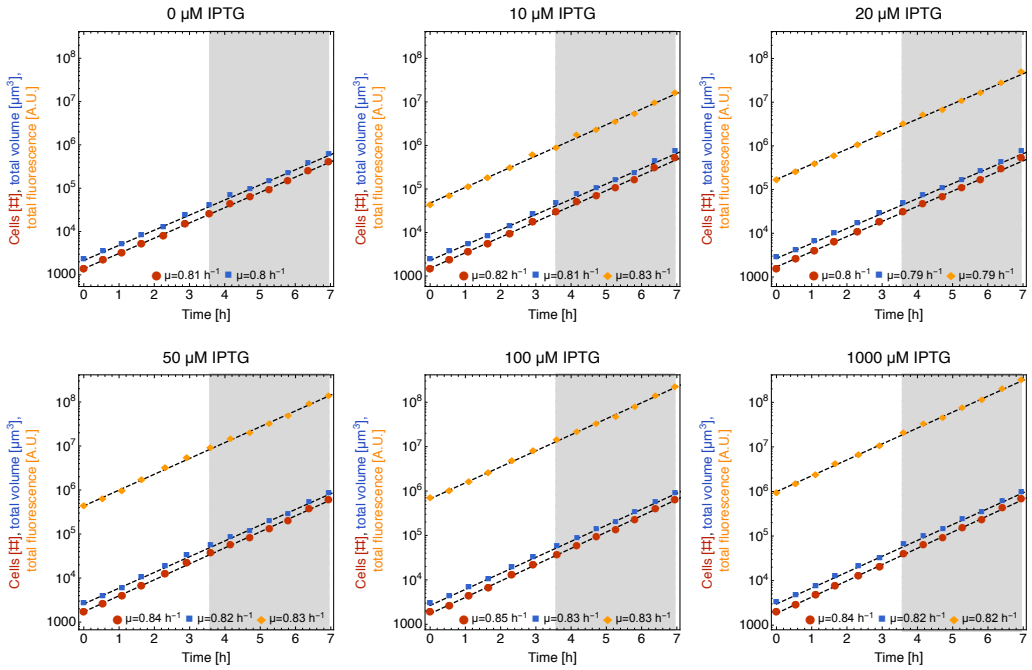

Figure S8: **Balanced growth of *B. subtilis* B15 on glucose, sample B at different IPTG concentrations.** See figure S11 for further detail.

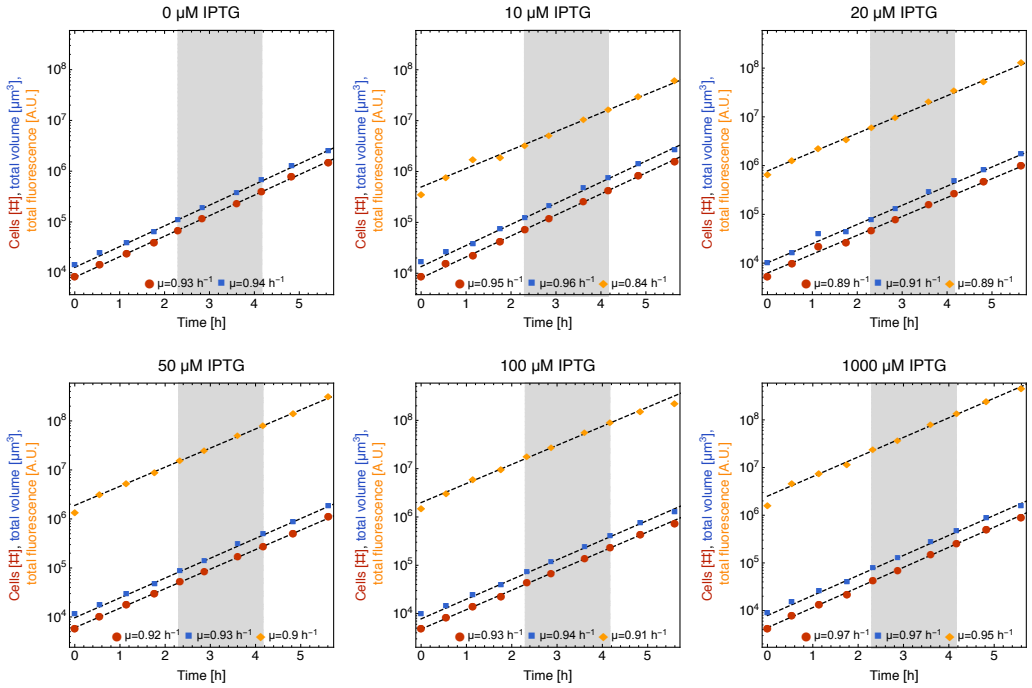

Figure S9: **Balanced growth of *B. subtilis* B15 on glucose + malate at different IPTG concentrations.** See figure S11 for further detail.

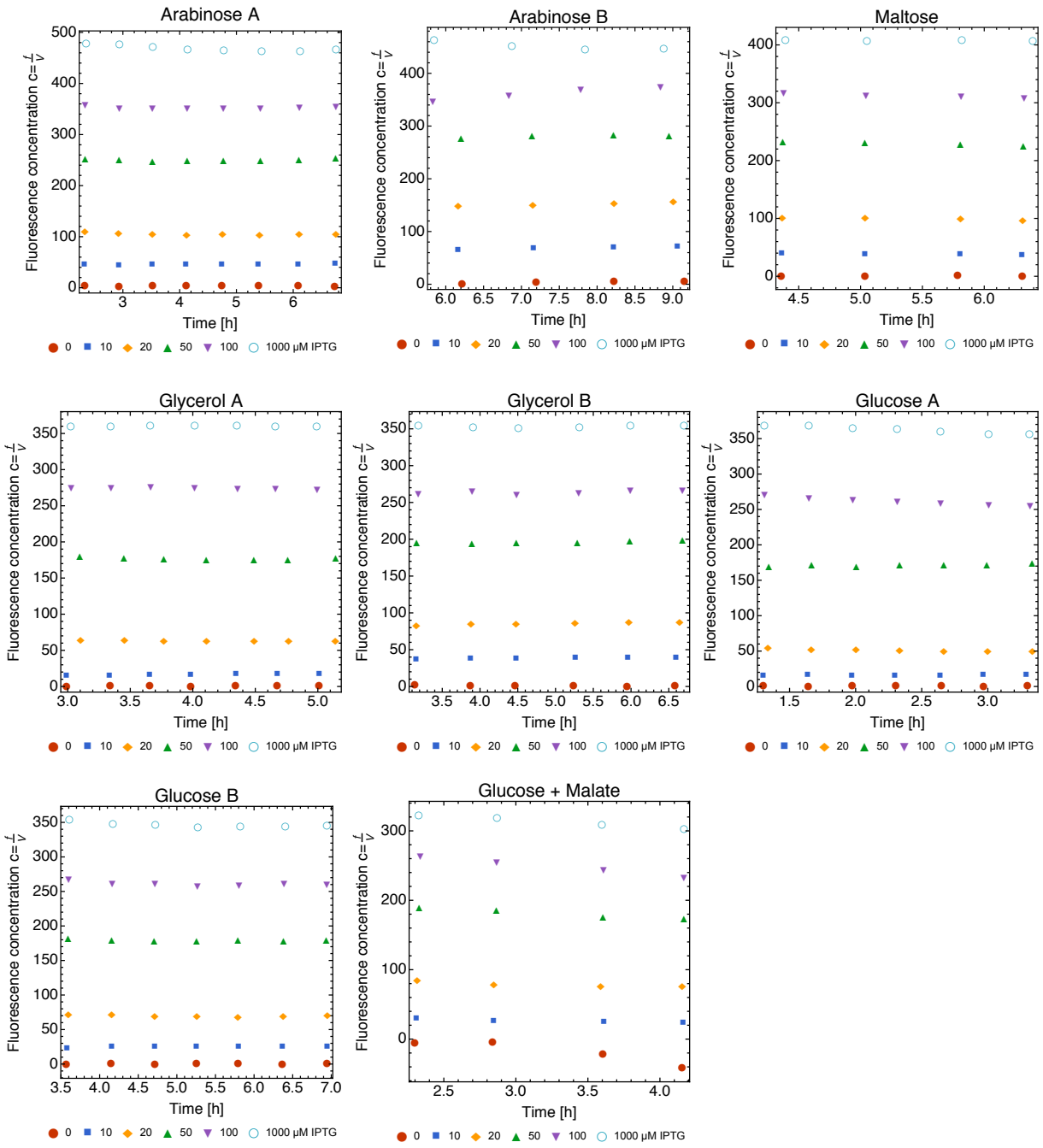

Figure S10: **Concentration homeostasis during balanced growth.** For each experiment, the region of balanced growth is shown (cmp. Figures S2-9). Capital letters (A,B) indicate biological replicates. Per experiment, the average of all time points from the region of balanced growth was used for further analyses.

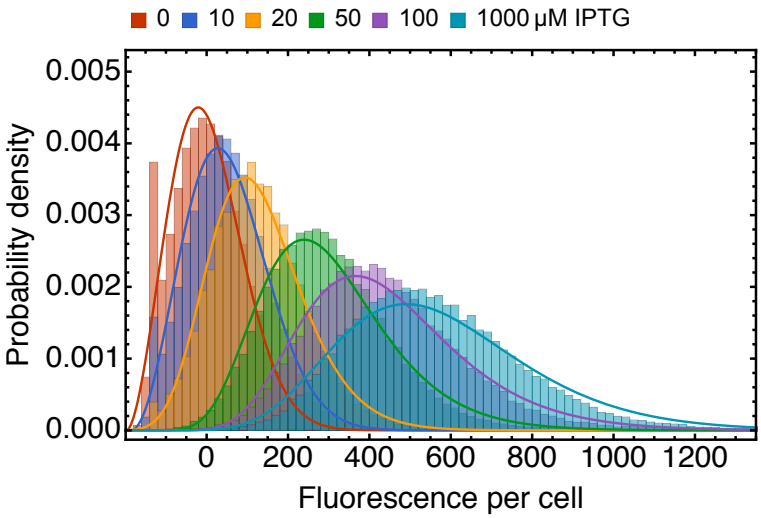

Figure S11: **Distributions of fluorescence per cell of *B. subtilis* B15 growing on arabinose at different IPTG concentrations.** This figure accompanies Figure 2b in the main text. The measured distributions are fitted to gamma distributions (solid lines).

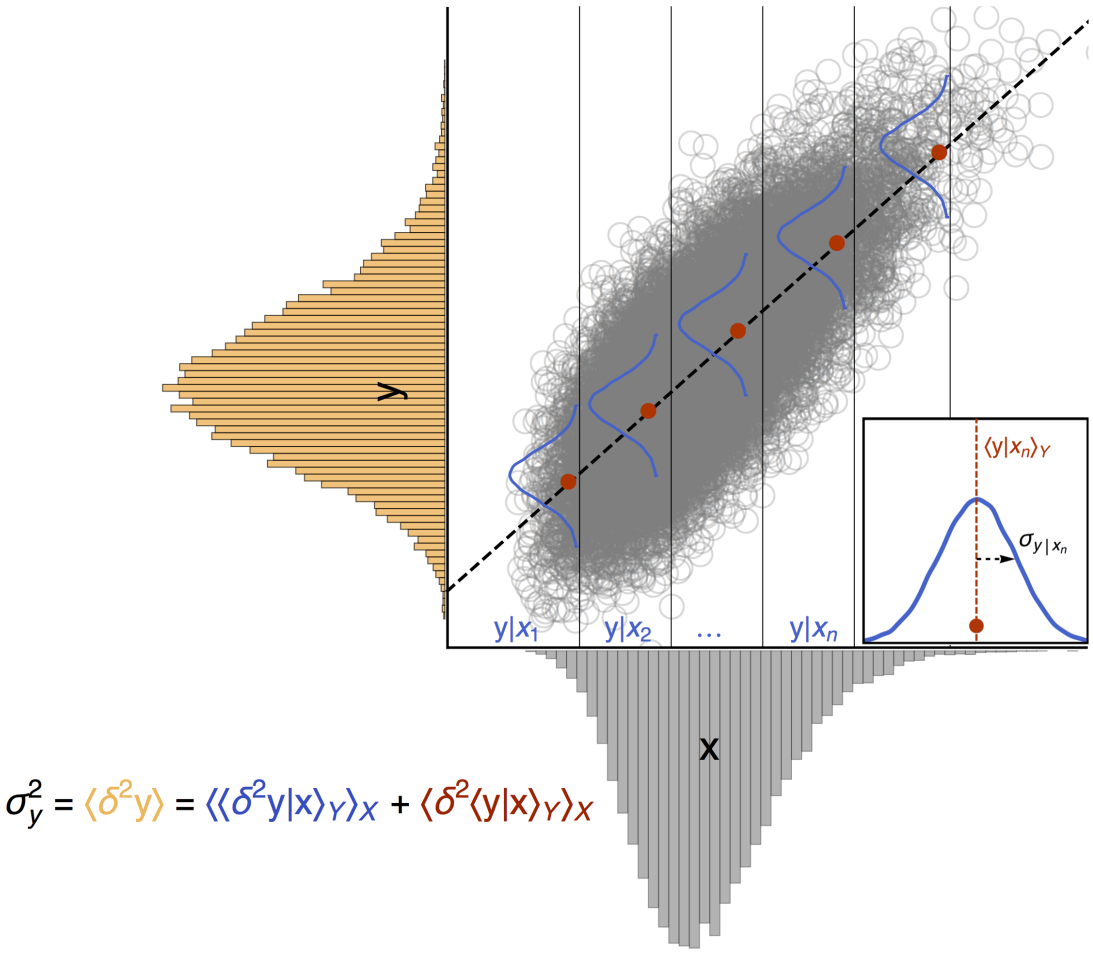

Figure S12: **Visualisation of the law of total variance.** The random variables X and Y are distributed according to the marginal distributions in gray and yellow, respectively. The values of Y depend on X by a function $f(x) = \langle y|x \rangle$ as indicated by the dashed line. At fixed x_n (inset), the values of Y follow a distribution (blue) with a mean, indicated in red, and a standard deviation $\sigma_{y|x_n}$, indicated by the black arrow. The variance of Y ($\langle \delta^2 y \rangle$, marked in yellow) is the sum of 1.) the mean variance of the conditional distributions ($\langle \langle \delta^2 y|x \rangle_Y \rangle_X$, marked in blue) and 2.) the variance of the conditional means ($\langle \delta^2 \langle y|x \rangle_Y \rangle_X$, marked in red). Variations in $y|x$, captured by $\langle \langle \delta^2 y|x \rangle_Y \rangle_X$, are solely due to fluctuations in y that are intrinsic to y and independent of x, whereas the variations in $\langle y|x \rangle$, given by $\langle \langle \delta^2 y|x \rangle_Y \rangle_X$, are extrinsic to y and can be attributed to changes in x. When X and Y are independent, the latter term becomes zero (which is the case for concentration at balanced growth).

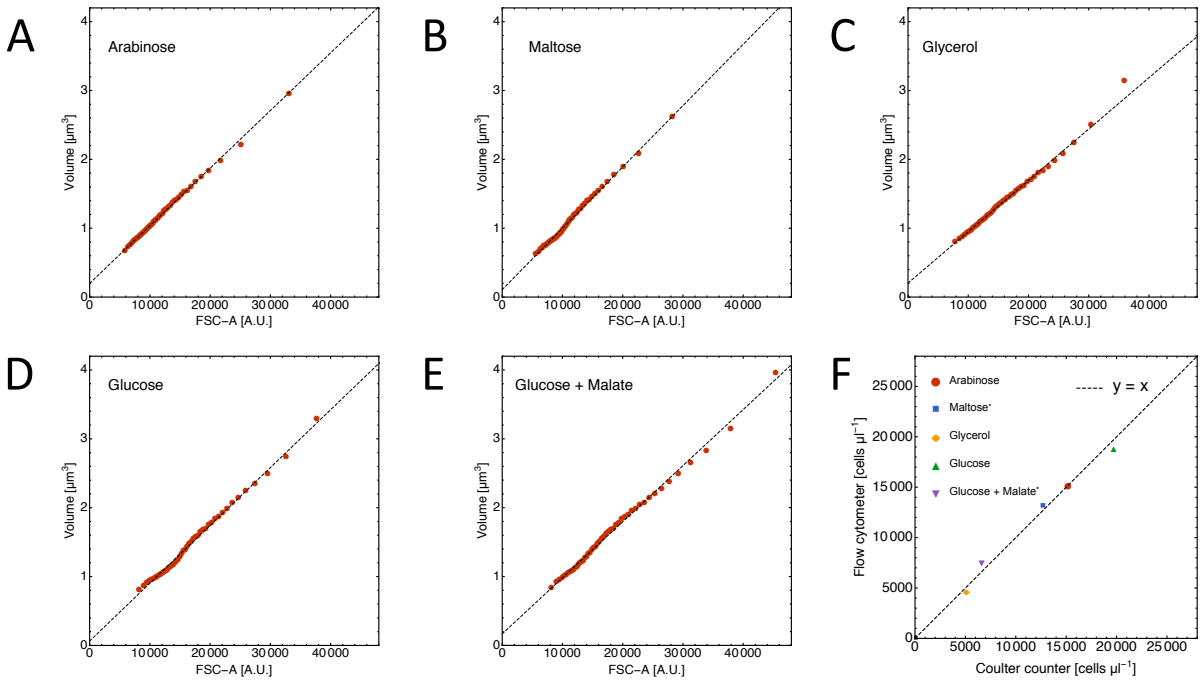

Figure S13: **Cross calibration of forward scatter to volume. A-E.** Cross-calibration of forward scatter area (FSC-A) to volume. Data points indicate quantiles in FSC-A and volume distributions mapped against each other. Dashed lines indicate the individual linear fits that are used to convert FSC-A to volume. For further detail, refer to the Methods (main text). **F.** After correcting for dilution, flow cytometer and Coulter counter registered the same number of cells per sample.

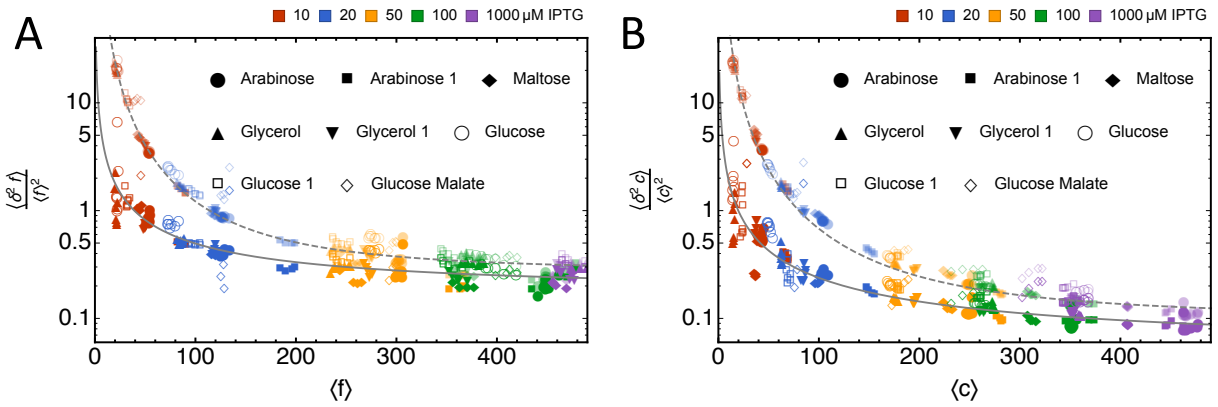

Figure S14: **Variance of background fluorescence distorts the scaling of noise with mean expression levels.** Noise in total cell fluorescence (A.) and fluorescence concentration (B.) as function of the respective mean across growth rates and promoter activities (i.e. IPTG concentrations), with (dense symbols) and without (light symbols) corrections for the variance of background fluorescence. Solid and dashed lines indicate $\frac{\langle \delta^2 x \rangle}{\langle x \rangle^2} \propto \frac{a}{\langle x \rangle}$ and $\frac{\langle \delta^2 x \rangle}{\langle x \rangle^2} \propto \frac{\langle \langle \delta^2 x_{bg} \rangle \rangle}{\langle x \rangle^2}$, respectively. The solid lines are the same as in figure 4, main text. In both plots, all time points from the region of balanced growth are shown (see figure S10).

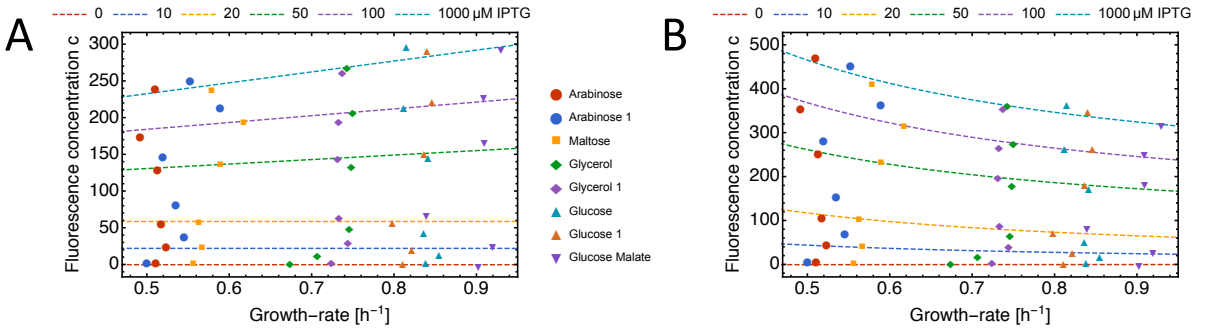

Figure S15: **Reduced protein expression by dilution by growth is partially compensated for by enhanced protein synthesis rate at higher growth rates.** Supplemental figure to plot 3 BC, of the main text, which shows all individual experiments. Each data point is the average of all time points shown in figure S10. Dashed lines, fits as in figure 3 of the main text.

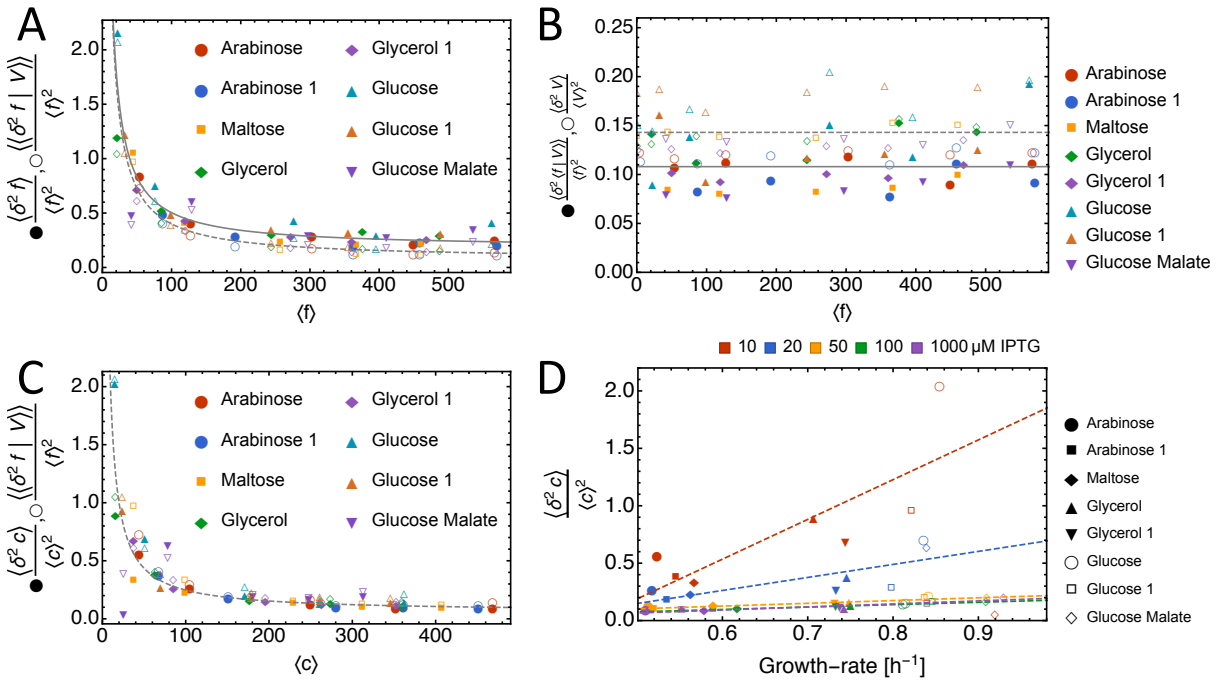

Figure S16: **Effects of promoter activity and growth rate on noise are indistinguishable and fall on an invariant relation between noise and mean of protein expression.** Supplemental figure to figure 4, main text, showing the results of all individual experiments. **A.** Noise in total cell fluorescence (filled symbols) and its intrinsic, 'biochemical' contribution $\frac{\langle\langle \delta^2 f|V\rangle\rangle}{\langle f\rangle^2}$ (open symbols). **B.** Fluorescence variation scales with volume as indicated by the relation $\frac{\langle \delta^2\langle f|V\rangle\rangle}{\langle f\rangle^2} = \frac{\langle \delta^2 V\rangle}{\langle V\rangle^2}$ which holds at balanced growth. From our experimental data, we see that $\frac{\langle \delta^2\langle f|V\rangle\rangle}{\langle f\rangle^2} \approx \frac{\langle \delta^2 V\rangle}{\langle V\rangle^2}$. **C.** At balanced growth, noise in fluorescence concentration directly captures protein expression noise due to biochemical origins (i.e. intrinsic sources). **D.** Dependence of noise in fluorescence concentration on the cellular growth rate at different magnitudes of promoter activity (IPTG concentration). For each carbon source, data points from 10 to 1000 μM IPTG are shown. Each data point is the average of all time points at balanced growth shown in figure S10.

Chapter 4

Single *Bacillus subtilis* cells display systematic deviations from exponential growth and biphasic growth behaviour along their cell cycle

Niclas Nordholt, Johan H. van Heerden, Frank J. Bruggeman

Abstract

The growth of a bacterial cell is the result of a multitude of molecular biosynthetic processes and their coordination. Each of these processes is subject to stochastic fluctuations. Yet, the average bacterial cell manages to double its volume and molecular content during its life time, under conditions of steady state growth. Thus, cells compensate for stochastic fluctuations, which requires continuous coordination of the biosynthetic rates with transient disruptive events such as DNA replication and septum formation. Such disruptive events can cause perturbations of metabolic homeostasis and balanced growth, forcing a change in the growth rate of cells. Here we studied the growth rate of single *B. subtilis* cells as function of their cell cycle, at three different growth conditions. We found that, under conditions of balanced growth, the growth profiles of single cells show systematic deviations from exponential growth that depend on growth conditions, cell-cycle progression and cell size at birth. Constitutive gene expression changed in synchrony with the instantaneous growth rate of cells, resulting in homeostatic expression levels throughout the cell cycle. Growth rate as function of the time-to-division indicates a biphasic pattern of cell growth. The second phase of growth initiates at a fairly constant time before cell division, suggesting the existence of a 'checkpoint' after which cell growth changes qualitatively and similarly across cells, for instance due to initiation of DNA replication or septum formation.

Introduction

Bacterial growth is an autocatalytic process in which a cell duplicates its molecular content to form two new, viable cells through cell division. The biochemical reactions that underlie growth are inherently stochastic and result in cell-to-cell variability in populations of isogenic cells, even under constant growth conditions[146,49]. Despite the inevitable randomness of these molecular reactions, bacterial populations are able to maintain time-invariant, condition-dependent distributions of cell size, generation time and macromolecular composition[216,52,149]. How bacteria achieve the homeostatic state required for 'balanced growth' has been the subject of decades of microbial studies, both on the level of the population[174] and on the level of single cells[34,195,29,215,66,184]. With recent technological advances it is now feasible to study the cell cycle of thousands of individual cells simultaneously, at high temporal resolution[216]. This has facilitated the discovery of phenomenological principles of cell size control[195,29] and their underlying mechanisms[215,66,184].

An implicit assumption of most recent studies is that growth of a single cell throughout the cell cycle proceeds exponentially at a fixed rate (box 1). While this approximation can easily be motivated by first principles that allude to the autocatalytic nature of bacterial growth[90,37], it cannot be ruled out that the physiological state of a cell may change with cell cycle progression such that cells deviate from exponential growth. For instance, since the genome occurs in such low copy numbers, its replication affects gene expression and in a strict sequence the copy number of genes per cell are increased. As a result, genes that are closer to the origin of replication are temporarily present in higher copy numbers than genes close to the terminal region of the chromosome, which can have consequences for gene expression[214] and the biosynthetic capacity of a cell, which can causes changes in growth rate (see[187] for a review on gene dosage effects in bacteria). Additionally, conformational changes of the nucleoid as function of the cell cycle have been observed in bacteria, which could possibly affect the accessibility of the DNA for transcription regulators[217,86]. Besides the effects on gene expression, the initiation of genome replication results in the expansion of the nucleoid volume, which can influence the volume dynamics of a cell (box 1).

Another example of a potentially disruptive event, in addition to DNA replication initiation, which can temporarily perturb cell homeostasis, is the process of cell wall (and/membrane) constriction prior to division. While growth of the cell wall in rod-shaped bacteria occurs continuously and uniformly distributed along the lateral cell wall during cell elongation[35], the rate of peptidoglycan (PG) incorporation accelerates at the constriction site, leading to an increased demand for PG precursors[221,220], possibly requiring and adjust of cellular metabolism to meet this enhanced demand. Cell wall constriction also necessitates the synthesis of a dedicated set of enzymes, the 'divisome', which is driven by hydrolysis of adenosine- or guanosine-triphosphate (ATP, GTP)[3,202]. Thus, the cell should re-allocate its limited resources between processes required for cell division and cell-component synthesis, which may influence the cellular growth rate. Besides the resource requirements that cell wall constriction imposes on the cell, in gram-positive bacteria such as *B. subtilis*, septum formation is finalised before division[133,26], resulting in a temporarily compartmentalised state of the cell prior to cell separation. All of this can disturb the metabolic homeostatic state of a cell associated with maintaining a constant growth rate.

Global changes in cell structure, and their temporal ordering during the cell cycle, all have to be completed before cell division can occur. The associated changes in the physiological state of the cell beg the question whether growth of an individual cell is at all times proportional to its size or whether there are distinct growth phases, associated with the onset – passing of checkpoints – and completion of global changes in cell structure. Early observations have been made that suggest the existence of such growth phases[34,97,26]. However, these studies relied on the inference of single cell growth rates from cell size distributions.

Here we characterise the growth rate dynamics of individual *B. subtilis* cells with sub-cell-cycle

resolution, using time-lapse fluorescence microscopy. We report that the during its cell cycle a *B. subtilis* cell grows in two phases. The exact values of the growth rate along the cell cycle depends on growth conditions. What we find across conditions is that cells that are born smaller than average grow faster than those that are born larger. The onset of the second phase occurs at a particular time prior to cell division, regardless of cell size, indicating that a global cellular event is initiated that takes a fixed amount of time, such as DNA replication. Despite large changes in their growth rate and, thus, in biosynthetic capacity, we find that cells are able to maintain almost perfect protein concentration homeostasis throughout the cell cycle. We explore scenarios that could underlie the observed growth patterns and discuss their role in the control of cell size homeostasis.

Box 1: Limitations of a balanced growth condition for single cells

The aim of this box is to derive i. the conditions for balanced growth, ii. the relation between the specific volume-growth rate ($\frac{d\ln V}{dt}$; V, cell volume) and the specific elongation rate ($\frac{d\ln l}{dt}$; l, cell length) for rod-shaped cells that grow in length, and iii. show how sudden initiation of replication can affect a cell's balanced-growth state.

Balanced growth conditions For single cells to grow balanced, their intracellular state, e.g. of metabolism, must be such that the cell's specific growth rate $\frac{1}{V}dVdt = \frac{d\ln V}{dt}$ equals a constant denoted by μ_V. The condition for this state is that all concentrations in a cell remain constant; since,

$$\begin{aligned} c &= \frac{\text{number of molecules of a particular species}}{\text{cell volume}} = \frac{n}{V} \\ \frac{dc}{dt} &= \frac{1}{V}\frac{dn}{dt} - \frac{n}{V^2}\frac{dV}{dt} \;\Rightarrow\; \frac{1}{n}\frac{dn}{dt} = \frac{1}{V}\frac{dV}{dt} = \mu_V. \end{aligned} \tag{4.1}$$

Thus, when the specific rate of molecule synthesis and volume are equal then concentrations are constant and will remain so and define the specific growth rate of a cell. Since, $\frac{dV}{dt} = \mu_V V$ we obtain $V(t) = V_b e^{\mu_V t}$. With V_b as the birth volume of a cell and the generation time, t_g, is defined as $\frac{V_d}{V_b} = e^{\mu_V t_g} = 2$, with V_d as the division volume, such that $t_g = \frac{\ln 2}{\mu_V}$.

Relation between the specific rate of volume-growth and length-growth The volume of an idealised rod-shaped cell equals the volume of a sphere, V_{cap}, plus that of a cylinder with length L, which equals $l - 2r$, with l as the length of the cell and r as its radius,

$$V(t) = \frac{4}{3}\pi r(t)^3 + \pi r(t)^2(l - 2r(t)) = \pi r(t)^2 l(t) - \frac{2}{3}\pi r(t)^3 = \pi r(t)^2 l(t) - \frac{1}{2}V_{cap}(t) \tag{4.2}$$

We illustrate this relationship in figure 4.1a. When we assume that the cell's volume grows by length growth[36] then $r(t)$ becomes a constant r and

$$\mu_V(t) = \frac{1}{V(t)}\frac{dV}{dt} = \frac{l(t)}{V(t)}\frac{\partial V(t)}{\partial l(t)}\frac{1}{l(t)}\frac{dl}{dt} = \frac{l(t)}{V(t)}\frac{\partial V(t)}{\partial l(t)}\mu_l = \frac{\pi r^2 l(t)}{\pi r^2 l(t) - \frac{1}{2}V_{cap}}\mu_l(t) \tag{4.3}$$

Thus when μ_V is constant during balanced growth μ_l is not; since,

$$\mu_l(t) = \frac{\pi r^2 l(t) - \frac{1}{2}V_{cap}}{\pi r^2 l(t)}\mu_V = \left(1 - \frac{\frac{2}{3}\pi r^3}{\pi r^2 l(t)}\right)\mu_V = \left(1 - \frac{2r}{3l(t)}\right)\mu_V \tag{4.4}$$

From equation 4.2 we can obtain $l(t)$ in terms of $V(t)$, for $V(t)$ we can substitute $V(t) = V_b e^{\mu_V t}$ and $V_b = \pi r^2 l_b - \frac{1}{2}V_{cap}$, which gives for $l(t)$ and $\mu_l(t)$,

$$l(t) = e^{\mu_V t}\left(l_b - \frac{2}{3}r\right) + \frac{2}{3}r \tag{4.5}$$

$$\mu_l(t) = \frac{1}{l}\frac{dl}{dt} = \mu_V\left(\frac{e^{\mu_V t}(l_b - \frac{2}{3}r)}{e^{\mu_V t}(l_b - \frac{2}{3}r) + \frac{2}{3}r}\right) \;\Rightarrow\; \frac{\mu_l(t)}{\mu_V} = \left(\frac{e^{\mu_V t}(1 - \frac{2}{3}\frac{r}{l_b})}{e^{\mu_V t}(1 - \frac{2}{3}\frac{r}{l_b}) + \frac{2}{3}\frac{r}{l_b}}\right) \text{ for } 0 \le t \le \frac{\ln 2}{\mu_V}. \tag{4.6}$$

Note that $l_b \ge 2r$ such that $0 \le \frac{r}{l_b} \le \frac{1}{2}$. This last equation indicates that $\mu_l \neq \mu_V$ under conditions of balanced growth when μ_V is fixed. Analysis of this equation indicates that μ_l as function of t/t_g is a rising function with no evidence of a rate change point (figure 4.1b). Below we will report experimental data that does indicate a rate change point, the results of figure 4.1b therefore indicate that a rate change point is not due to the measurement of cell length instead of cell volume, but rather due to a disturbance in the balanced growth rate of the cell.

Effect of replication of DNA on the growth rate of a cell can cause the emergence of a rate change point When we assume that after 55% of cell cycle progression a cell starts to grow an additional volume, say the nucleoid, then the volume dynamics of the cell equals,

$$\frac{dV_c}{dt} = \mu_c V_c \tag{4.7}$$

$$\frac{dV_n}{dt} = \begin{cases} 0 & 0 \le t \le t_{\text{rate change}} \\ k\left(1 - e^{-\frac{t - \frac{3}{5}\frac{\ln 2}{\mu_V}}{\tau}}\right) & t > t_{\text{rate change}} \end{cases} \tag{4.8}$$

$$V_c(0) = V_{c,0} \tag{4.9}$$

$$V_n(0) = V_{n,0}, \tag{4.10}$$

with V_c as cytosolic volume and V_n as nuclear volume, such that $V = V_c + V_n$. We added an expansion time τ for the nucleoid to account for slow structural changes and make the relation between the growth rate of the cell and cell-cycle progression time continuous. This system of equations can be solved and gives rise to a specific volume-growth rate (equal to $\frac{1}{V}\frac{dV}{dt} = \frac{1}{V_c + V_n}\left(\frac{dV_c}{dt} + \frac{dV_n}{dt}\right)$) profile as function of a cell's cell cycle as shown in figure 4.1c. Note that a rate change point emerges. Below we also report measurements that give similar profiles, suggesting the existence of a sudden rate change point due to, for instance, initiation of replication or any other global disruptive event (some are discussed in the introduction).

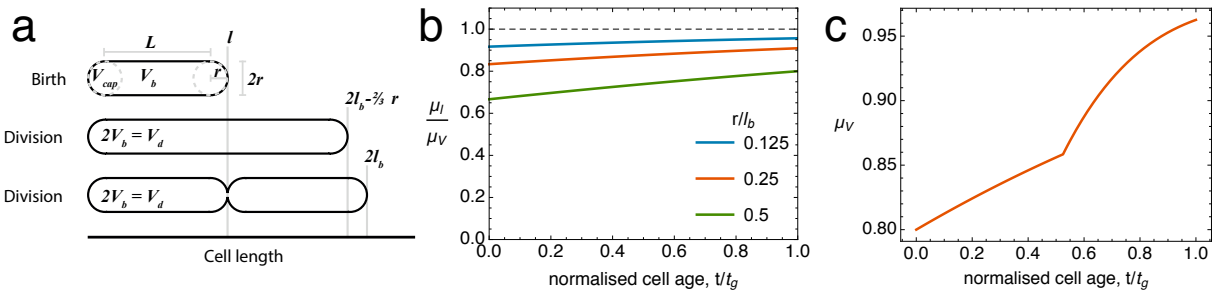

Figure 4.1: **Mathematics of single cell growth. a.** Schematic to illustrate the geometry of a rod-shaped bacterial cell that we use in box 1 to derive the relation between μ_V and μ_l. **b.** Variation of the specific length-growth rate of a perfect rod-shaped cell, growing only in length, as function of its cell cycle progression, during conditions of balanced growth. **c.** Profile of the specific growth rate of a cell if, after 55% of cell cycle progression, the volume-growth rate changes suddenly due to the addition of a zeroth order growth process, e.g. due to DNA replication. For details, see box 1.

Results

Table 4.1: Notations

Notation	Description	Units
a	cell age, time elapsed since birth of a cell	h
L	Length of a cell	μm
$ER\|a$	Instantaneous elongation rate, $\frac{dL}{dt}$, of a cell at age a	μm h^{-1}
$\langle ER\|a\rangle$	Average instantaneous elongation rate, $\frac{dL}{dt}$, over all cells of age a	μm h^{-1}
$sER\|a$	Specific instantaneous elongation rate, $\frac{1}{L}\frac{dL}{dt}$, of a cell at age a	h^{-1}
$\langle sER\|a\rangle$	Average specific instantaneous elongation rate, $\frac{1}{L}\frac{dL}{dt}$, over all cells of age a	h^{-1}
$\overline{sER}$	*sER* averaged over the cell cycle of a single cell	h^{-1}
$\langle sER\rangle$	mean sER of the population	h^{-1}
T	generation time	h
α	Normalised cell age, $\frac{a}{T}$, of a cell	0-1
L_b	Birth length of a cell	μm
L_d	Division length of a cell	μm
$\langle x\|\alpha\rangle$	*x* conditioned on α averaged over the population	[*x*]
$\langle x\|L_b,\alpha\rangle$	*x* subsetted by L_b, conditioned on α averaged over the L_b subset	[*x*]
Fluorescence (f) (per cell)	Sum of all pixel fluorescence intensities inside a cell	AU
Fluorescence concentration	Average pixel fluorescence intensity $\frac{f}{N_{pixels}}$ inside a cell	AU

Experimental approach

We used time-lapse fluorescence microscopy to monitor the growth and fluorescent reporter protein expression by individual *Bacillus subtilis* cells while they are growing on agar pads, under conditions of balanced growth. We considered three growth rates, which we varied by changing the carbon source. As carbon sources we considered arabinose, glucose and glucose plus four amino acids (methionine, histidine, glutamate and tryptophan). The population growth rates were 0.37 h^{-1}, 0.65 h^{-1}, 0.80 h^{-1}, with average interdivision times of 104 min, 62 min and 51 min, respectively. Throughout the text, we will refer to these conditions as slow, intermediate and fast growth, respectively. Distributions of birth length and division length were time-invariant over several generations, confirming balanced growth of the cell population (figure S1).

We determined the length of each cell with a certain age (a) and calculated the instantaneous absolute elongation rate ($ER|a$, [μm h^{-1}]) and the instantaneous specific elongation rate ($sER|a$, [h^{-1}]) for all cells for which we observed a complete cell cycle (i.e. observed birth and division). Length was used to characterise growth, because it is directly obtained from the recorded movies of cell growth and did not require any additional assumptions. We confirmed that the cell width remained relatively constant throughout the cell cycle (figure S2). The terms cell size and cell length will be used interchangeably hereafter. We note that the specific growth rate averaged over all cells ($\langle sER \rangle$) was in excellent agreement with the respective population growth rate, for each condition (figure S3). In table 4.1 a list of notations can be found that we use throughout the text.

In order to reveal systematic changes in elongation rate, such as deviations from exponential growth – and whether they occur at fixed times during the bacterial cell cycle, i.e. at 'checkpoints', we plot several cell features as function of the normalised cell age, which equals the ratio of a cell's current age over its generation time. For each growth condition, we group cells in normalised age bins (bin size 0.1) and study the correlation of particular growth characteristics of a cell, such as its instantaneous elongation rate.

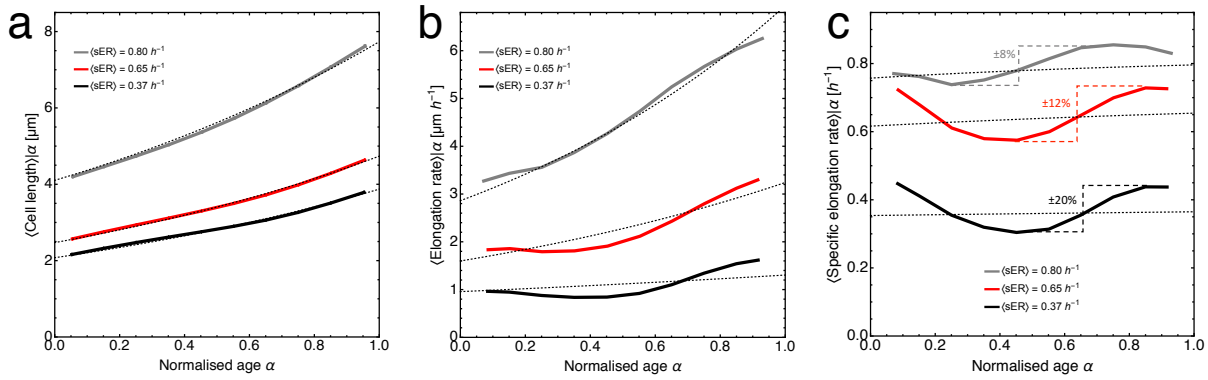

Figure 4.2: **Individual cells show systematic deviations from exponential growth along their cell cycle. a.** Average cell length as function of the normalised cell age α at three different growth conditions. Cell growth can be approximated by exponential growth, but systematic deviations are observed (dotted lines; see box 1 eq. 4.5). **b.** Absolute elongation rate (*ER*) as function of normalised cell age. If length increases exponentially, its time-derivative (*ER*) is also expected to increase exponentially (dotted lines; see box 1 eq. 4.5), which is not observed. **c.** Specific elongation rate (*sER*) as function of normalised cell age. If growth is exponential at steady state, *sER* follows the relation in box 1, equation 4.6 (dotted lines). For all analyses in these figures, only cells with a complete cell cycle (i.e. both birth and division observed) were included, totalling N = 2907, 12555, 15939 cells for the population average specific elongation rate (sER) = 0.80, 0.65, 0.37 h^{-1}, respectively. Standard error bars are smaller than the plot lines. Dotted lines are the best fits to the respective equation from box 1, with μ_V as the only unknown parameter.

Individual cells show systematic deviations from exponential growth along their cell cycle

Figure 4.2 shows the average growth behaviour of single *B. subtilis* cells growing at three different population growth rates. As expected, cell length approximately doubles on average during the cell cycle. Birth, division and average length increase with increasing growth rate (figure 4.2a), which is in agreement with earlier findings by others[184]. The increase of a cell's length with its age can be approximated by an exponential function (figure 4.2a, cf. equation 4.5 in box 1). However, when carefully evaluated, this approximation reveals the presence of systematic deviations from exponential growth along a cell's cell cycle, indicating that under all three conditions, cells do not grow at a constant rate. Rather, the instantaneous growth rate shows systematic deviations around the expected, exponentially increasing value (figure 4.2b, cf. box 1, eq. 4.5).

The deviations from exponential growth are smaller at fast growth than at slow growth. At fast growth, the instantaneous elongation rate increases monotonically with cell age, but not in an exponential manner as is expected for exponential growth (figure 4.2b). At intermediate and slow growth, the elongation rate is constant or even slightly decreasing during the first half of the cell cycle (figure 4.2b), while it increases faster than expected from the population growth rate during the second half of the cell cycle (figure 4.2b, cf. box 1, eq. 4.5). In line with this observation, the specific elongation rate displays large systematic deviations from the expected value (the dotted line in figure 4.2c) of up to $\pm$20% during the cell cycle (figure 4.2c).

We conclude that the average instantaneous growth rate displays systematic deviations from exponential growth. Thus, cells do not display a constant growth rate during their cell cycle. The observed growth-rate-vs-cell age dependency (figure 4.2b) suggests the existence of two distinct growth phases in *B. subtilis*: a first growth phase characterised by a nearly constant elongation rate and a second growth phase characterised by increasing elongation rate. Since balanced growth is inherently related to metabolic homeostasis (see box 1) we can conclude that cells do not maintain a balanced metabolism during their cell cycle, and that metabolic homeostasis is perturbed upon cell birth and later in the cell cycle, for instance because of the start of replication or septum formation.

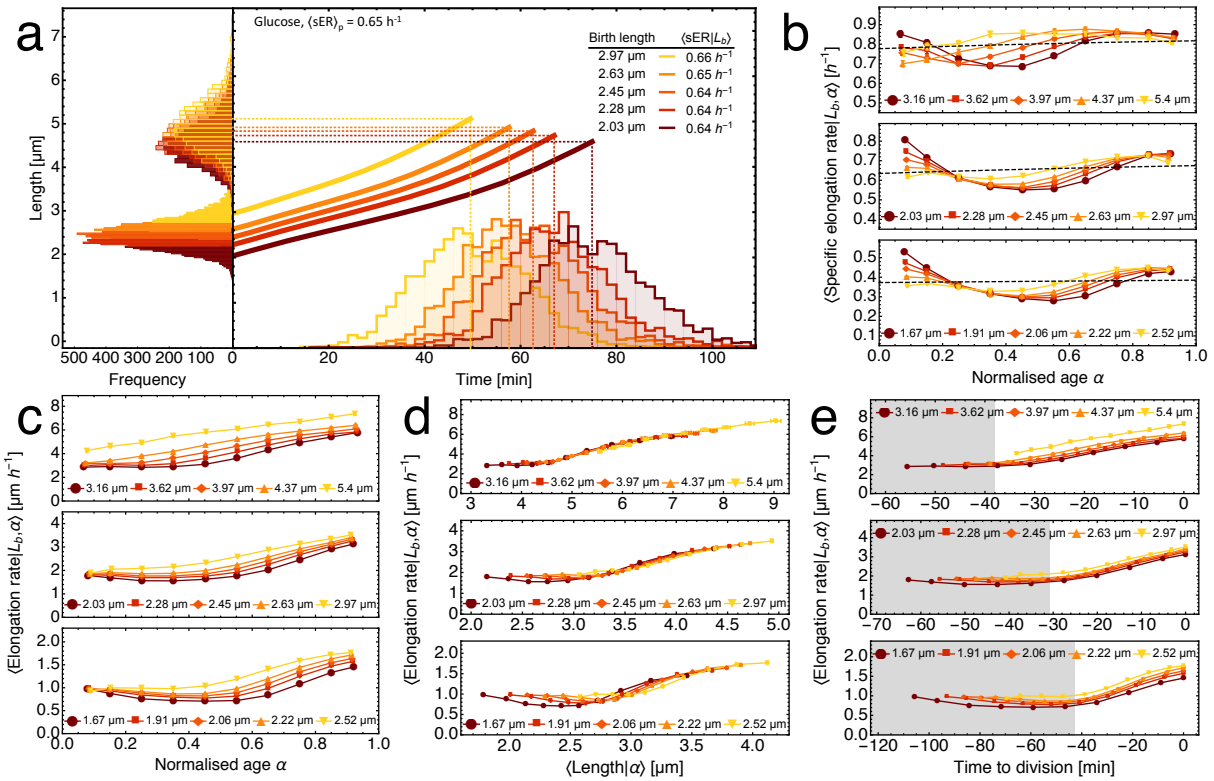

Figure 4.3: **Systematic deviations of single-cell growth rates correlate with birth size and time-to-division. a.** Average length profiles of cells as function of time, classified according to birth length classes (growth is on glucose). The frequency distributions along the y-axis show the length distributions at birth (left bottom) and division (left top). Interdivision-time distributions of the individual birth length classes are shown on the x-axis. Horizontal and vertical dashed lines indicate the mean division length and interdivision time of each birth length class, respectively. **b.** Specific elongation rate of different birth length classes as function of cell age for fast (top), intermediate (middle) and slow (bottom) growth. The legends indicate the mean birth length of the respective birth length class. The dashed line is the specific elongation rate according to equation 4.6 and the same as in figure 4.2a. Note that the mean $\langle sER|L_b, \alpha\rangle$ for the different birth length classes was the same as the population average, $\langle sER\rangle$. **c.-e.** Absolute elongation rate as function of the normalised cell age (**c.**), current cell length (**d.**) and time to division (**e.**). The grey area indicates the first growth phase, with transition to the second phase at 41, 31 and 38 minutes prior to division at slow, intermediate and fast growth, respectively. The number of cells per birth length class: N = 3188, 2511, 582 for slow, intermediate and fast growth, respectively.

Systematic deviations of single cell growth rates from exponential growth correlate with birth size and time-to-division

To better understand the systematic deviations from exponential growth, we classified cells according to their birth length (we made 5 such classes, i.e. 'bins') and studied how the growth rate of those cell classes varied along their cell cycles. Each class contains 20% of all cells for which complete cell cycles (birth and division) were observed (figure 4.3a, left marginal distribution). Comparison of figures 4.2a, 4.3a and 4.3b indicates the cells of each birth-size class display systematic deviations from exponential growth. Figure 4.3a shows the frequency distributions of birth and division length, coloured according to the different classes. While the birth length distributions are separated at birth, their division length distributions overlap, indicating a compensating mechanism for cell size homeostasis. Cells that are born larger than average, have on average a shorter generation time (figure 4.3a, distributions on x-axis) and a slightly higher average growth rate (table in figure 4.3a).

Figure 4.3b and c indicate that the exact deviations that cells show from exponential growth along their cell cycle are dependent on birth size. Cells that are born comparatively small deviate most from exponential growth (figure 4.3b). Under all conditions, the progression of the elongation rate along the cell cycle displays a biphasic growth pattern. The duration of the first, sub-exponential growth phase is longer in small cells (figure 4.3b and c). An exception to the biphasic growth pattern is observed only for cells that were born larger than average in the fast growth condition (top figure in figure 4.3c, yellow lines). The elongation rate of these cells increases throughout the cell cycle.

To understand whether the differences in the duration of the growth phases are related to cell length, we plot the elongation rate as function of cell length (figure 4.3d). These curves deviate from the expected exponential curve and the effect of birth size is greatest at the slow-growth condition. The overall curvature is very similar across the three growth conditions: it is biphasic, first the elongation rate is fairly constant while it rises in the second phase. Not that the lengths at which the growth rate rises is dependent on the growth condition, but is always larger than ≈ 3 μm.

In figure 4.3e we plot the average elongation rate of cells in the five different birth-size classes as function of the time to division. We find that elongation rate increases at a constant time before cell division under all conditions, independent of birth length (figure 4.3e). The exact time at which the growth phase transition occurs depends on the growth condition (figure 4.3e). By fitting a piecewise function to the data (see Methods), we estimated the point of growth-phase transition at slow, intermediate and fast growth to be 43, 31 and 38 minutes prior to division, respectively (figure 4.3e, grey area).

We conclude that the growth rate of cells as function of the cell cycle is not exponential, it is biphasic and birth-size dependent. For a specific growth condition, cells start the second phase of growth at a similar time before the cell division, regardless of their birth size.

Cells achieve protein concentration homeostasis by compensating for protein dilution disturbances due to growth rate variation

Protein concentration is influenced by the growth rate of a cell and the translation rate[89,180,139]. That cells display a biphasic growth-rate pattern raises the question whether a single cell can maintain protein concentration homeostasis throughout its cell cycle. We therefore integrated the coding sequence of a fluorescent protein (GFP) under the control of an inducible promoter into the genome of *B. subtilis* and expressed it constitutively (for details see[139]). We used this construct to investigate how the systematic variation in growth rate influences constitutive gene expression throughout the cell cycle. Furthermore, the rate of fluorescent protein production per cell length can yield information about the state of the protein synthesis machinery of the cell.

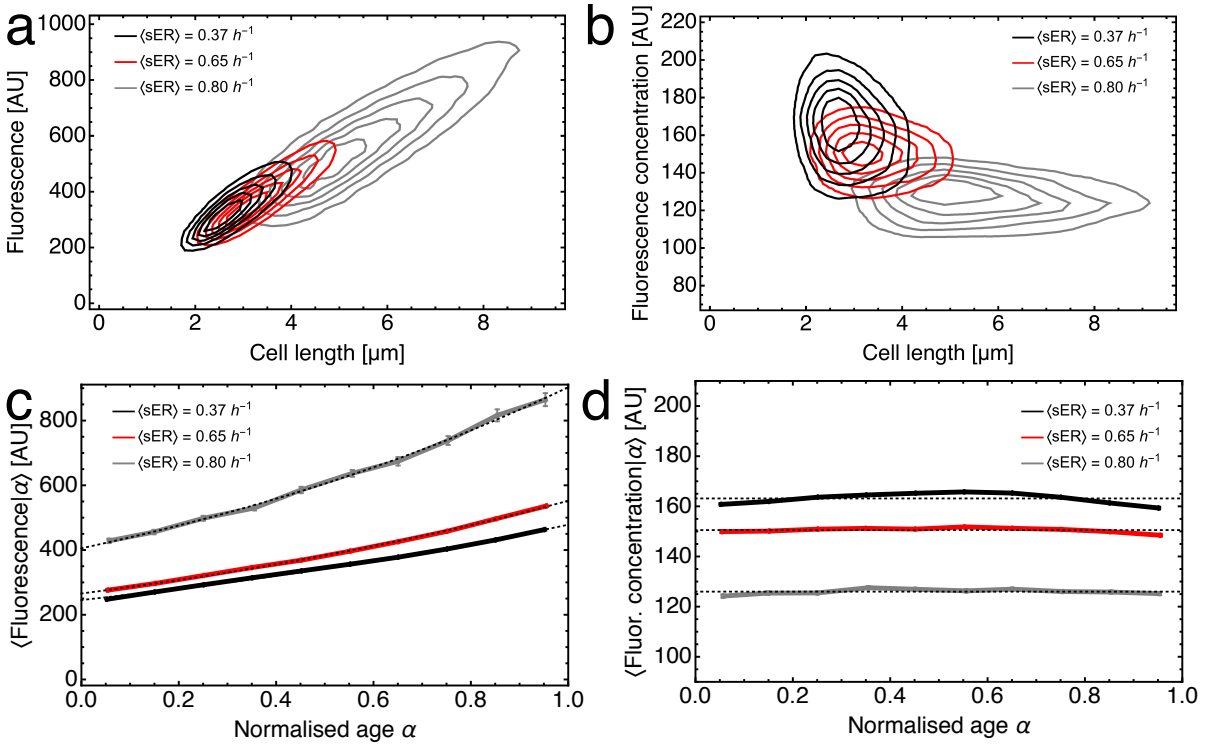

Figure 4.4: **Constitutive protein expression on the level of the population and single cells. a.** Absolute fluorescence as function of cell length at fully induced protein expression. **b.** Fluorescence concentration as function of cell length. Fluorescence concentration is almost independent of cell length and decreases with increasing population growth rate. **c.** Absolute fluorescence as function of the cell cycle increases similarly to cell length (cf. figure 4.2a), with larger cells containing more protein. The dotted line is obtained by rearranging equation 4.1. **d.** Fluorescence concentration stays approximately constant over the whole cell cycle, showing only a slight increase between age 0.5 - 0.7. Cells included for the analysis N = 4244, 1776, 580 for slow, intermediate and fast growth, respectively. Dotted lines indicate the mean fluorescence concentration.

Figure 4.4a indicates that the mean protein expression per cell (not the concentration) increases with mean cell size, which is larger at higher growth rates, as is expected for constitutive expression. This is in agreement with what we found earlier with this construct, using flow cytometry[139]. The mean fluorescence per cell increases with cell length, resulting in an approximately constant protein concentration (figure 4.4b). There exists a weak negative correlation between cell size and protein concentration, which is largest at slow growth (Pearson correlation coefficients: ρ_{slow}=-0.23, $\rho_{intermediate}$=-0.14, ρ_{fast}=-0.13). The population average protein concentration is condition dependent, showing a decrease with increasing growth rate (figure 4.4b). This is in line with the expectations and indicates the effect of protein dilution by growth[71,89,139].

When evaluated as function of cell-cycle progression, cellular protein abundance increases with the normalised age, showing only minor deviations from the expected, exponential increase (figure 4.4c, cf. figure 4.2a). The protein concentration therefore stays approximately constant during the entire cell cycle, except for a slight increase close the middle of the cell cycle (figure 4.4d) at the low growth rate condition. The stability of protein concentration throughout the cell cycle is quite remarkable, as it indicates that the variations in growth rate during the cell cycle only have a slight effect on protein concentration homeostasis inside the cell.

To gain further insight into the protein expression along the cell cycle, we considered temporal protein expression in single cells to elucidate how they maintain fairly constant expression levels. Analogous to the growth analysis in figure 4.3, we grouped cells according to their birth length. Due to the smaller sample size (see Methods for details) we reduced the number of birth length classes to three, with each class representing a third of the cells per condition (see Methods for details).

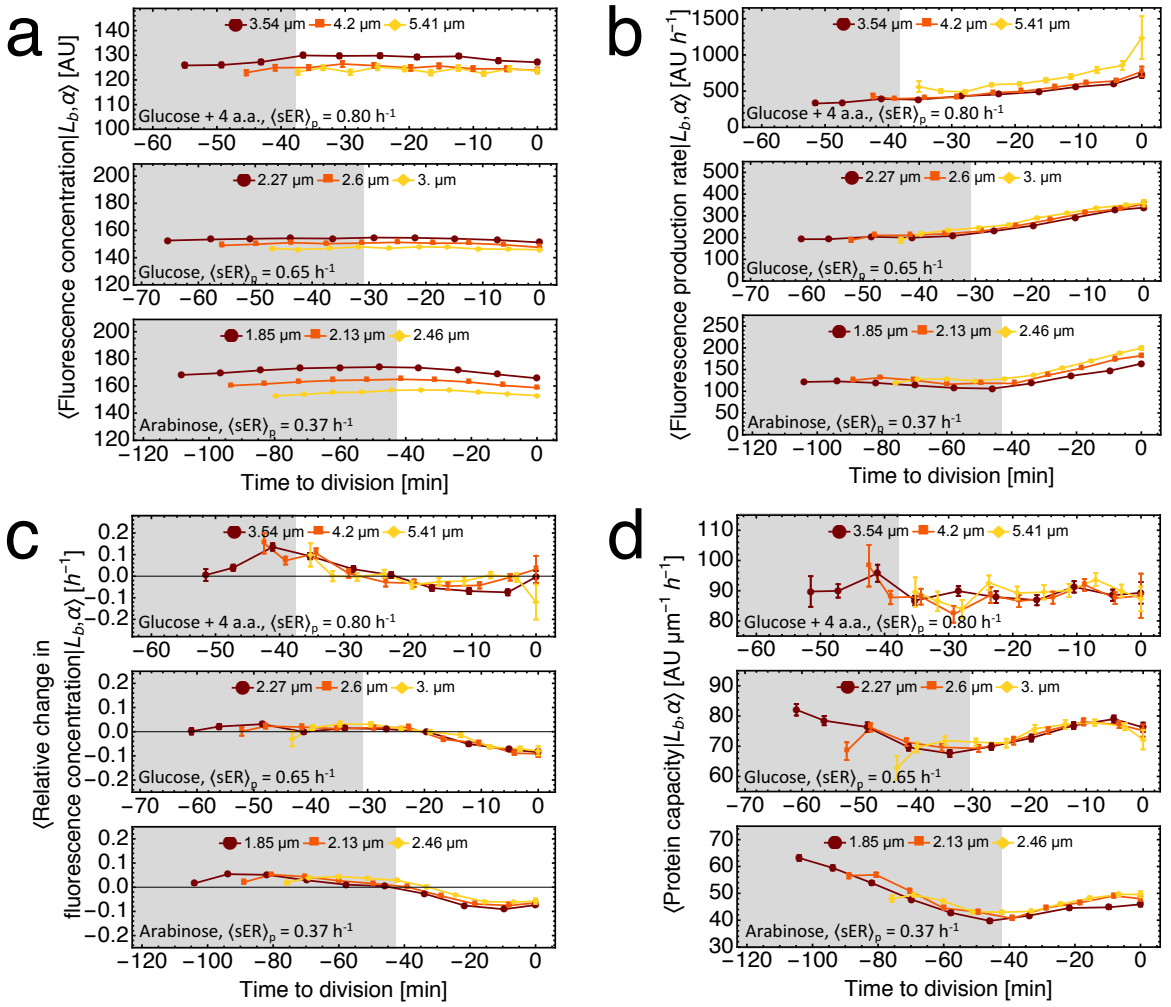

Figure 4.5: **Protein expression dynamics buffer growth rate effects independent of birth size.** Fluorescence concentration (**a.**) fluorescence production rate (**b.**) relative rate of change in fluorescence concentration (**c.**) and protein capacity (**d.**) as function of time to division. The grey area corresponds to the first growth phase, as shown in figure 4.3e. **a.** Concentration homeostasis is maintained throughout the cell cycle and cells that are born small maintain a higher than average expression level. **b.** Fluorescence production rate increases at a set time to division, similar to elongation rate (cf. figure 4.3e). **c.** Fluorescence concentration increases in the first phase and starts to decrease at a set time to division. **d.** Protein capacity, i.e. protein produced per length and unit time, decreases up to a set time before division. The mean birth length of each class is given in the plot legends. The grey area marks the first growth phase and is the same as in figure 4.3e. Cells per birth length class: N = 1415, 593, 194 $\pm$1 for slow, intermediate and fast growth, respectively. Error bars indicate the standard error of the mean and are possibly smaller than the symbols.

The results are shown in figure 4.5. Under all conditions, expression levels were approximately constant and cells that were born small maintained the highest expression concentration throughout the cell cycle (figure 4.5a). The differences to the mean expression level range from $\approx$ 2% at fast growth to $\approx$ 5% at slow growth. Which is considerably lower than the variation in growth rate ($\langle sER \rangle_p \pm$8-20%) that we observed as function of the cell cycle (figure 4.2c).

We determined the fluorescence production rate by calculating the differences in fluorescence per cell over time along the cell cycle (see Methods for details). Fluorescence production rate is slightly higher in large cells than in small cells (figure 4.5b). At conditions of slow and intermediate growth, we find that the production rate is initially constant and increases at a characteristic time before division, in synchrony with elongation rate (figure 4.5b, cf. figure 4.3e). At the fast growth condition, we see a steady increase in protein production, which is in agreement with the elongation rate dynamics in figure 4.3e. Thus, the rate of protein expression mirrors that of cell elongation.

These findings indicate that cells buffer the sudden increase in elongation rate by a concomitant increase in protein production to maintain a fixed protein concentration. However, the cells are unable to fully compensate for the effects of protein dilution by growth. This becomes clear when we inspect the relative change in fluorescence concentration per unit time (figure 4.5c). In the first growth phase, protein accumulates, as can be seen from the positive values in figure 4.5c. Upon the onset of the second growth phase at the characteristic time before division, fluorescence concentration starts to decrease, as the relative rate of change becomes negative. The resulting changes in fluorescence concentration are between $\pm$ 2-5% of the mean, depending on growth rate, with a maximal concentration at the transition point between the two growth phases (figure 4.5a, cf. also figure S4). It is also noteworthy that the relative rate of change in fluorescence concentration is almost independent of birth length.

Figures 4.5a-c illustrate the consequences of the biphasic growth patterns on the expression levels of a constitutive gene. A different way to interpret the data is to evaluate them in the context of protein produced per unit length per time. We call this measure the 'protein capacity' of the cell (figure 4.5d). The protein capacity can provide insights into the amount of protein a cell can produce per unit length, which is a proxy for the state of the protein synthesis machinery of the cell.

In figure 4.5d the protein capacity is plotted against time-to-division for the different growth conditions. Under all conditions, protein capacity is independent of birth length, indicating that the capacity to synthesise protein is independent of cell length and is solely set by the nutrient conditions. In agreement with earlier findings, we find that protein capacity increases with growth rate[180,44] (figure S4). At fast growth, protein capacity stays nearly constant over the whole cell cycle (figure 4.5d). The protein capacity at slow and intermediate growth shows biphasic behaviour, with an initial decrease and a minimum at the characteristic time to division, as indicated by the grey area in figure 4.5d. At slow and intermediate growth, protein capacity mirrors specific elongation rate (figure 4.3b). This indicates that the ability of a cell to synthesise protein changes in synchrony with the cell elongation rate throughout the cell cycle.

Discussion

In this paper we identify distinct growth phases in the cell cycle of *B. subtilis* under conditions of balanced growth. While population growth and single-cell endpoint measurements follow the classical growth law[28,174], monitoring growth of single cells with high temporal resolution revealed deviations from exponential growth. We found two distinct growth stages. The first phase is characterised by a constant elongation rate and a variable duration that depends on the birth length of a cell. The onset of the second phase occurs at a fixed time before division, independent of birth

length, and is characterised by an increase of elongation rate as cell length increases.

Despite the large changes in growth rate, we observed that cells can maintain protein-concentration homeostasis throughout the cell cycle by adapting their protein synthesis. These findings challenge the dogma that single cell growth is exponential with a rate that is set solely by the growth conditions.

Here we will discuss the implications of the observed growth and expression patterns for cell size homeostasis and explore scenarios that could underlie these systematic deviations from exponential growth.

Implications for cell size homeostasis

In our data, cells that are born smaller than average have a generation time that is above average, in line with previous observations for other bacterial species[145,29,195](figure S5). Here we found that this results from a prolonged first growth phase, as the duration of the second growth phase is independent of birth length (figure 4.3). Conversely, large cells that have a generation time shorter than the duration of the second phase do not exhibit biphasic growth at all. Additionally, small cells add more length before division[215] (figure S5). This suggests that the biphasic growth plays a role in the coordination of biomass production with cell cycle progression to ensure cell size homeostasis. The relatively narrow window of cell lengths at which the onset of the second growth phase occurs (figure 4.3d), suggests that reaching a certain size is a prerequisite for the transition between growth phases, which is in agreement with recent experiments by others[184,215]. The variable duration of the first growth phase allows cells that were born small to 'catch up' in size. This indicates that cells behave as 'sizers' during the first growth phase. Whether cells actually 'aim' for a certain size, or whether this is merely a consequence of a different mechanism, such as reported in Si et al.[184], cannot directly be concluded from our data. In the second growth phase, growth is proportional to length and proceeds for a fixed time interval, resulting in an 'adder'-like behaviour[29,195]. This would also explain, why cells at slow growth rather exhibit 'sizer'-like behaviour, whereas cells at fast growth exhibit 'adder'-like behaviour[215,195]. Small cells, which have a comparably long generation time, spend a much larger fraction of their life in the first growth phase ('sizer'), whereas large cells with a shorter generation time exist mostly, or even completely, in the second growth phase ('adder'). Interestingly, we found that, within a condition, cells of different birth lengths (which correlate with generation time) show no marked difference in their average specific elongation rate. This suggests that, at the level of single cells, specific elongation rate is not the determining factor for biphasic growth. It is rather related to cell size at birth and generation time. From these observations one could argue that cells that are born larger are also born 'older', which suggests a close coupling of cell cycle progression and cell size. In the following section we will speculate on the possible origins of these phenomenological descriptions, which we will derive from previous studies and augment with the protein expression data that we generated.

Cell cycle events that could cause disruption of the metabolic state of a cell and result in biphasic growth

We observed that despite growth rate fluctuations, cells are able to maintain a remarkably stable expression level of a constitutively expressed gene (figure 4.5). Our data suggest that this is achieved by a compensating change of protein synthesis with growth. The increase in gene expression at a set time to division could be an indication for a gene duplication event[214]. The GFP is situated at $\approx 28^\circ$ on the genome in the *amyE* locus. However, the increase in GFP-production and acceleration of growth rate occur simultaneously. The ribosomal genes that would be the main suspect for the accelerated growth rate are mostly situated closer to the *oriC*[99]. From this, one would expect the increase in elongation rate to occur before the increase in GFP production, so we can likely rule out gene dosage effects as the sole reason for the biphasic growth. However,

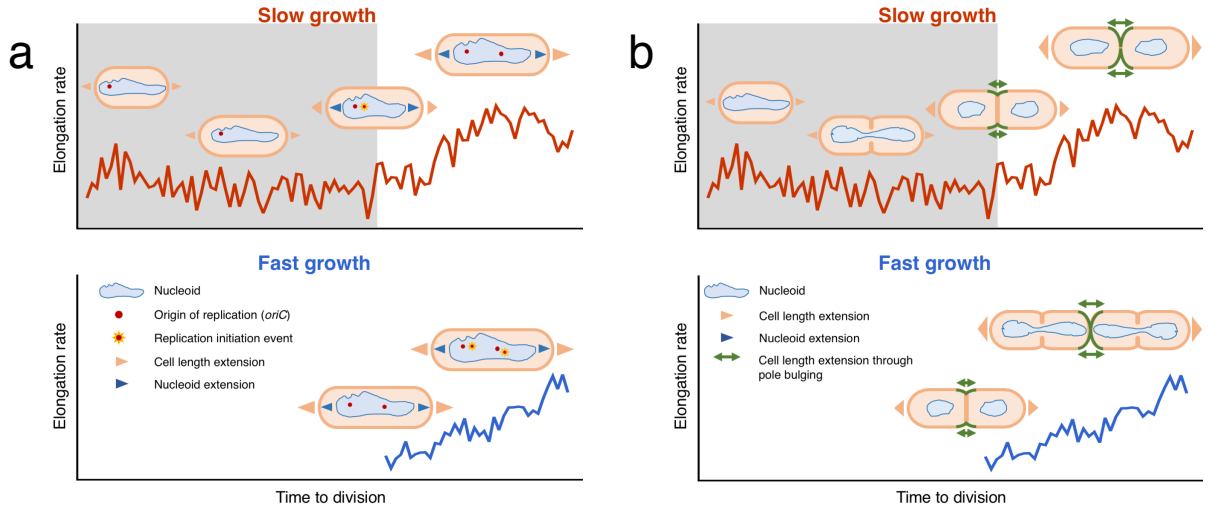

Figure 4.6: **Cell cycle events that could cause disruption of the metabolic state of a cell and result in biphasic growth. a.** Initiation of DNA replication and subsequent nucleoid expansion results in an increase in growth rate. **b.** Septum formation and cell separation in conjunction with pole bulging as origin of the growth rate increase.

even under conditions that are similar to the slow growth condition tested here, *B. subtilis* cells are born partially diploid, with more than 50% of their chromosome replicated, which means that DNA replication is initiated in the previous generation before cell separation occurs[217]. Subsequent to replication initiation, the nucleoid volume expands until replication is completed. Nucleoid expansion could offer a mechanistic explanation for the change in growth rate that we describe as 'biphasic growth' (figure 4.6a, box1). At fast growth, there may be multiple overlapping rounds of replication, resulting in the absence of the first growth phase[38] (figure 4.6a). A pivotal question is whether cells that are born larger progressed further through the cell cycle before division, i.e. have a partial chromosome that is closer to completion. Previous measurements suggest that this is the case[72,183]. However, we are not aware of any publication that directly shows this.

Alternatively, or in addition, the dynamic changes in protein capacity could be the result of a coordinated resource reallocation towards the synthesis of other macromolecules, such as DNA and cell wall precursors. Especially the latter lends itself as a possible candidate. In the second growth phase, we observe accelerated growth that could be due to length extension as a result of an increased cell wall synthesis (figure 4.6b). This could explain the slow increase in protein capacity in comparison with length growth and the resulting decrease in protein concentration: The smaller a cell is, the closer its shape resembles a sphere. As a consequence, the ratio of surface area to volume increases, meaning that the cell wall constitutes a larger fraction of the total biomass in smaller cells, resulting in a larger fraction of resources that has to be dedicated to cell wall synthesis. It was shown that cell wall thickness and strain on the cell wall in *B. subtilis* are constant across conditions[127], which supports the idea that the relative burden of cell wall synthesis is larger on small (and slower growing) cells.

The synthesis of the cell wall is thought to be a continuous process that occurs uniformly along the longitudinal axes of the cell[35,90]. This implies that the synthesis of the external cell wall is unlikely to cause the biphasic growth pattern. However, *B. subtilis* forms a septum well before cell division[26]. This could also offer an explanation for the biphasic growth pattern, and the fixed time before division where the minimal elongation rate and protein capacity is reached: when septum formation is initiated after nucleoid segregation, the Z-ring forms and constricts at the division site, closely followed by peptidoglycan (PG) synthases[3,20] (figure 4.6b). This process requires energy, i.e. guanosine-triphosphate (GTP), which is also required for the initiation of ribosomal synthesis and thus directly related to the protein capacity[96]. This may result in a reduction of the protein capacity of the cell at a characteristic time before division. Furthermore, through the septal cell

wall synthesis, PG is sequestered towards the septal site[220]. Upon completion of the septum, 'normal' longitudinal growth resumes and more resources are available for protein synthesis, which is indicated by an increase in the protein capacity. Subsequently, the PG-layer that connects the new poles is hydrolysed. The hydrolysis of the connecting tissue together with the positive turgor pressure inside the cell leads to bulging of the new poles, which 'pushes' apart the newborn cells[91], leading to a perceived increase in length growth, i.e. the second growth phase (figure 4.6b).

The hypothesis that septum synthesis and pole formation are responsible for the increase in growth rate is supported by the relatively fixed time of the onset of the second growth phase: it was recently shown, that cell wall constriction time is growth rate independent[20]. Furthermore, since cell width does not change within conditions and hardly across conditions (figure S2 and S7), the septum area is fixed too. The consequences of this are twofold: 1.) cells have to synthesise the same amount of cell wall at the septal site, regardless of birth size and condition, resulting in a relatively larger resource requirement and thus stronger deviation from exponential growth in smaller cells. And 2.) the area which can be attacked by hydrolases to separate the newborn cells is roughly equal, and independent of birth size or condition, resulting in a constant time from completion of the septum to cell division[183]. At fast growth, the generation time can be shorter than the time that is required for septum formation and cell separation, meaning that septum formation gets initiated in the previous generation and we do not see the first growth phase at all (figure 4.6b).

Septum formation as the 'checkpoint' at which phase transition occurs is also supported by the relation between length and elongation rate. The size that is reached in the first phase, even by the smallest cells, is around 2.5 to 3 μm. The length of a single chromosome nucleoid has been determined to be 1.5 $\pm$ 0.25 μm in *B. subtilis*[183]. Cells that grow faster than the time that is required for DNA replication (C-period) and the time between replication termination and division (D-period) contain multiple partially replicated chromosomes, resulting in a larger nucleoid. Thus, septum formation can only occur at a length that is large enough to accommodate two nucleoids, whose size will depend on the generation time of the cell. This suggests that nucleoid separation and septum formation mark the transition between the two growth phases. Ultimately, cell cycle progression is concerted around DNA replication[26,38,215].

The constant elongation rate in the first growth phase implies that cell growth is linear during this period. Linear growth in an autocatalytic system indicates a limitation of some sort. In figure 4.5b we also observed a constant protein production rate, which indicates that protein synthesis is subject to this constraint as well. The existence of the biphasic expression pattern is independent of expression strength (figure S4). Again, one can speculate that resource limitation due to allocation to different processes is the underlying cause: DNA replication or synthesis of the divisome and PG-precursors in preparation of septum formation would be possible candidates, but also changes in the surface-area-to-volume ratio might play a role[66]. The accumulation of excess cell wall precursors was proposed recently as a mechanism that initiates cell wall constriction[66].

Conclusion

In this paper, we provided experimental evidence for the existence of distinct growth phases during the bacterial cell cycle that are likely a consequence of a mechanism that ensures cell size homeostasis. These dynamics could only be revealed through single cell measurements with high temporal resolution, as the population and end point measurements of single cells fulfilled the criteria for balanced, exponential growth.

We propose mechanisms that consolidate our growth and expression data with previous knowledge on DNA replication, segregation and cell septation. The validation or falsification of the proposed

models requires further investigation with simultaneous measurements of cell growth, DNA replication progression and cell wall synthesis with high temporal resolution.

Although the exact mechanisms of nucleoid segregation and cell division differ, it is reasonable to expect similar growth dynamics in other bacterial species, especially if resource (re)allocation dynamics lie at the heart of the behaviour we observe. Resource allocation and its management has in recent years received a lot of attention and has been shown to explain the often complex relationship between growth, metabolism and other physiological processes, for both prokaryotic and eukaryotic microbes[180,143,13,166], albeit not at a sub-cell-cycle resolution. Here we are left to speculate, that cell growth generates conditions inside a cell that requires the dynamic management of resources to ensure protein concentration homeostasis. This results in growth patterns that are more complex than explained by simply thinking of a cell as an unlimited autocatalytic system.

Moreover, the requirement to coordinate biosynthesis with cell cycle progress, suggests the existence of 'checkpoints' that need to be met before a cell can divide, in agreement with recent findings by other. Lastly, the low copy number of genomic DNA and continuous biosynthesis may cause temporal imbalances between these two processes that impact cell growth.

Methods

Strains and medium composition

For growth experiments, prototrophic *Bacillus subtilis* strain BSB1 [138] was revived in a defined morphilinopropanesulphonic acid (MOPS) - buffered minimal medium (MM) containing: 40 mM MOPS (adjusted to pH 7.4), 2 mM potassium phosphate (pH 7.0), 15 mM $(NH_4)_2SO_4$, and a trace element solution (final concentrations: 811 μM $MgSO_4$, 80 nM $MnCl_2$, 5 μM $FeCl_3$, 10 nM $ZnCl_2$, 30 nM $CoCl_2$ and 10 nM $CuSO_4$) [160]. Tris-Spizizen-salts (TSS) minimal medium composition was as following: 37.4 mM NH_4Cl, 1.5 mM K_2HPO_4, 49.5 mM TRIS, 1mM $MgSO_4$, 0.004% FeCl3 / 0.004% Na_3-citrate*$2H_2O$ [68] and trace elements as in the MM-medium. For solid TSS medium, 1.5% w/v low melt agarose was added.
The media were supplemented with different carbon sources to the following final concentrations: 6 mM arabinose, 5 mM glucose and 5 mM glucose with the amino acids methionine, histidine, glutamate and tryptophan to a final concentration of 1 mM each. We refer to these media as arabinose, glucose and glucose + 4 a.a., respectively. From a 1 M stock solution of isopropyl β-D-1-thiogalactopyranoside (IPTG) an appropriate amount was added to the medium to reach a final concentration of 50 or 1000 μM.
Escherichia coli strain JM109 (Promega) was used for cloning and amplification of plasmids. For cloning, *E. coli* and *Bacillus subtilis* were grown in LB + 0.5% w/v glucose supplemented with the appropriate antibiotic in the following concentrations: ampicillin, 100 μg/ml; spectinomycin 150 μg/ml. For LB plates, 1.5% w/v agar were added prior to autoclaving.
Plasmid pDR111-N015-superfolderGFP was constructed by amplifying the coding sequence of superfolderGFP (sfGFP) by PCR with primers N015 (ggtggtgctagcaggaggtgatccagtatgtctaaaggtgaagaactg) and N017 (ggtggtgcatgcttatttgtagagctcatccat), digestion of the product and backbone pDR111 [126] (*bla amyE' spc*^{R} $P_{hyperspank}$ *lacI 'amyE*; kind gift from David Rudner) with NheI and SphI and subsequent ligation. After transformation of chemocompetent *Escherichia coli* JM109 (Promega) and plasmid isolation, the identity of pDR111-N015-sfGFP was confirmed by sequencing. *Bacillus subtilis* strain B15 (BSB1 *spc*^{R} $P_{hyper-spank}$*-sfGFP lacI::amyE*) was constructed as following: pDR111-N015-sfGFP was linearised with SacII, added to a BSB1 culture grown in MM+glucose until starvation phase, and incubated for one hour before addition of fresh MM and plating on LB+glucose+spc for selection. Genomic insertion into *amyE* was confirmed by amylase deficiency, PCR and sequencing. The *amyE* locus is situated at $\approx 28^\circ$ on the genome.

Growth experiments

Cells were revived by inoculation directly from single-use 15% glycerol stocks into 50 ml Greiner tubes with 5 ml MM supplemented with IPTG and grown at 37° Celsius and 200 rpm. After 8 to 15 generations, the cultures reached an OD_{600} between 0.01 and 0.2 and were diluted in 50 ml Greiner tubes with 5 ml liquid TSS supplemented with IPTG and grown at 37° Celsius and 200 rpm for another 4 to 5 generations. After dilution to an OD_{600} of 0.01, 2 μl of the culture was transferred to a 1.5% low melt agarose pad freshly prepared with TSS.
Once seeded with cells, agarose pads were inverted and placed onto a glass bottom microwell dish (35 mm dish, 14 mm microwell, No. 1.5 coverglass) (Matek, USA), which was sealed with parafilm and immediately taken to the microscope for time-lapse imaging. Per carbon source, we carried out 5 independent growth experiments: *B. subtilis* B15 with 0, 50 and 1000 μM IPTG and the parent strain *B. subtilis* BSB1 with 0 and 1000 μM IPTG. For each experiment, we monitored growth at 4 different positions on the agar pad. For the analysis of the growth dynamics, we combined the data from all 5 independent experiments per carbon source, as we did not detect significant differences in the specific elongation rates, length at birth and length at division between strains and conditions (figure S8). The analysis of protein expression was carried out on the data sets of *B. subtilis* B15 at full induction (1000 μM IPTG).

Microscopy and data analysis

Imaging was performed with a Nikon Ti-E inverted microscope (Nikon, Japan) equipped with 100X oil objective (Nikon, CFI Plan Apo ? NA 1.45 WD 0.13), Zyla 5.5 sCmos camera (Andor, UK), brightfield LED light source (CoolLED pE-100), fluorescence LED light source (Lumencor, SOLA light engine), GFP filter set (Nikon Epi-Fl Filter Cube GFP-B), computer controlled shutters, automated stage and incubation chamber for temperature control. Temperature was set to 37°C at least three hours prior to starting an experiment. Nikon NIS-Elements AR software was used to control the microscope. Brightfield images (80 ms exposure time at 3.2% power) were acquired every minute for 8-15 hours. GFP fluorescence images (1 second exposure at 25% power) were acquired every 10 min. Time-lapse data were processed with custom MATLAB functions developed within our group. Briefly, an automated pipeline segmented every image, identifying individual cells and calculating their spatial features. Cells were assigned unique identifiers and were tracked in time, allowing for the calculation of time-dependent properties including cell ages, cell sizes (areas and lengths), elongation rates and generation times. In addition, the genealogy of every cell was recorded. The fluorescence values that we report here are the sum of all pixel intensities in the area of a cell contour. As a measure for fluorescence concentration we calculated the average pixel intensity in a fixed area in the centre of the cell. The output from the MATLAB pipeline was further analysed with MATHEMATICA, version 10 (Wolfram Research, Champaign, IL, USA), using custom scripts.

Calculation of instantaneous rates

Instantaneous (specific) elongation rate was calculated using a sliding-window approach. Briefly, a window of a given size (5, 10 or 15 minutes for fast, intermediate and slow growth, respectively) was moved along the time series of length measurements for each cell and the difference or Log-difference of the first and last data point of the window was calculated as elongation rate or specific elongation rate, respectively. This resulted in a time-series of instantaneous (specific) elongation rates for each cell. The average of each of these time-series per cell is reported as $\langle ER \rangle$ or $\langle sER \rangle$. Protein production rate was calculated similarly with a window size of 10 minutes, i.e. every time point where fluorescence was recorded, under all conditions. Protein capacity was obtained by normalising the protein production rate by cell length.

Binning by cell age

We binned time series data of all cells into 10 age bins of width 0.1 each. To avoid sampling bias resulting from varying interdivision times (IDT), i.e. overrepresentation of cells with long IDT per age bin due to fixed imaging intervals, we first binned the time series of individual cells into 10 age bins and averaged over each bin, before binning the data over the whole population/ birth length class.

Estimation of the growth phase transition prior to division

We estimated the time-to-division at which the elongation rate increases (figure 4.3e) by fitting a piecewise function to the data, using Wolfram MATHEMATICA's *FindFit* function. The piecewise function that we used describes the elongation rate as function of time-to-division and assumes that elongation rate is constant initially (a) and increases exponentially at a certain time-to-division (t_D):

$$\begin{cases} a & t < t_D \\ aE^{m(t-t_D)} & t \geq t_D \end{cases}$$

The function was fitted to the ensemble of data points from each birth length class, yielding 5 fits per growth condition.

Correction for fluorescence drift over the time course of an experiment

To correct for an increase of background fluorescence that occurred over the time course of an experiment, we normalised the fluorescence values of each experiment by estimating the background fluorescence over time (for an example see figure S9). For this, per position, we defined 2 regions where no cell growth occurred and measured the evolution of fluorescence over the duration of the experiment. Using MATLAB, we fitted a polynomial to the rescaled background fluorescence and normalised the fluorescence values of all cells by the fitted function.

Appendix

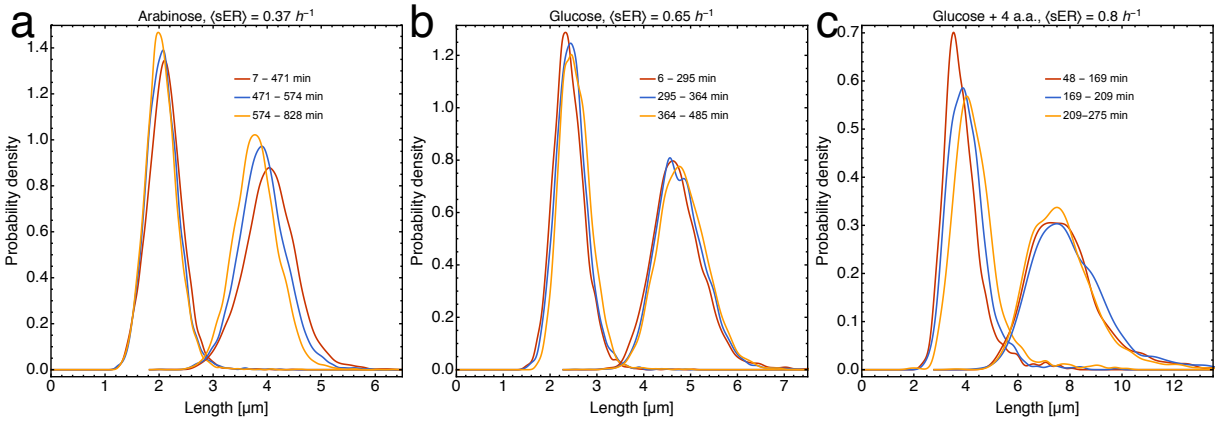

Figure S1: **Distributions of birth length and division length are stable for several generations, indicating balanced population growth.** Each distribution represents a third of all cells from the period of balanced growth (cf. figure S3). The legend indicates the time frame in which cells from the respective distribution were born.

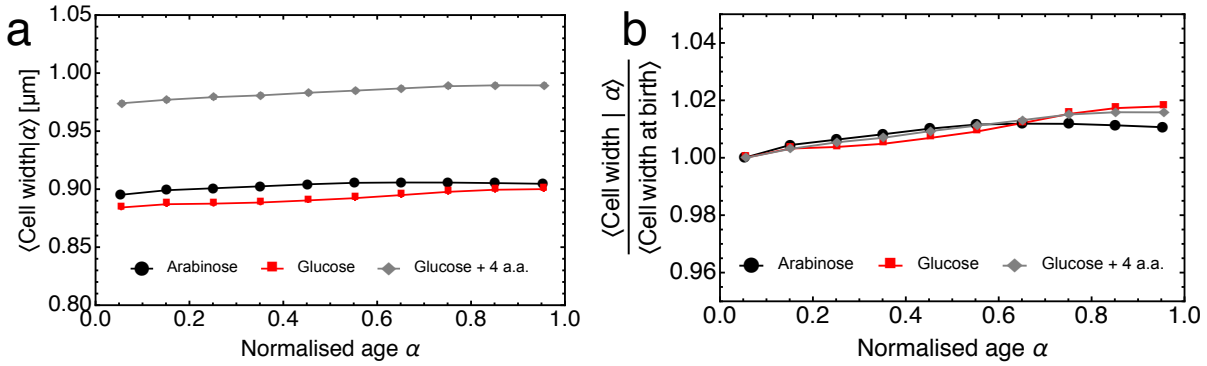

Figure S2: **Average cell width changes by less than 2% throughout the cell cycle.** Standard error bars are smaller than plot markers.

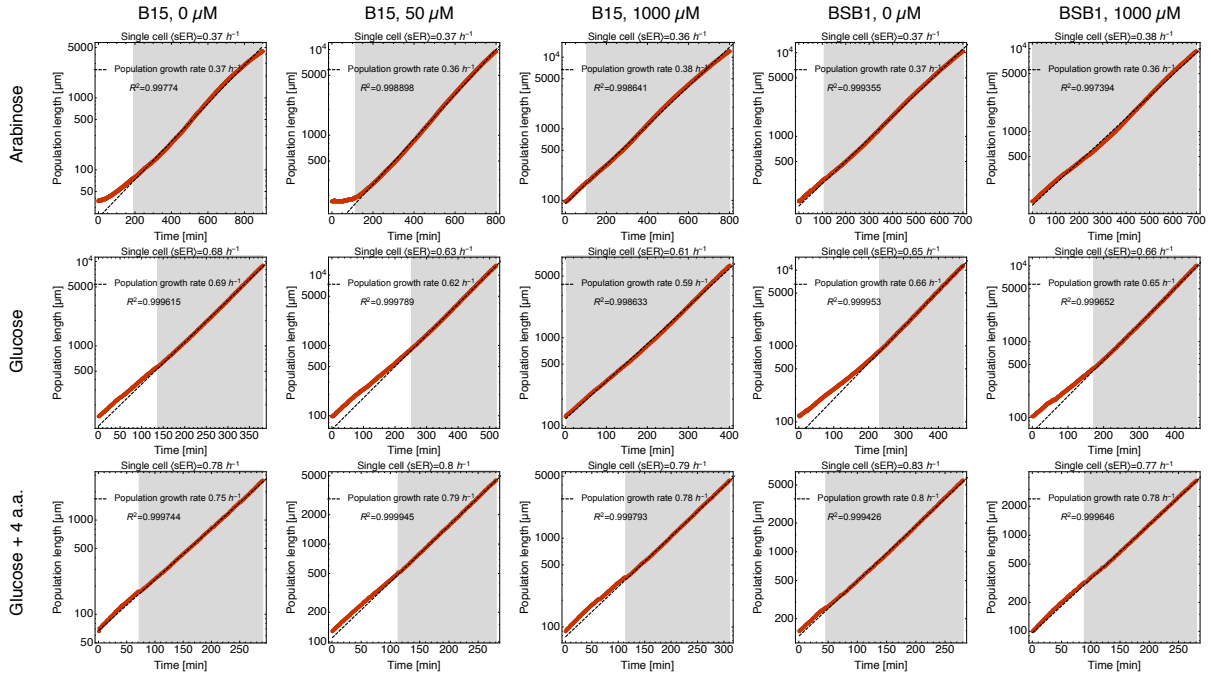

Figure S3: **Comparison between single cell average $\langle sER \rangle$ and population growth rate as measured by the length increase of the whole population.** The dashed line is a linear fit to the log-transformed total cell length of the population, the slope of which yields the specific growth rate. We define the region of exponential growth by an R^2-cutoff ($R^2 \geq 0.995$) of the fit to the log-transformed data (grey area). In all analyses in the main text, we only use cells that were born within the grey area.

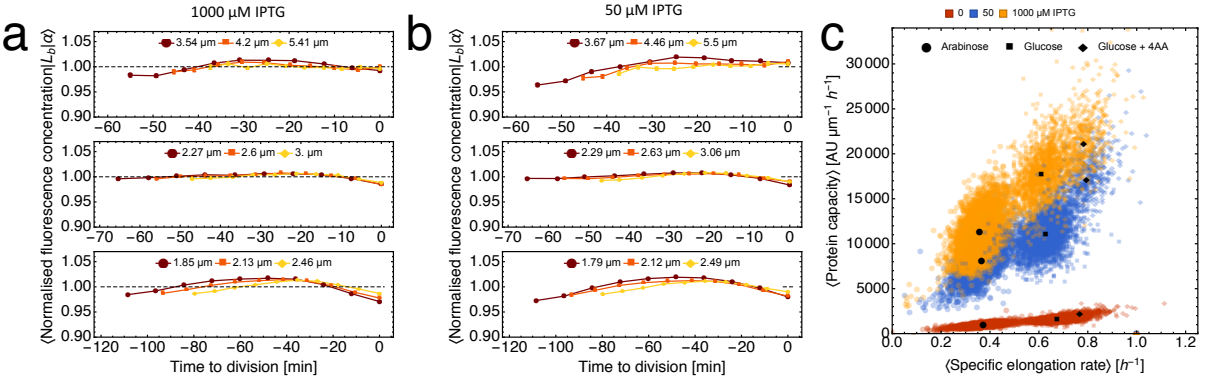

Figure S4: Normalised fluorescence concentration at induction with 1000 μM (**a.**, as in the main text) and 50 μM (**b.**) IPTG. **c.** Protein capacity increases with specific elongation rate. This indicates a scaling with the translational machinery [180].

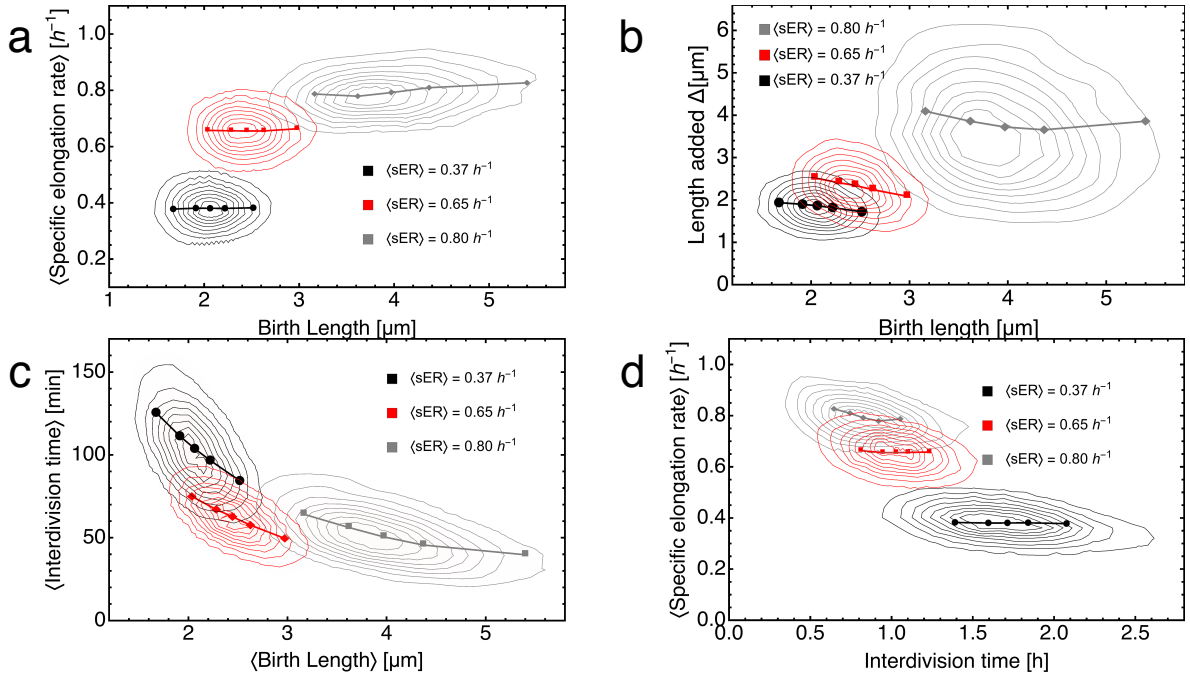

Figure S5: **Correlations related to cell size homeostasis. a.** Specific elongation rate is independent of birth length. **b.** The amount a cell grows before division is negatively correlated with birth length, i.e. smaller cells grow more. **c.** Interdivision time decreases with increasing birth length. **d.** Interdivision time and specific elongation rate are hardly correlated. The symbols represent the birth length classes from figures 4.3 and 4.5.

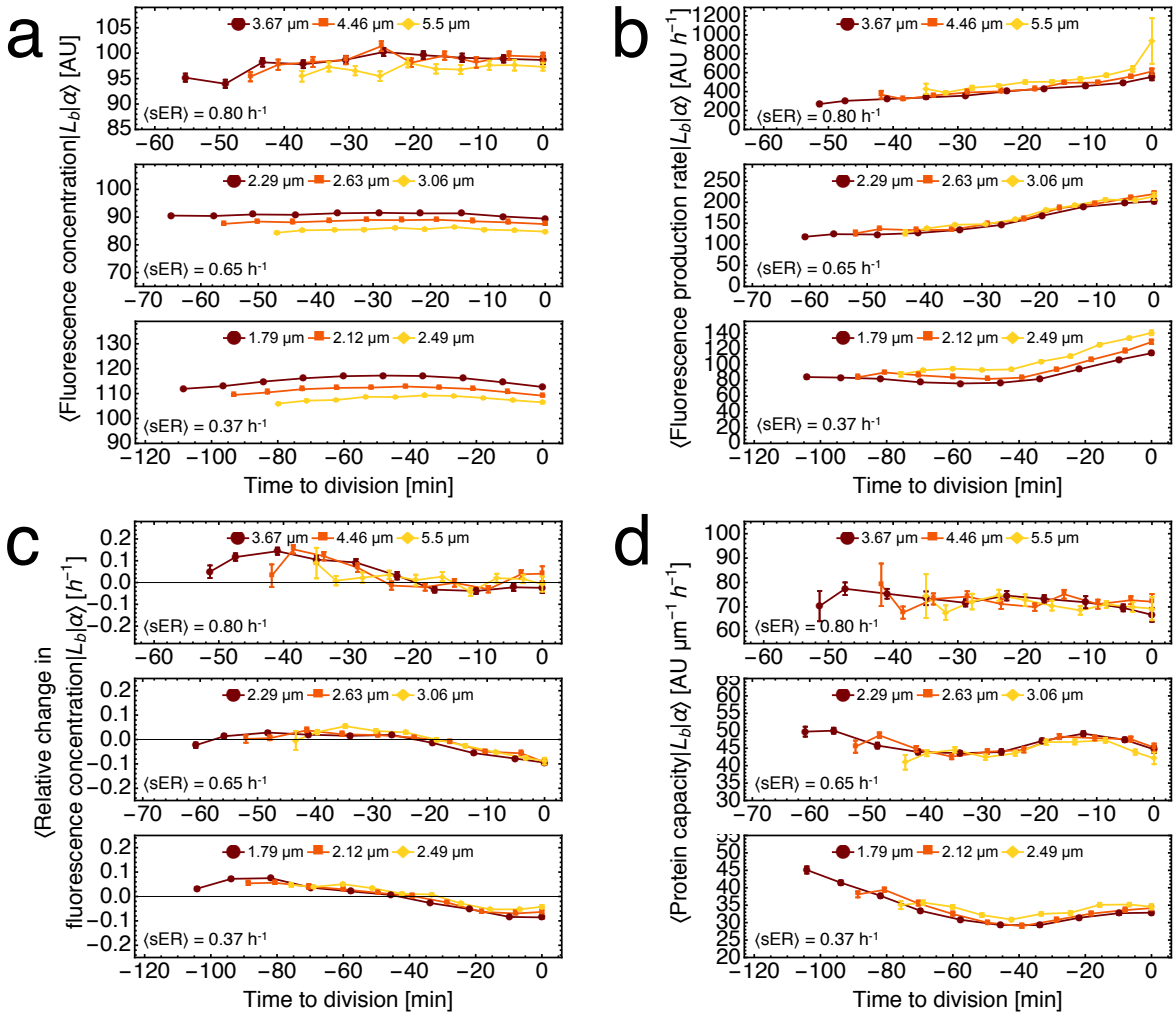

Figure S6: **Expression strength does not influence expression dynamics.** Same as figure 4.5, but with 50 μM IPTG added to the growth medium, instead of 1000 μM IPTG.

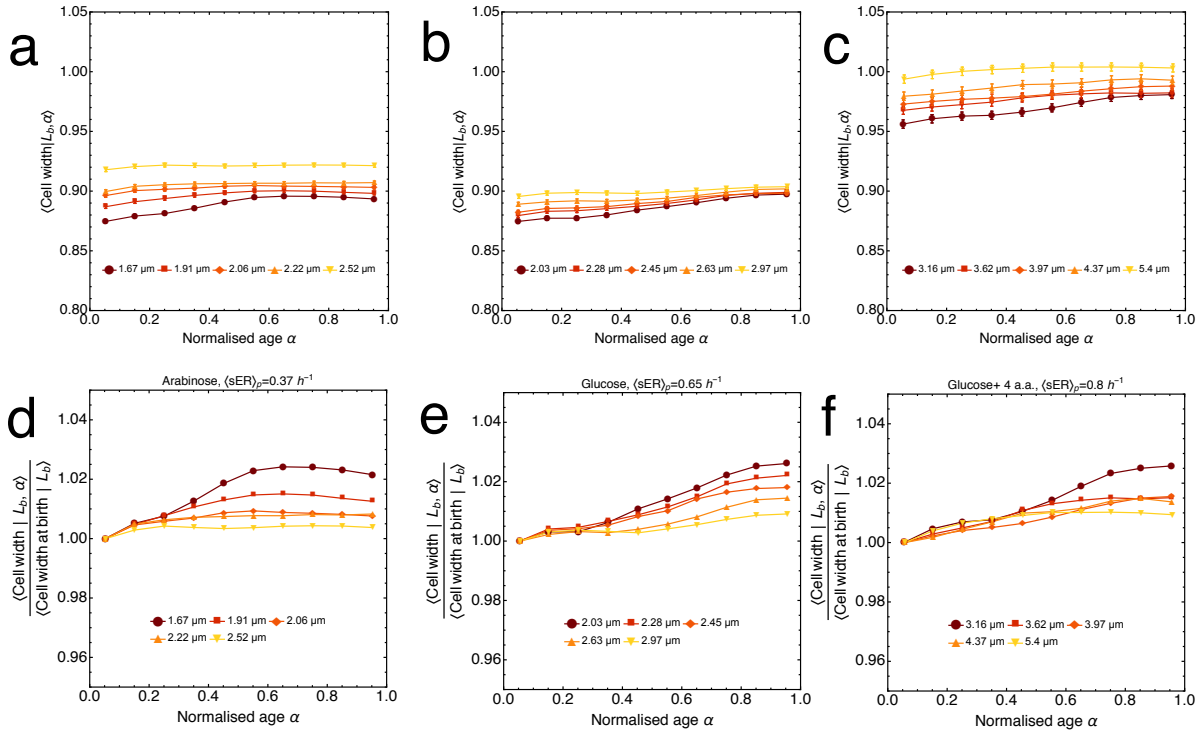

Figure S7: Average cell width of different birth length classes changes by $\leq$ 3% along the cell cycle.

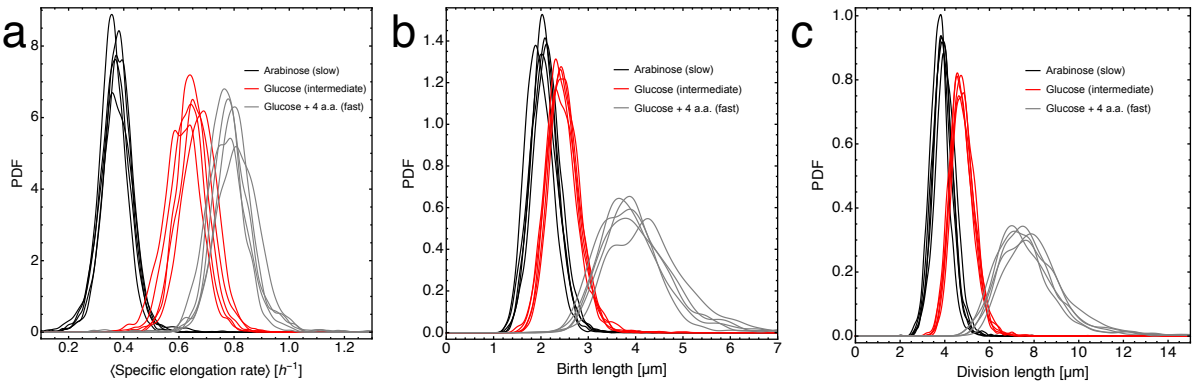

Figure S8: Distributions of specific elongation rate (**a.**), birth lengths (**b.**) and division lengths (**c.**) for all 5 experiments per carbon source. All 5 experiments per carbon source were combined for the growth analyses in the main text.

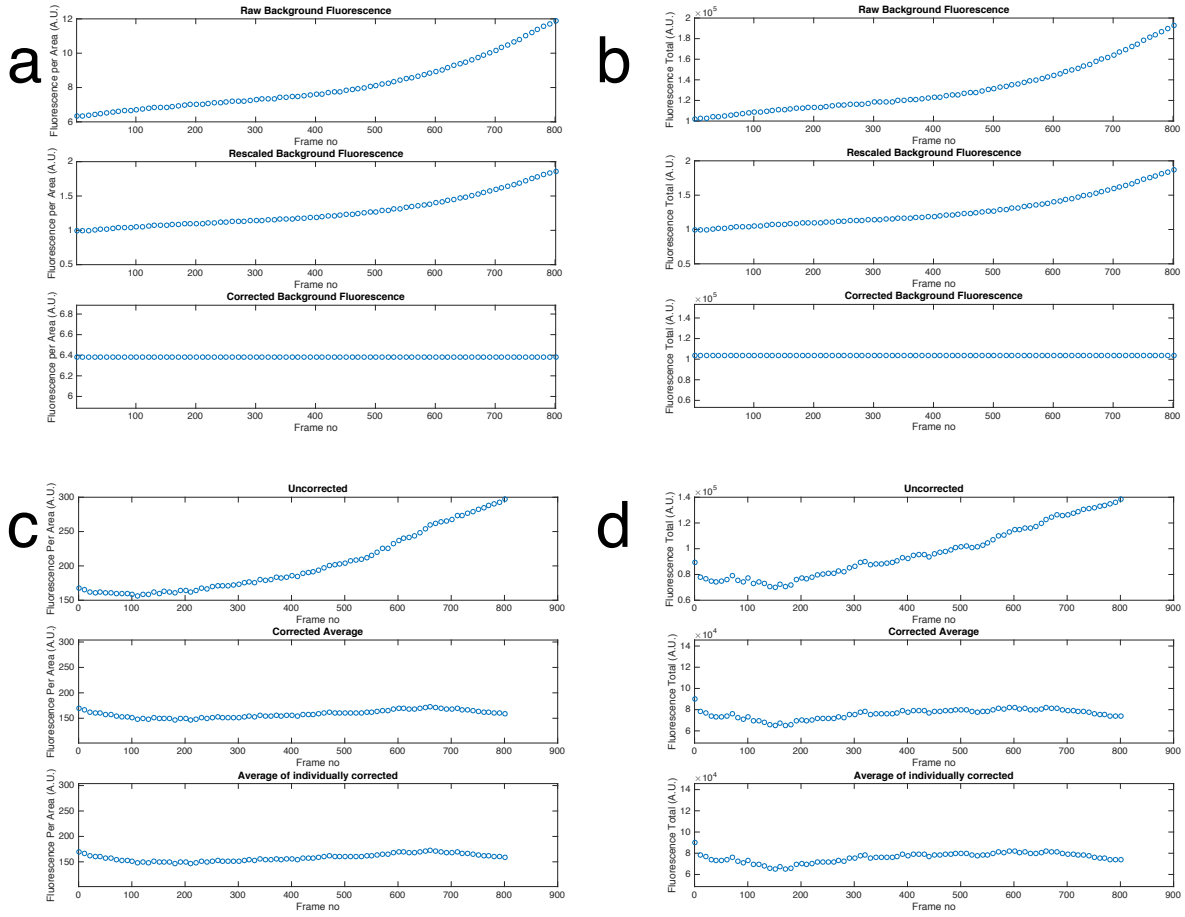

Figure S9: **Correction for fluorescence drift.** The drift in fluorescence over the course of each experiment was estimated from an area in the field of view without cell growth (**a., b.**, upper panel, see Methods for details). A polynomial function was fitted to the rescaled background fluorescence and used to normalise the fluorescence values of all cells (**c., d.**). The example shown here is for B15, grown on arabinose with 1000 μM IPTG added.

Chapter 5

General discussion

Introduction

In this chapter I will discuss some of our findings in the greater context of bacterial growth and gene expression. Based on current literature, and the results from this thesis, I will identify gaps in our understanding of bacterial growth and suggest future research directions and potential experiments to clarify some of these unknowns.

The advantages of studying single microbial cells sampled from a population at balanced growth

In this work we studied growth and gene expression, and their interrelation, in single *Bacillus subtilis* cells. All experiments were carried out specifically under conditions of balanced growth. The concept of balanced growth was introduced already in the 1950s-1970s, as a phenomenological description of a state of bacterial growth under which the distributions of cellular properties become time invariant[159,28,149]. This property makes the state of balanced growth an invaluable tool to study microbial growth, for several reasons.

From a practical perspective, the state of balanced growth is readily reproducible and it can be easily confirmed whether a population has reached this state or not. Carrying out experiments with a microbial population that is in a clearly defined physiological state eliminates many variables and improves reproducibility of the experimental results. By keeping the environmental conditions constant, we can focus more on the processes that take place inside a cell. Additionally, time invariance of the distributions of individual cellular properties immensely simplifies the mathematical treatment of microbial populations[159,149]. Another, minor practical advantage is, because the population properties are time-invariant, the exact time point of sampling from the population is not critical to the results of an experiment.

From a conceptual perspective, the characteristics of the stationary probability distributions of cellular properties in a certain constant environment bear a lot of information about the microorganism that is studied. For one, the shape, mean and variance of a distribution of a certain cellular property or molecule copy number are closely related to the processes that generate them, in this particular case growth and gene expression[179,153,7,39,172]. For instance, the age distribution of a population of asynchronously growing cells has a characteristic shape, with twice as many newborn than dividing cells (figure 1.1, top left). But even if we look at cells of the same age, their sizes, growth rates and molecular contents differ, due to stochastic fluctuations on the molecular and cellular scale[152,177,204]. Hence, the distributions of single-cell properties in a microbial population at balanced growth can be seen as a map of possible states that a single cell of this microorganism can potentially realise in a certain environment by virtue of its molecular and cellular organisation and the stochasticity that affects it.

The fact that microbial populations are at all able to achieve homeostasis in virtually any cellular property indicates the existence of compensating mechanisms that steer cells towards an environment dependent average. Without these mechanisms, the state of balanced growth would not exist. However, little is known about the underlying principles and molecular implementations of these control mechanisms, even in well studied model organisms such as *Escherichia coli* and *Bacillus subtilis*. These long standing problems have recently been revisited with modern single-cell measurement techniques, which enable us to confirm previous conjectures and provide a fresh perspective on unanswered questions.

Phenomenological principles of microbial growth and what we can learn from them

How cells achieve the state of balanced growth has been revisited extensively in recent years, using modern single-cell measurement techniques. These efforts resulted in phenomenological growth principles that describe how cells are able to maintain size homeostasis under various conditions[5,29,195]. Much like the microscopic growth theory by Powell[159], Painter & Marr[149] and Richmond & Collins[34], such phenomenological principles serve to identify and quantitatively describe relations between, for instance, the cellular growth rate and cell size[184,79]. These growth laws are often applicable to several species, in this specific case to all microorganisms that divide by binary fission[145,29,195,66]. However, even the meticulous and quantitative description of a biological phenomenon does not offer an explanation of the underlying mechanism, whose molecular implementations might differ between species.

If such laws and principles are merely descriptive, then what can we learn from them? The answer is, that these phenomenological principles clearly delineate the requirements a mechanism should meet. This can guide our intuition and help us to ask the right questions that ultimately lead to a mechanistic understanding, and the identification of the underlying molecular circuitry, of a phenomenological principle. To use an analogy: solving a jigsaw puzzle is much easier when we know what the final result is supposed to look like. Knowing the purpose a mechanism is supposed to achieve makes it easier to imagine the architecture of a mechanism or molecular circuit that could fulfil this purpose. For instance, observing the cell cycles of thousands of individual cells revealed that size homeostasis in several bacterial species is achieved by the addition of a roughly fixed cell length between birth and division, the so called 'adder' principle[5,29,195]. The molecular mechanisms that underlie this phenomenological principle are not understood, and they might differ between organisms. The validation of this decade-old 'adder' (or 'incremental') conjecture[211] with modern single-cell techniques inspired investigations that focus more on the mechanistic basis of cell size homeostasis in bacteria[215,184], again building on previous theory whose validation was limited by the time's technology[46]. The results of these studies suggest that cell size homeostasis is a side effect of the coordination of cell growth with DNA replication, rather than an active size-adaptation mechanism to environmental conditions[79,6,215]. Using mathematical modelling, it was demonstrated that the proposed mechanism could successfully reproduce deviations from the 'adder' behaviour at slow growth[215].

These findings bring us back to an earlier statement: the close relation between the distributions of single-cell properties and the process that generates these distributions. In order to understand how a microorganism achieves a state of balanced growth, and why the stationary distributions of cellular properties might or might not change depending on the environmental conditions, one needs to ultimately study the process that generates these distributions: the cell cycle of individual cells. To reflect this change in perspective, one can reformulate the question 'How does a population achieve time-invariant size distributions at balanced growth?' to 'How does a cell know when to divide?'.

Studying the growth behaviour of single bacterial cells as function of their cell cycle

Before a bacterial cell can divide and produce two newborn cells, it has to synthesise all molecular components that constitute a viable cell. In this process, the average cell doubles its size and mass and has to provide (at least) one complete copy of the genome per newborn cell. How bacterial cells ensure this and divide 'just in time' is still poorly understood. This reflects our rather limited

understanding of the bacterial cell cycle. The bacterial cell cycle itself is the amalgamation of countless, highly dynamic processes, which are also subject to stochastic fluctuations. These processes need to be coordinated, and stochastic fluctuations compensated, in order for a cell to grow and successfully divide. As a result, the size and molecular composition of a cell constantly changes throughout the cell cycle, which has consequences for the metabolic/physiological state of the cell.

A good indicator for the physiological state of a cell is its growth rate, which is closely tied to the metabolic state of the cell. Many cellular properties such as the macromolecular composition[44,180], cell size[195] and genome copy number[38] scale with growth rate. It also has the advantage that it is readily quantifiable for individual cells in any time-lapse microscopy setup. In order for a single cell to exhibit balanced growth, its metabolic state must be such that the cell grows exponentially with a fixed growth rate. The condition for this is that all intracellular concentrations remain constant. For simplicity, it is often assumed that, when a microbial population exhibits balanced growth, its individuals are in a balanced state as well[215,195]. In chapter 4 we have shown that this is not the case, and that individual cells systematically deviate from the expected growth behaviour. Thinking about the dynamic nature of the cell cycle and the multitude of processes that have to be coordinated, this result is not too surprising. Besides the stochastic fluctuations that affect the rates of biochemical reactions inside the cell, there are also 'deterministic' fluctuations throughout the cell cycle, such as the steady increase of cell size and the number of macromolecules, and transient events, such as cell division, DNA replication and segregation, or septum formation, that can all potentially perturb the metabolic homeostasis of a cell. Thus, balanced growth and metabolism of a single cell are the exception, rather than the rule. Campbell already anticipated this when he proposed the definition of balanced growth in the 1950s[28]. Whether a systemic, 'metabolic imbalance' is involved in the coordination of the bacterial cell cycle with cell growth is unknown. A recent study found that metabolic oscillations play a crucial role in the cell cycle progression of *S. cerevisiae*[151]. And also our results indicate that the systematic changes in the growth rate of individual cells at a fixed time to division might be involved in the coordination of the bacterial cell cycle with cell size and protein concentration homeostasis (chapter 4, discussion).

Adjusting its metabolic state might be necessary for a cell to compensate for the dynamic rearrangements that it undergoes during its lifetime, both on the molecular and cellular level. Our results from chapter 4 indicate such adjustments accompanied by systematic growth-rate changes along the cell cycle. The mechanisms that underlie these systematic deviations from exponential growth in *B. subtilis* can not immediately be deduced from our microscopy data. However, the combination of data on growth and gene expression allow for some 'educated guesses'.

The emerging picture: global events cause systematic deviations from exponential growth of single cells and activate compensating mechanisms

In chapter 4 we have identified two distinct growth phases in the cell cycle of *B. subtilis*. The first phase is characterised by a constant, or even decreasing, growth rate and a variable duration. In the second phase, the growth rate starts to increase at a set time to cell division. Despite the large systematic variations of growth rate, homeostasis in the concentration of a fluorescent reporter protein is maintained. In this section I will speculate on the identity of events in the bacterial cell cycle that might cause these deviations from exponential growth, for instance by altering the metabolic state of the cell. I will extend some of the ideas from chapter 4 and discuss alternative mechanistic explanations.

The criteria for an event, or a combination of events, that could potentially cause the systematic changes of growth rate as function of the cell cycle are:

- It should (on average) occur once in the lifetime of a cell
- It should affect the cell on a global level, in such a way that it increases the cell's growth rate
- It should be transient and take a fixed amount of time, regardless of the environmental conditions

One process that fulfils these criteria is genome replication. The genome of most bacteria consists of a single, circular chromosome. Replication gets initiated at a particular locus in the genome (the origin of replication, *oriC*) and proceeds bidirectionally down both arms of the chromosome until the replication forks meet at the terminus. The replication forks proceed at a presumably fixed, condition independent rate, which results in a constant time for the replication of a chromosome. The generation times of a bacterium, such as *B. subtilis* or *E. coli*, range from hours to minutes, depending on the environmental conditions. In order to achieve generation times that are shorter than the replication time of a chromosome, bacterial cells have to timeously initiate replication in previous generations. This results in multiple ongoing rounds of replication at once[38]. On the other hand, when the generation time is longer than the replication time, there are periods in a cell's life where DNA replication is absent. In these periods, the cell volume keeps expanding while the volume that is occupied by the nucleoid remains constant. This leads to an increase of the nucleoid-free fraction of the cytoplasm. As the nucleoid is not accessible for protein complexes, such as ribosomes[9], the increase in nucleoid-free volume might affect biochemical reaction rates through effects on molecular crowding[88]. This might contribute to the dynamic changes of growth rate and protein capacity.

Upon initiation of DNA replication, the nucleoid volume starts expanding, which again might cause a change in the ratio of cell volume to nucleoid volume. Additionally, it might lead to an increase of the rate of cell volume expansion, with a clearly defined rate-change point (RCP) as our modelling efforts have shown (chapter 4, box 1). After a roughly fixed time that is required for completion of replication and DNA segregation[38,183,215], the cell divides and the cycle starts anew. At fast growth there are no periods without DNA replication, making the effects of initiation of another round of DNA replication less pronounced (i.e. the changes are quantitative, not qualitative).

In our data, the RCP under all conditions occurs 30 - 40 minutes before division. The time for DNA replication in *B. subtilis* was estimated to be between 45 - 60 minutes, with another 20 - 30 minutes for the time between termination of replication and septum completion, adding up to a total of 65 - 90 minutes for a single round of replication and segregation[133,183]. When we consider cell birth (i.e. separation of sister cells) as the start of the cell cycle, and we maintain the constraint of a single replication initiation event per cell cycle, then it seems unlikely that replication initiation is responsible for the systematic changes in growth rate. However, septum formation occurs 20 - 35 minutes before cell separation in *B. subtilis*, which means that DNA replication and segregation have to be completed even before that[133,26,183]. When we redefine cell division (and birth) as the moment of septum completion, rather than cell separation, then the assumption of replication initiation contributing to the change in growth rate appears reasonable. DNA replication might then be already initiated after septum completion, way before cell separation. This redefinition is reasonable as it marks the time point after which partitioning of cellular resources into the new daughter cells is concluded. The fact that newly separated *B. subtilis* cells have a second, partially completed chromosome even under conditions where the generation time exceeds the time required for replication and segregation, supports this hypothesis[183,217]. In addition, cell division is a transient disruptive event that can introduce intracellular fluctuations and lead to metabolic imbalances, due to random, uneven partitioning of volume and cellular resources. Growth behaviour that indicates this was observed for *E. coli* in our lab (van Heerden *et al.*, unpuplished). These imbalances might

occur upon septum completion in *B. subtilis* and manifest as growth rate changes.

Despite the organisational differences between the two organisms, the famous model by Helmstetter & Cooper[38] for DNA replication in *E. coli* might be applicable to *B. subtilis* under the condition that septum completion is defined as the start of a new cell cycle.

In chapter 4 we discuss in more detail additional factors that might contribute to the dynamic changes in growth rate. These factors are:

- septum formation itself, as it could require the cell to reallocate resources towards cell wall synthesis
- hydrolysis of the peptidoglycan bond in order to separate septated cells, which might lead to bulging of the new poles, 'pushing' the cells apart prior to complete separation

Regardless of the mechanistic basis for the change in growth rate along the cell cycle of *B. subtilis*, our results indicate that cells do not only modulate their generation time[145], but also adjust their growth rate and metabolic state throughout the cell cycle as a way to compensate for intracellular fluctuations and to steer them towards an environment dependent, balanced state. The homeostasis in the expression levels that we observed for a constitutively expressed fluorescent protein in single cells, as well as the balanced state of the population, supports this conclusion. What properties a cell monitors in order to trigger such compensation mechanisms, and how it senses them, remains unknown. Changes in the surface-area to volume ratio, critical cell size or the ratio of the number of *oriC*'s to volume sensed by the concentration of an initiator molecule have all been suggested[215,184,46,50]. More generally, the changes in growth rate might be a consequence of a change in the rate limiting step of growth, for instance an altered ratio of cell volume to surface area[66].

Cost and benefit of non-genetic heterogeneity and gene expression noise in an evolutionary context

In chapter 2 we review current literature on the impact of non-genetic heterogeneity on the ability to survive in dynamic environments. As we point out in the discussion of that chapter, there are still many open questions regarding the biological function and evolutionary costs of non-genetic heterogeneity and molecular noise. To what extent does non-genetic heterogeneity in isogenic populations fulfil a function or a purpose and to what extent is it merely an inevitable side effect of molecular reactions? What are the evolutionary and metabolic costs of molecular noise and how can they be tuned?

Molecular stochasticity is ubiquitous and can have detrimental effects on the life of a microbial cell, by scrambling signals and reducing the accuracy of responses to environmental cues. In the most extreme cases, this can lead to maladaption of the cell to its environment with fatal consequences[205]. However, there are many examples where molecular stochasticity, and non-genetic heterogeneity that can arise from it, is harnessed by microorganisms to fulfil a biological function[118,1,140]. When evaluating stochasticity in biological systems with respect to a possible biological function, it is important to consider it in an evolutionary context. In their natural habitat, most microorganisms experience unpredictable environmental fluctuations, for instance in terms of temperature, nutrient availability or the occurrence of extinction-threatening conditions. In such environments, non-genetic heterogeneity can function to diversify the phenotypes in a microbial population and increase the chances of a genotype to survive sudden environmental changes in the future[10,21,31,175]. This can result in the formation of physiologically distinct subpopulations, such as persister cells, that are able to endure adverse conditions[10]. The frequency of persister formation

and the duration of this physiologically distinct state can be evolved, which illustrates the impact of non-genetic heterogeneity on the fitness of a genotype in dynamic environments[55,176,108].

The biological functions of molecular stochasticity and its impact on fitness can also be more subtle. For instance, it can affect the expression levels of metabolic enzymes across a population of microbes in order to 'prepare' a fraction of the population for sudden shifts between carbon sources[31,137,186]. Elevated expression noise is a way to increase gene expression plasticity, i.e. the responsiveness of expression across changing conditions, but at the same time it decreases accuracy in constant environments[106]. In unsteady conditions, plasticity might therefore be desirable and lead to the selection for increased expression noise of certain genes[186,222]. Counter-intuitively, random fluctuations in a signal molecule, e.g. a transcription factor, can even enhance signal transmission by increasing its sensitivity, by covering a wider range[155,154,123,80]. Transcriptional regulation can act to both attenuate and increase the expression noise of its target gene[24,222].

The examples discussed here illustrate that gene expression noise and non-genetic heterogeneity can confer a fitness advantage in uncertain, dynamic environments. They can act as rudimentary sensor systems in new or infrequent environments, where constitutive expression of a dedicated sensor and transporter system is too costly. Moreover, they are evolvable traits. However, their impact on fitness is difficult to quantify directly, as their objective and the environmental regimes under which they evolved are rarely known. These circumstances are further complicated by the fact that fitness is the result of a multi-parametric optimisation problem, where costs and benefits are set off against each other. I.e. for a comprehensive evaluation of the costs and benefits of gene expression noise in a single enzyme under natural conditions, one needs to measure the costs and benefits in different 'currencies', such as response time to environmental changes, energy requirements, occupation of biosynthetic capacity, accuracy or plasticity. These often involve trade-offs amongst each other. For instance, accuracy might come at the expense of plasticity. Alternatively, fitness might be measured in terms of parameters that are themselves the result of multidimensional inputs, for instance growth rate. However, growth rate is only directly related to fitness in the specific case where the objective is to produce offspring as fast as possible in order to outcompete other genotypes.

In contrast to the 'desirable' noise that can brace populations for sudden environmental changes, noise can also be detrimental and costly when the objective is to function robustly in constant conditions. As discussed in the previous paragraphs, constant growth permissive environments are likely the exception for most microorganisms in their natural habitat. However, cells are able to maintain fairly stable intracellular conditions. This is reflected by the relatively low noise levels that are exhibited by essential genes that form the scaffold of a cell, such as DNA maintenance, amino acid synthesis or cell division[137,186]. Accuracy is more important here, as being 'off' comes at immediate costs. Large fluctuations in these genes can have drastic consequences for the integrity and viability of a cell, thus they likely evolved to minimise expression noise. Noise minimisation can be achieved by brute force, i.e. high expression levels or long signal integration times, both of which entail costs (i.e. protein synthesis or reaction time, respectively)[107,105,146]. Alternatively, negative feedback regulation can be employed to reduce noise in the expression of a target gene[153,39]. This does not totally eliminate noise, but shifts it to a different component of the feedback loop[24]. Moreover, the proteins that constitute the loop come at an additional biosynthetic and energetic cost. The prevalence of such regulatory motifs is proof that these costs are offset by the benefit of low noise in the target gene. Despite the evolutionary efforts to minimise noise and non-genetic heterogeneity in certain genes, there are fundamental lower limits of expression noise ('noise floors') that can not be surpassed[107,196,105].

Understanding and quantifying the constraints that are imposed on gene expression noise and non-genetic heterogeneity, and their inherent limits, can help us to not only infer the evolutionary context in which a molecular circuit evolved[7,39]. It also is a requirement for targeted manipulation of

noise under artificial conditions, for example in biotechnological or medical settings. Under these predictable and often tightly controlled conditions, random fluctuations are often undesirable as they can reduce accuracy and therefore product yield and treatment efficiency. Due to the difficulties of quantifying the cost and benefits of noise experimentally, most studies that deal with this topic are of theoretical nature[203,218]. Formulating a unifying fitness theory, that provides a theoretical framework to guide our experimental efforts, is one of the big challenges in this field.

Perspective

The aim of this work was to characterise the interrelation between growth and gene expression, and the stochastic fluctuations therein, in a quantitative manner. The insights that we gained from our experimental results can aid our understanding of the complex cellular architecture that keeps *Bacillus subtilis* in balance under varying conditions.

We also find that there are still many gaps in our understanding of the bacterial cell cycle and its coordination with growth, especially from a mechanistic perspective. Most recent studies on this topic focussed on the gram-negative model bacterium *E. coli*[184,215]. However, our results indicate that the situation in *B. subtilis* and related bacteria might be different, despite some phenomenological similarities.

Further investigations on the level of single cells and tracking of individual molecules will be able to fill these gaps. In our particular case, simultaneous real-time observation of cell wall synthesis, DNA replication and nucleoid dynamics, and ideally ribosomal content and activity along the cell cycle could provide a mechanistic explanation for the growth dynamics which we observe in chapter 4 and the coordination of the cell cycle of *B. subtilis* in general. Septum formation and DNA replication dynamics may be tracked *in vivo* with time-lapse fluorescence microscopy and appropriate mutants (see Bisson-Filho *et al.*[20], Wang *et al.*[217], Wallden *et al.*[215]). Consolidating these measurements with dynamic growth measurements might serve to further our understanding of the bacterial cell cycle and its coordination with growth.

Directly quantifying the effects of gene expression noise on fitness might be achieved by an extensive cost-benefit analysis, similar to the approach by Dekel & Alon[43]. The experimental design could be modified to use a promoter library[132,222,82] in order to modulate expression noise and levels of the proteins involved in the utilisation of lactose, *lacZ* and *lacI*. Using promoters with similar averages and different noise levels could be used to quantify the effect of noise on fitness. Modulating the expression noise of *lacZ* could give insights about the costs of noise in a metabolic enzyme, whereas modulating the expression noise of *lacI* can tell us the effects of noisy regulation on fitness. Modifying the binding kinetics of *lacI*, or the number of DNA binding sites are alternative ways to change the noise in *lacI* activity. The read-out for fitness will be the cellular growth rate. Expression levels and noise may be monitored *in vivo*, using a fusion of the target proteins to fluorescent protein of different colours. Growth and expression levels/noise may be monitored in real-time with a time-lapse microscopy setup that uses microfluidics, similar to the one by Taniguchi *et al.*[196]. It allows the simultaneous observation of many genetic constructs, constant and dynamic environmental conditions (i.e. lactose pulsing), all on the level of single cells.

Questions that could be answered with such a setup are:

- What are the costs and benefits of noisy expression in constant and dynamic environments?
- Can noisy transcriptional regulation serve to increase plasticity while decreasing the protein costs for metabolic enzymes?

- Is the impact of noise on fitness constant across expression levels?
- How are the levels of gene expression noise related to the environmental dynamics?

Bibliography

Bibliography

[1] ACAR, M., METTETAL, J. T., AND VAN OUDENAARDEN, A. Stochastic switching as a survival strategy in fluctuating environments. *Nature genetics 40*, 4 (2008), 471–475.

[2] ACKERMANN, M., STECHER, B., FREED, N. E., SONGHET, P., HARDT, W.-D., AND DOEBELI, M. Self-destructive cooperation mediated by phenotypic noise. *Nature 454*, 7207 (Aug. 2008), 987–990.

[3] ADAMS, D. W., AND ERRINGTON, J. Bacterial cell division: assembly, maintenance and disassembly of the Z ring. *Nature reviews. Microbiology 7*, 9 (sep 2009), 642–53.

[4] AMATO, S. M., ORMAN, M. A., AND BRYNILDSEN, M. P. Metabolic control of persister formation in escherichia coli. *Molecular cell 50*, 4 (2013), 475–487.

[5] AMIR, A. Cell size regulation in bacteria. *Physical Review Letters 112*, 20 (may 2014), 208102.

[6] AMIR, A. Is cell size a spandrel? *eLife 6*, 7 (jul 2017), 1876–1885.

[7] AUSTIN, D. W., ALLEN, M. S., MCCOLLUM, J. M., DAR, R. D., WILGUS, J. R., SAYLER, G. S., SAMATOVA, N. F., COX, C. D., AND SIMPSON, M. L. Gene network shaping of inherent noise spectra. *Nature 439*, 7076 (feb 2006), 608–611.

[8] BAKSHI, S., DALRYMPLE, R. M., LI, W., CHOI, H., AND WEISSHAAR, J. C. Partitioning of RNA polymerase activity in live Escherichia coli from analysis of single-molecule diffusive trajectories. *Biophysical journal 105*, 12 (dec 2013), 2676–86.

[9] BAKSHI, S., SIRYAPORN, A., GOULIAN, M., AND WEISSHAAR, J. C. Superresolution imaging of ribosomes and RNA polymerase in live Escherichia coli cells. *Molecular microbiology 85*, 1 (2012), 21–38.

[10] BALABAN, N. Q., MERRIN, J., CHAIT, R., KOWALIK, L., AND LEIBLER, S. Bacterial Persistence as a Phenotypic Switch. *Science 305*, 5690 (2004).

[11] BAR-EVEN, A., PAULSSON, J., MAHESHRI, N., CARMI, M., O'SHEA, E., PILPEL, Y., AND BARKAI, N. Noise in protein expression scales with natural protein abundance. *Nature genetics 38*, 6 (jun 2006), 636–43.

[12] BAR-ZIV, R., VOICHEK, Y., AND BARKAI, N. Dealing with Gene-Dosage Imbalance during S Phase. *Trends in Genetics 32*, 11 (2016), 717–723.

[13] BASAN, M., HUI, S., OKANO, H., ZHANG, Z., SHEN, Y., WILLIAMSON, J. R., AND HWA, T. Overflow metabolism in Escherichia coli results from efficient proteome allocation. *Nature 528*, 7580 (dec 2015), 99–104.

[14] BEAUMONT, H. J., GALLIE, J., KOST, C., FERGUSON, G. C., AND RAINEY, P. B. Experimental evolution of bet hedging. *Nature 462*, 7269 (Nov 2009), 90–93.

[15] BECSKEI, A., AND SERRANO, L. Engineering stability in gene networks by autoregulation. *Nature 405*, June (jun 2000), 590–593.

[16] BENZER, S. Induced synthesis of enzymes in bacteria analyzed at the cellular level. *Biochimica et biophysica acta 11* (1953), 383–395.

[17] BERG, O. G. A model for the statistical fluctuations of protein numbers in a microbial population. *J Theor Biol 71*, 4 (Apr 1978), 587–603.

[18] BERGSTROM, C. T., AND LACHMANN, M. Shannon information and biological fitness. In *Information Theory Workshop, 2004. IEEE* (2004), IEEE, pp. 50–54.

[19] BERKHOUT, J., BOSDRIESZ, E., NIKEREL, E., MOLENAAR, D., DE RIDDER, D., TEUSINK, B., AND BRUGGEMAN, F. J. How biochemical constraints of cellular growth shape evolutionary adaptations in metabolism. *Genetics 194*, 2 (2013), 505–512.

[20] BISSON-FILHO, A. W., HSU, Y.-P., SQUYRES, G. R., KURU, E., WU, F., JUKES, C., SUN, Y., DEKKER, C., HOLDEN, S., VANNIEUWENHZE, M. S., BRUN, Y. V., AND GARNER, E. C. Treadmilling by FtsZ filaments drives peptidoglycan synthesis and bacterial cell division. *Science 355*, 6326 (2017), 739–743.

[21] BLAKE, W. J., BALÁZSI, G., KOHANSKI, M. A., ISAACS, F. J., MURPHY, K. F., KUANG, Y., CANTOR, C. R., WALT, D. R., AND COLLINS, J. J. Phenotypic Consequences of Promoter-Mediated Transcriptional Noise. *Molecular Cell 24*, 6 (dec 2006), 853–865.

[22] BOLDOGH, I. R., AND PON, L. A. Interactions of mitochondria with the actin cytoskeleton. *Biochimica et Biophysica Acta (BBA) - Molecular Cell Research 1763*, 5-6 (may 2006), 450–462.

[23] BOULINEAU, S., TOSTEVIN, F., KIVIET, D. J., TEN WOLDE, P. R., NGHE, P., AND TANS, S. J. Single-cell dynamics reveals sustained growth during diauxic shifts. *PLoS One 8*, 4 (2013).

[24] BRUGGEMAN, F. J., BLÜTHGEN, N., AND WESTERHOFF, H. V. Noise management by molecular networks. *PLoS Computational Biology 5*, 9 (sep 2009), e1000506.

[25] BULL, J. Evolution of phenotypic variance. *Evolution* (1987), 303–315.

[26] BURDETT, I. D. J., KIRKWOOD, T. B. L., AND WHALLEY, J. B. Growth kinetics of individual Bacillus subtilis cells and correlation with nucleoid extension. *Journal of Bacteriology 167*, 1 (jul 1986), 219–230.

[27] CAI, L., FRIEDMAN, N., AND XIE, X. S. Stochastic protein expression in individual cells at the single molecule level. *Nature 440*, 7082 (mar 2006), 358–362.

[28] CAMPBELL, A. Synchronization of cell division. *Bacteriological reviews 21*, 4 (dec 1957), 263–72.

[29] CAMPOS, M., SUROVTSEV, I. V., KATO, S., PAINTDAKHI, A., BELTRAN, B., EBMEIER, S. E., AND JACOBS-WAGNER, C. A constant size extension drives bacterial cell size homeostasis. *Cell 159*, 6 (dec 2014), 1433–46.

[30] CHABOT, J. R., PEDRAZA, J. M., LUITEL, P., AND VAN OUDENAARDEN, A. Stochastic gene expression out-of-steady-state in the cyanobacterial circadian clock. *Nature 450*, 7173 (dec 2007), 1249–1252.

[31] CHOI, P. J., CAI, L., FRIEDA, K., AND XIE, X. S. A Stochastic Single-Molecule Event Triggers Phenotype Switching of a Bacterial Cell. *Science 322*, 5900 (2008), 442–446.

[32] CHONG, S., CHEN, C., GE, H., AND XIE, X. S. Mechanism of transcriptional bursting in bacteria. *Cell 158*, 2 (jul 2014), 314–326.

[33] COHEN, A. A., KALISKY, T., MAYO, A., GEVA-ZATORSKY, N., DANON, T., ISSAEVA, I., KOPITO, R. B., PERZOV, N., MILO, R., SIGAL, A., AND ALON, U. Protein dynamics in individual human cells: Experiment and theory. *PLoS ONE 4*, 4 (2009).

[34] COLLINS, J. F., AND RICHMOND, M. H. Rate of growth of Bacillus cereus between divisions. *Journal of general microbiology 28*, May (1962), 15–33.

[35] COOPER, S. Rate and Topography of Cell-Wall Synthesis During the Division Cycle of Salmonella typhimurium. *Journal of Bacteriology 170*, 1 (jan 1988), 422–430.

[36] COOPER, S. The Constrained Hoop : Length during an Explanation of the Overshoot a Shift-Up of Escherichia colit in Cell. *J. Bacteriol. 171*, 10 (1989), 5239–5243.

[37] COOPER, S. Bacterial growth and division : biochemistry and regulation of prokaryotic and eukaryotic division cycles.

[38] COOPER, S., AND HELMSTETTER, C. E. Chromosome replication and the division cycle of Escherichia coli. *Journal of Molecular Biology 31*, 3 (feb 1968), 519–540.

[39] COX, C. D., MCCOLLUM, J. M., ALLEN, M. S., DAR, R. D., AND SIMPSON, M. L. Using noise to probe and characterize gene circuits. *Proceedings of the National Academy of Sciences of the United States of America 105*, 31 (aug 2008), 10809–14.

[40] DAR, R. D., RAZOOKY, B. S., SINGH, A., TRIMELONI, T. V., MCCOLLUM, J. M., COX, C. D., SIMPSON, M. L., AND WEINBERGER, L. S. Transcriptional burst frequency and burst size are equally modulated across the human genome. *Proceedings of the National Academy of Sciences of the United States of America 109*, 43 (oct 2012), 17454–9.

[41] DAR, R. D., RAZOOKY, B. S., WEINBERGER, L. S., COX, C. D., AND SIMPSON, M. L. The low noise limit in gene expression. *PLoS ONE 10*, 10 (oct 2015), e0140969.

[42] DAS NEVES, R. P., JONES, N. S., ANDREU, L., GUPTA, R., ENVER, T., AND IBORRA, F. J. Connecting Variability in Global Transcription Rate to Mitochondrial Variability. *PLoS Biology 8*, 12 (dec 2010), e1000560.

[43] DEKEL, E., AND ALON, U. Optimality and evolutionary tuning of the expression level of a protein. *Nature 436*, 7050 (jul 2005), 588–92.

[44] DENNIS, P. P., AND BREMER, H. Macromolecular composition during steady-state growth of Escherichia coli B-r. *Journal of bacteriology 119*, 1 (jul 1974), 270–81.

[45] DERIS, J. B., KIM, M., ZHANG, Z., OKANO, H., HERMSEN, R., GROISMAN, A., AND HWA, T. The Innate Growth Bistability and Fitness Landscapes of Antibiotic-Resistant Bacteria. *Science 342*, 6162 (Nov. 2013), 1237435–1237435.

[46] DONACHIE, W. D. Relationship between Cell Size and Time of Initiation of DNA Replication. *Nature 219*, 5158 (sep 1968), 1077–1079.

[47] DONALDSON-MATASCI, M. C., BERGSTROM, C. T., AND LACHMANN, M. The fitness value of information. *Oikos 119*, 2 (2010), 219–230.

[48] ELDAR, A., AND ELOWITZ, M. B. Functional roles for noise in genetic circuits. *Nature 467*, 7312 (2010), 167–173.

[49] ELOWITZ, M. B., LEVINE, A. J., SIGGIA, E. D., AND SWAIN, P. S. Stochastic gene expression in a single cell. *Science (New York, N.Y.) 297*, 5584 (aug 2002), 1183–6.

[50] FANTES, P., GRANT, W., PRITCHARD, R., SUDBERY, P., AND WHEALS, A. The regulation of cell size and the control of mitosis. *Journal of Theoretical Biology 50*, 1 (1975), 213–244.

[51] FENG, J., KESSLER, D. A., BEN-JACOB, E., AND LEVINE, H. Growth feedback as a basis for persister bistability. *Proceedings of the National Academy of Sciences 111*, 1 (2014), 544–549.

[52] FISHOV, I., ZARITSKY, A., AND GROVER, N. B. On microbial states of growth. *Molecular Microbiology 15*, 5 (mar 1995), 789–794.

[53] FRANK, S. A. Natural selection. i. variable environments and uncertain returns on investment. *Journal of evolutionary biology 24*, 11 (2011), 2299–2309.

[54] FRANKEL, N. W., PONTIUS, W., DUFOUR, Y. S., LONG, J., HERNANDEZ-NUNEZ, L., AND EMONET, T. Adaptability of non-genetic diversity in bacterial chemotaxis. *Elife 3* (2014), e03526.

[55] FRIDMAN, O., GOLDBERG, A., RONIN, I., SHORESH, N., AND BALABAN, N. Q. Optimization of lag time underlies antibiotic tolerance in evolved bacterial populations. *Nature 513*, 7518 (2014), 418–421.

[56] FRIEDMAN, N., CAI, L., AND XIE, X. S. Linking stochastic dynamics to population distribution: An analytical framework of gene expression. *Physical Review Letters 97*, 16 (oct 2006), 168302.

[57] FUNG, D. K., CHAN, E. W., CHIN, M. L., AND CHAN, R. C. Delineation of a bacterial starvation stress response network which can mediate antibiotic tolerance development. *Antimicrobial agents and chemotherapy 54*, 3 (2010), 1082–1093.

[58] FUTCHER, B. Metabolic cycle, cell cycle, and the finishing kick to Start. *Genome biology 7*, 4 (jan 2006), 107.

[59] GAÁL, B., PITCHFORD, J. W., AND WOOD, A. J. Exact results for the evolution of stochastic switching in variable asymmetric environments. *Genetics 184*, 4 (2010), 1113–1119.

[60] GOLDING, I., PAULSSON, J., ZAWILSKI, S. M., AND COX, E. C. Real-time kinetics of gene activity in individual bacteria. *Cell 123*, 6 (dec 2005), 1025–1036.

[61] GREULICH, P., SCOTT, M., EVANS, M. R., AND ALLEN, R. J. Growth-dependent bacterial susceptibility to ribosome-targeting antibiotics. *Molecular systems biology 11*, 3 (2015), 796.

[62] GUIDO, N. J., LEE, P., WANG, X., ELSTON, T. C., AND COLLINS, J. J. A pathway and genetic factors contributing to elevated gene expression noise in stationary phase. *Biophysical journal 93*, 11 (dec 2007), L55–7.

[63] GUIMARAES, J. C., ROCHA, M., AND ARKIN, A. P. Transcript level and sequence determinants of protein abundance and noise in Escherichia coli. *Nucleic Acids Research 42*, 8 (2014), 4791–4799.

[64] HACCOU, P., AND IWASA, Y. Optimal mixed strategies in stochastic environments. *Theoretical population biology 47*, 2 (1995), 212–243.

[65] HANSEN, A. S., AND O'SHEA, E. K. Promoter decoding of transcription factor dynamics involves a trade-off between noise and control of gene expression. *Molecular Systems Biology 9*, 1 (apr 2013), 704.

[66] HARRIS, L. K., AND THERIOT, J. A. Relative rates of surface and volume synthesis set bacterial cell size. *Cell 165*, 6 (jun 2016), 1479–1492.

[67] HARVEY, R. J., MARR, A. G., AND PAINTER, P. R. Kinetics of growth of individual cells of Escherichia coli and Azotobacter agilis. *J. Bacteriol. 93*, 2 (Feb 1967), 605–617.

[68] HARWOOD, C. R., AND CUTTING, S. M. *Molecular biological methods for Bacillus*. Wiley, 1990.

[69] HILFINGER, A., AND PAULSSON, J. Separating intrinsic from extrinsic fluctuations in dynamic biological systems. *Proceedings of the National Academy of Sciences of the United States of America 108*, 29 (jul 2011), 12167–12172.

[70] HILL, N. S., KADOYA, R., CHATTORAJ, D. K., AND LEVIN, P. A. Cell size and the initiation of DNA replication in bacteria. *PLoS Genetics 8*, 3 (mar 2012), e1002549.

[71] HINTSCHE, M., AND KLUMPP, S. Dilution and the theoretical description of growth-rate dependent gene expression. *Journal of biological engineering 7*, 1 (jan 2013), 22.

[72] HOLMES, M., RICKERT, M., AND PIERUCCI, O. Cell division cycle of Bacillus subtilis: Evidence of variability in period D. *Journal of Bacteriology 142*, 1 (apr 1980), 254–261.

[73] HORNUNG, G., BAR-ZIV, R., ROSIN, D., TOKURIKI, N., TAWFIK, D. S., OREN, M., AND BARKAI, N. Noise-mean relationship in mutated promoters. *Genome Research 22*, 12 (dec 2012), 2409–2417.

[74] HUGHES, A. L., AND GOTTSCHLING, D. E. An early age increase in vacuolar pH limits mitochondrial function and lifespan in yeast. *Nature 492*, 7428 (nov 2012), 261–265.

[75] HUH, D., AND PAULSSON, J. Non-genetic heterogeneity from stochastic partitioning at cell division. *Nature genetics 43*, 2 (2011), 95–100.

[76] HUH, D., AND PAULSSON, J. Random partitioning of molecules at cell division. *Proceedings of the National Academy of Sciences of the United States of America 108*, 36 (sep 2011), 15004–9.

[77] HUI, S., SILVERMAN, J. M., CHEN, S. S., ERICKSON, D. W., BASAN, M., WANG, J., HWA, T., AND WILLIAMSON, J. R. Quantitative proteomic analysis reveals a simple strategy of global resource allocation in bacteria. *Molecular systems biology 11*, 2 (2015), 784.

[78] JONES, D. L., BREWSTER, R. C., AND PHILLIPS, R. Promoter architecture dictates cell-to-cell variability in gene expression. *Science 346*, 6216 (2014), 1533–1536.

[79] JUN, S., AND RUST, M. J. A Fundamental Unit of Cell Size in Bacteria. *Trends in Genetics 33*, 7 (jul 2017), 433–435.

[80] KELLOGG, R. A., AND TAY, S. Noise facilitates transcriptional control under dynamic inputs. *Cell 160*, 3 (2015), 381–392.

[81] KEMPE, H., SCHWABE, A., CRÉMAZY, F., VERSCHURE, P. J., AND BRUGGEMAN, F. J. The volumes and transcript counts of single cells reveal concentration homeostasis and capture biological noise. *Molecular biology of the cell 26*, 4 (feb 2015), 797–804.

[82] KEREN, L., HAUSSER, J., LOTAN-POMPAN, M., VAINBERG SLUTSKIN, I., ALISAR, H., KAMINSKI, S., WEINBERGER, A., ALON, U., MILO, R., AND SEGAL, E. Massively Parallel Interrogation of the Effects of Gene Expression Levels on Fitness. *Cell 166*, 5 (aug 2016), 1282–1294.e18.

[83] KEREN, L., VAN DIJK, D., WEINGARTEN-GABBAY, S., DAVIDI, D., JONA, G., WEINBERGER, A., MILO, R., AND SEGAL, E. Noise in gene expression is coupled to growth rate. *Genome Research 25*, 12 (dec 2015), 1893–1902.

[84] KEREN, L., ZACKAY, O., LOTAN-POMPAN, M., BARENHOLZ, U., DEKEL, E., SASSON, V., AIDELBERG, G., BREN, A., ZEEVI, D., WEINBERGER, A., ALON, U., MILO, R., AND SEGAL, E. Promoters maintain their relative activity levels under different growth conditions. *Molecular systems biology 9* (jan 2013), 701.

[85] KIVIET, D. J., NGHE, P., WALKER, N., BOULINEAU, S., SUNDERLIKOVA, V., AND TANS, S. J. Stochasticity of metabolism and growth at the single-cell level. *Nature 514*, 7522 (sep 2014), 376–379.

[86] KLECKNER, N., FISHER, J. K., STOUF, M., WHITE, M. A., BATES, D., AND WITZ, G. The bacterial nucleoid: Nature, dynamics and sister segregation, dec 2014.

[87] KLUMPP, S., AND HWA, T. Bacterial growth: global effects on gene expression, growth feedback and proteome partition. *Current Opinion in Biotechnology 28* (aug 2014), 96–102.

[88] KLUMPP, S., AND SCOTT, M. Molecular crowding limits translation and cell growth. *Proceedings of the National Academy of Sciences of the United States of America*, 1 (sep 2013), 1–6.

[89] KLUMPP, S., ZHANG, Z., AND HWA, T. Growth rate-dependent global effects on gene expression in bacteria. *Cell 139*, 7 (dec 2009), 1366–75.

[90] KOCH, A. Growth and form of the bacterial cell wall. 327–341.

[91] KOCH, A. L., AND DOYLE, R. J. The growth strategy of the Gram-positive rod. *FEMS Microbiology Letters 32*, 3-4 (1986), 247–254.

[92] KOCHANOWSKI, K., VOLKMER, B., GEROSA, L., VAN RIJSEWIJK, B. R. H., SCHMIDT, A., AND HEINEMANN, M. Functioning of a metabolic flux sensor in escherichia coli. *Proceedings of the National Academy of Sciences 110*, 3 (2013), 1130–1135.

[93] KORCH, S. B., HENDERSON, T. A., AND HILL, T. M. Characterization of the hipa7 allele of escherichia coli and evidence that high persistence is governed by (p) ppgpp synthesis. *Molecular microbiology 50*, 4 (2003), 1199–1213.

[94] KORT, R., KEIJSER, B., AND CASPERS, M. Transcriptional activity around bacterial cell death reveals molecular biomarkers for cell viability. *BMC . . . 9* (jan 2008), 590.

[95] KOTTE, O., VOLKMER, B., RADZIKOWSKI, J. L., AND HEINEMANN, M. Phenotypic bistability in Escherichia coli's central carbon metabolism. *Molecular systems biology 10*, 7 (jul 2014), 736.

[96] KRÁSNÝ, L., AND GOURSE, R. L. An alternative strategy for bacterial ribosome synthesis: Bacillus subtilis rRNA transcription regulation. *The EMBO journal 23*, 22 (nov 2004), 4473–83.

[97] KUBITSCHEK, H. E. Bilinear cell growth of Escherichia coli. *Journal of Bacteriology 148*, 2 (nov 1981), 730–733.

[98] KUDLA, G., MURRAY, A. W., TOLLERVEY, D., AND PLOTKIN, J. B. Coding-sequence determinants of gene expression in Escherichia coli. *Science (New York, N.Y.) 324*, 5924 (apr 2009), 255–8.

[99] KUNST, F., OGASAWARA, N., MOSZER, I., ALBERTINI, A. M., ALLONI, G., AZEVEDO, V., BERTERO, M. G., BESSIÈRES, P., BOLOTIN, A., BORCHERT, S., BORRISS, R., BOURSIER, L., BRANS, A., BRAUN, M., BRIGNELL, S. C., BRON, S., BROUILLET, S., BRUSCHI, C. V., CALDWELL, B., CAPUANO, V., CARTER, N. M., CHOI, S. K., CODANI, J. J., CONNERTON, I. F., AND DANCHIN, A. The complete genome sequence of the gram-positive bacterium Bacillus subtilis. *Nature 390*, 6657 (nov 1997), 249–56.

[100] KUSSELL, E. Evolution in microbes. *Annual review of biophysics 42* (2013), 493–514.

[101] KUSSELL, E., KISHONY, R., BALABAN, N. Q., AND LEIBLER, S. Bacterial persistence. *Genetics 169*, 4 (2005), 1807–1814.

[102] KUSSELL, E., AND LEIBLER, S. Phenotypic diversity, population growth, and information in fluctuating environments. *Science 309*, 5743 (2005), 2075–2078.

[103] LAM, F. H., STEGER, D. J., AND O'SHEA, E. K. Chromatin decouples promoter threshold from dynamic range. *Nature 453*, 7192 (2008), 246–250.

[104] LAMBERT, G., AND KUSSELL, E. Memory and fitness optimization of bacteria under fluctuating environments. *PLoS Genet 10*, 9 (2014), e1004556.

[105] LEHNER, B. Selection to minimise noise in living systems and its implications for the evolution of gene expression. *Molecular systems biology 4*, 170 (2008), 170.

[106] LEHNER, B. Conflict between noise and plasticity in yeast. *PLoS Genetics 6*, 11 (nov 2010), e1001185.

[107] LESTAS, I., VINNICOMBE, G., AND PAULSSON, J. Fundamental limits on the suppression of molecular fluctuations. *Nature 467*, 7312 (sep 2010), 174–178.

[108] LEVIN-REISMAN, I., RONIN, I., GEFEN, O., BRANISS, I., SHORESH, N., AND BALABAN, N. Q. Antibiotic tolerance facilitates the evolution of resistance. *Science 355*, 6327 (2017), 826–830.

[109] LEVINE, J. H., FONTES, M. E., DWORKIN, J., AND ELOWITZ, M. B. Pulsed feedback defers cellular differentiation. *PLoS Biology 10*, 1 (jan 2012), e1001252.

[110] LEVY, S. F., ZIV, N., AND SIEGAL, M. L. Bet hedging in yeast by heterogeneous, age-correlated expression of a stress protectant. *PLoS biology 10*, 5 (jan 2012), e1001325.

[111] LEWIS, K. Persister Cells. *Annu. Rev. Microbiol 64*, 1 (oct 2010), 357–72.

[112] LI, G.-W., BURKHARDT, D., GROSS, C., AND WEISSMAN, J. S. Quantifying absolute protein synthesis rates reveals principles underlying allocation of cellular resources. *Cell 157*, 3 (apr 2014), 624–35.

[113] LI, G.-W., AND XIE, X. S. Central dogma at the single-molecule level in living cells. *Nature 475*, 7356 (2011), 308–315.

[114] LI, S. C., AND KANE, P. M. The yeast lysosome-like vacuole: Endpoint and crossroads. *Biochimica et Biophysica Acta (BBA) - Molecular Cell Research 1793*, 4 (2009), 650–663.

[115] LIN, W.-H., AND KUSSELL, E. Complex interplay of physiology and selection in the emergence of antibiotic resistance. *Current Biology 26*, 11 (2016), 1486–1493.

[116] LINDNER, A. B., MADDEN, R., DEMAREZ, A., STEWART, E. J., AND TADDEI, F. Asymmetric segregation of protein aggregates is associated with cellular aging and rejuvenation. *Proceedings of the National Academy of Sciences 105*, 8 (feb 2008), 3076–3081.

[117] LOCKE, J. C., AND ELOWITZ, M. B. Using movies to analyse gene circuit dynamics in single cells. *Nature Reviews Microbiology 7*, 5 (2009), 383–392.

[118] MAAMAR, H., RAJ, A., AND DUBNAU, D. Noise in gene expression determines cell fate in Bacillus subtilis. *Science 317*, 5837 (jul 2005), 526–529.

[119] MAGNUSSON, L. U., FAREWELL, A., AND NYSTRÖM, T. ppGpp: a global regulator in Escherichia coli. *Trends in microbiology 13*, 5 (may 2005), 236–42.

[120] MAISONNEUVE, E., CASTRO-CAMARGO, M., AND GERDES, K. (p) ppGpp controls bacterial persistence by stochastic induction of toxin-antitoxin activity. *Cell 154*, 5 (2013), 1140–1150.

[121] MALONEY, P. C., AND ROTMAN, B. Distribution of suboptimally induces -d-galactosidase in escherichia coli. the enzyme content of individual cells. *J Mol Biol 73*, 1 (Jan 1973), 77–91.

[122] MATHIS, R., AND ACKERMANN, M. Response of single bacterial cells to stress gives rise to complex history dependence at the population level. *Proceedings of the National Academy of Sciences* (mar 2016), 201511509.

[123] MCDONNELL, M. D., AND ABBOTT, D. What is stochastic resonance? Definitions, misconceptions, debates, and its relevance to biology, may 2009.

[124] MCINERNY, C. J. Cell cycle-regulated transcription in fission yeast. *Biochemical Society transactions 32*, Pt 6 (dec 2004), 967–72.

[125] MCQUARRIE, D. A. Stochastic approach to chemical kinetics. *Journal of Applied Probability 4*, 3 (1967), 413–478.

[126] MEESKE, A. J., RILEY, E. P., ROBINS, W. P., UEHARA, T., MEKALANOS, J. J., KAHNE, D., WALKER, S., KRUSE, A. C., BERNHARDT, T. G., AND RUDNER, D. Z. SEDS proteins are a widespread family of bacterial cell wall polymerases. *Nature 537* (2016), 1–15.

[127] MISRA, G., ROJAS, E. R., GOPINATHAN, A., AND HUANG, K. C. Mechanical consequences of cell-wall turnover in the elongation of a gram-positive bacterium. *Biophysical Journal 104*, 11 (jun 2013), 2342–2352.

[128] MOLENAAR, D., VAN BERLO, R., DE RIDDER, D., AND TEUSINK, B. Shifts in growth strategies reflect tradeoffs in cellular economics. *Molecular systems biology 5*, 1 (2009), 323.

[129] MONOD, J. The Growth of Bacterial Cultures. *Annual Review of Microbiology 3*, 1 (oct 1949), 371–394.

[130] MUNSKY, B., NEUERT, G., AND VAN OUDENAARDEN, A. Using Gene Expression Noise to Understand Gene Regulation. *Science 336*, 6078 (apr 2012), 183–187.

[131] MURPHY, K. F., BALÁZSI, G., AND COLLINS, J. J. Combinatorial promoter design for engineering noisy gene expression. *Proceedings of the National Academy of Sciences of the United States of America 104*, 31 (jul 2007), 12726–31.

[132] MUTALIK, V. K., GUIMARAES, J. C., CAMBRAY, G., LAM, C., CHRISTOFFERSEN, M. J., MAI, Q.-A., TRAN, A. B., PAULL, M., KEASLING, J. D., ARKIN, A. P., AND ENDY, D. Precise and reliable gene expression via standard transcription and translation initiation elements. *Nature methods 10*, 4 (apr 2013), 354–60.

[133] NANNINGA, N., AND KOPPES, L. J. H. The Cell Cycle of Bacillus subtilis as Studied by Electron Microscopy. *Archives of Microbiology 181* (1979), 173–181.

[134] NARULA, J., KUCHINA, A., ZHANG, F., FUJITA, M., SÜEL, G. M., AND IGOSHIN, O. A. Slowdown of growth controls cellular differentiation. *Molecular systems biology 12*, 5 (may 2016), 871.

[135] NATHAN, L. P.-T., GLENN, D. L., AND JOHAN, V. Synchronous long-term oscillations in a synthetic gene circuit. *Nature 538*, 7626 (oct 2016), 1–4.

[136] NEW, A. M., CERULUS, B., GOVERS, S. K., PEREZ-SAMPER, G., ZHU, B., BOOGMANS, S., XAVIER, J. B., AND VERSTREPEN, K. J. Different levels of catabolite repression optimize growth in stable and variable environments. *PLoS biology 12*, 1 (jan 2014), e1001764.

[137] NEWMAN, J. R. S., GHAEMMAGHAMI, S., IHMELS, J., BRESLOW, D. K., NOBLE, M., DERISI, J. L., AND WEISSMAN, J. S. Single-cell proteomic analysis of S. cerevisiae reveals the architecture of biological noise. *Nature 441*, 7095 (jun 2006), 840–6.

[138] NICOLAS, P., MÄDER, U., DERVYN, E., ROCHAT, T., LEDUC, A., PIGEONNEAU, N., BIDNENKO, E., MARCHADIER, E., HOEBEKE, M., AYMERICH, S., BECHER, D., BISICCHIA, P., BOTELLA, E., DELUMEAU, O., DOHERTY, G., DENHAM, E. L., FOGG, M. J., FROMION, V., GOELZER, A., HANSEN, A., HÄRTIG, E., HARWOOD, C. R., HOMUTH, G., JARMER, H., JULES, M., KLIPP, E., LE CHAT, L., LECOINTE, F., LEWIS, P., LIEBERMEISTER, W., MARCH, A., MARS, R. A. T., NANNAPANENI, P., NOONE, D., POHL, S., RINN, B., RÜGHEIMER, F., SAPPA, P. K., SAMSON, F., SCHAFFER, M., SCHWIKOWSKI, B., STEIL, L., STÜLKE, J., WIEGERT, T., DEVINE, K. M., WILKINSON, A. J., VAN DIJL, J. M., HECKER, M., VÖLKER, U., BESSIÈRES, P., AND NOIROT, P. Condition-dependent transcriptome reveals high-level regulatory architecture in Bacillus subtilis. *Science (New York, N.Y.) 335*, 6072 (mar 2012), 1103–6.

[139] NORDHOLT, N., VAN HEERDEN, J., KORT, R., AND BRUGGEMAN, F. J. Effects of growth rate and promoter activity on single-cell protein expression. *Scientific Reports 7*, 1 (2017), 6299.

[140] NORMAN, T. M., LORD, N. D., PAULSSON, J., AND LOSICK, R. Memory and modularity in cell-fate decision making. *Nature 503*, 7477 (nov 2013), 481–6.

[141] NORMAN, T. M., LORD, N. D., PAULSSON, J., AND LOSICK, R. Stochastic switching of cell fate in microbes. *Annual review of microbiology 69* (2015), 381–403.

[142] NOVICK, A., AND WEINER, M. Enzyme induction as an all-or-none phenomenon. *Proceedings of the National Academy of Sciences 43*, 7 (1957), 553–566.

[143] O'BRIEN, E. J., LERMAN, J. A., CHANG, R. L., HYDUKE, D. R., AND PALSSON, B. Ø. Genome-scale models of metabolism and gene expression extend and refine growth phenotype prediction. *Molecular systems biology 9*, 693 (apr 2013), 693.

[144] ORMAN, M. A., AND BRYNILDSEN, M. P. Inhibition of stationary phase respiration impairs persister formation in e. coli. *Nature communications 6* (2015).

[145] OSELLA, M., NUGENT, E., AND COSENTINO LAGOMARSINO, M. Concerted control of Escherichia coli cell division. *Proceedings of the National Academy of Sciences 111*, 9 (mar 2014), 3431–3435.

[146] OZBUDAK, E. M., THATTAI, M., KURTSER, I., GROSSMAN, A. D., AND VAN OUDENAARDEN, A. Regulation of noise in the expression of a single gene. *Nature genetics 31*, 1 (may 2002), 69–73.

[147] OZBUDAK, E. M., THATTAI, M., LIM, H. N., SHRAIMAN, B. I., AND VAN OUDENAARDEN, A. Multistability in the lactose utilization network of escherichia coli. *Nature 427*, 6976 (2004), 737–740.

[148] PAGE, R., AND PETI, W. Toxin-antitoxin systems in bacterial growth arrest and persistence. *Nature chemical biology 12*, 4 (2016), 208–214.

[149] PAINTER, P. R., AND MARR, A. G. Mathematics of microbial populations. *Annual review of microbiology 22* (jan 1968), 519–48.

[150] PAPAGIANNAKIS, A., NIEBEL, B., WIT, E. C., AND HEINEMANN, M. Autonomous metabolic oscillations robustly gate the early and late cell cycle. *Molecular Cell* (2016).

[151] PAPAGIANNAKIS, A., NIEBEL, B., WIT, E. C., AND HEINEMANN, M. Autonomous Metabolic Oscillations Robustly Gate the Early and Late Cell Cycle. *Molecular Cell 0*, 0 (dec 2016), 516–526.

[152] PAULSSON, J. Summing up the noise in gene networks. *Nature 427*, 6973 (2004), 415–8.

[153] PAULSSON, J. Models of stochastic gene expression. *Physics of Life Reviews 2*, 2 (jun 2005), 157–175.

[154] PAULSSON, J., BERG, O. G., AND EHRENBERG, M. Stochastic focusing: fluctuation-enhanced sensitivity of intracellular regulation. *Proceedings of the National Academy of Sciences of the United States of America 97*, 13 (jun 2000), 7148–53.

[155] PAULSSON, J., AND EHRENBERG, M. Random signal fluctuations can reduce random fluctuations in regulated components of chemical regulatory networks. *Physical review letters 84*, 23 (jun 2000), 5447–5450.

[156] PÉDELACQ, J.-D., CABANTOUS, S., TRAN, T., TERWILLIGER, T. C., AND WALDO, G. S. Engineering and characterization of a superfolder green fluorescent protein. *Nature biotechnology 24*, 1 (jan 2006), 79–88.

[157] PEDRAZA, J. M., AND PAULSSON, J. Effects of molecular memory and bursting on fluctuations in gene expression. *Science 319*, January (2008), 339–343.

[158] PEDRAZA, J. M., AND VAN OUDENAARDEN, A. Noise propagation in gene networks. *Science (New York, N.Y.) 307*, 5717 (mar 2005), 1965–9.

[159] POWELL, E. O. Growth Rate and Generation Time of Bacteria, with Special Reference to Continuous Culture. *Journal of general microbiology 15*, 3 (dec 1956), 492–511.

[160] QUE, Q., AND HELMANN, J. D. Manganese homeostasis in Bacillus subtilis is regulated by MntR, a bifunctional regulator related to the diphtheria toxin repressor family of proteins. *Molecular Microbiology 35*, 6 (jan 2002), 1454–1468.

[161] QUISEL, J. D., BURKHOLDER, W. F., AND GROSSMAN, A. D. In vivo effects of sporulation kinases on mutant Spo0A proteins in bacillus subtilis. *Journal of Bacteriology 183*, 22 (nov 2001), 6573–6578.

[162] RADZIKOWSKI, J. L., VEDELAAR, S., SIEGEL, D., ORTEGA, Á. D., SCHMIDT, A., AND HEINEMANN, M. Bacterial persistence is an active σs stress response to metabolic flux limitation. *Molecular Systems Biology 12*, 9 (2016), 882.

[163] RAJ, A., AND VAN OUDENAARDEN, A. Nature, nurture, or chance: stochastic gene expression and its consequences. *Cell 135*, 2 (2008), 216–226.

[164] RANG, C. U., PENG, A. Y., POON, A. F., AND CHAO, L. Ageing in Escherichia coli requires damage by an extrinsic agent. *Microbiology 158*, Pt_6 (jun 2012), 1553–1559.

[165] REED, J. L., AND PALSSON, B. Ø. Genome-scale in silico models of e. coli have multiple equivalent phenotypic states: assessment of correlated reaction subsets that comprise network states. *Genome Research 14*, 9 (2004), 1797–1805.

[166] REIMERS, A.-M., KNOOP, H., BOCKMAYR, A., AND STEUER, R. Cellular trade-offs and optimal resource allocation during cyanobacterial diurnal growth. *Proceedings of the National Academy of Sciences 114*, 31 (aug 2017), 201617508.

[167] RIVOIRE, O., AND LEIBLER, S. The value of information for populations in varying environments. *Journal of Statistical Physics 142*, 6 (2011), 1124–1166.

[168] ROSENFELD, N., YOUNG, J. W., ALON, U., SWAIN, P. S., AND ELOWITZ, M. B. Gene regulation at the single-cell level. *Science (New York, N.Y.) 307*, 5717 (mar 2005), 1962–5.

[169] ROTEM, E., LOINGER, A., RONIN, I., LEVIN-REISMAN, I., GABAY, C., SHORESH, N., BIHAM, O., AND BALABAN, N. Q. Regulation of phenotypic variability by a threshold-based mechanism underlies bacterial persistence. *Proceedings of the National Academy of Sciences of the United States of America* (2010), 1–6.

[170] RUSTICI, G., MATA, J., KIVINEN, K., LIÓ, P., PENKETT, C. J., BURNS, G., HAYLES, J., BRAZMA, A., NURSE, P., AND BÄHLER, J. Periodic gene expression program of the fission yeast cell cycle. *Nature genetics 36*, 8 (aug 2004), 809–17.

[171] SANCHEZ, A., CHOUBEY, S., AND KONDEV, J. Regulation of Noise in Gene Expression [review]. *Annual review of biophysics 42*, March (may 2013), 1–23.

[172] SANCHEZ, A., GARCIA, H. G., JONES, D., PHILLIPS, R., AND KONDEV, J. Effect of promoter architecture on the cell-to-cell variability in gene expression. *PLoS Computational Biology 7*, 3 (mar 2011), e1001100.

[173] SANCHEZ, A., AND GOLDING, I. Genetic Determinants and Cellular Constraints in Noisy Gene Expression. *Science 342*, 6163 (dec 2013), 1188–1193.

[174] SCHAECHTER, M., MAALOE, O., AND KJELDGAARD, N. O. Dependency on Medium and Temperature of Cell Size and Chemical Composition during Balanced Growth of Salmonella typhimurium. *Journal of General Microbiology 19*, 3 (dec 1958), 592–606.

[175] SCHREIBER, F., LITTMANN, S., LAVIK, G., ESCRIG, S., MEIBOM, A., KUYPERS, M., AND ACKERMANN, M. Phenotypic heterogeneity driven by nutrient limitation promotes growth in fluctuating environments. *Nature Microbiology in press*, May (may 2016), 1–7.

[176] SCHUMACHER, M. A., BALANI, P., MIN, J., CHINNAM, N. B., HANSEN, S., VULIĆ, M., LEWIS, K., AND BRENNAN, R. G. HipBA–promoter structures reveal the basis of heritable multidrug tolerance. *Nature 524*, 7563 (jul 2015), 59–64.

[177] SCHWABE, A., AND BRUGGEMAN, F. J. Contributions of cell growth and biochemical reactions to nongenetic variability of cells. *Biophysical Journal 107*, 2 (jul 2014), 301–313.

[178] SCHWABE, A., AND BRUGGEMAN, F. J. Single yeast cells vary in transcription activity not in delay time after a metabolic shift. *Nature communications 5* (2014), 4798.

[179] SCHWABE, A., DOBRZYŃSKI, M., RYBAKOVA, K., VERSCHURE, P., AND BRUGGEMAN, F. J. Origins of stochastic intracellular processes and consequences for cell-to-cell variability and cellular survival strategies. *Methods in enzymology 500* (jan 2011), 597–625.

[180] SCOTT, M., GUNDERSON, C., AND MATEESCU, E. Interdependence of cell growth and gene expression: origins and consequences. *Science 330*, 6007 (nov 2010), 1099–1102.

[181] SHAHREZAEI, V., AND MARGUERAT, S. Connecting growth with gene expression: of noise and numbers. *Current opinion in microbiology 25* (jun 2015), 127–35.

[182] SHARON, E., VAN DIJK, D., KALMA, Y., KEREN, L., MANOR, O., YAKHINI, Z., AND SEGAL, E. Probing the effect of promoters on noise in gene expression using thousands of designed sequences. *Genome Research 24*, 10 (oct 2014), 1698–1706.

[183] SHARPE, M. E., HAUSER, P. M., SHARPE, R. G., AND ERRINGTON, J. Bacillus subtilis cell cycle as studied by fluorescence microscopy: constancy of cell length at initiation of DNA replication and evidence for active nucleoid partitioning. *Journal of bacteriology 180*, 3 (feb 1998), 547–55.

[184] SI, F., LI, D., COX, S. E., SAULS, J. T., AZIZI, O., SOU, C., SCHWARTZ, A. B., ERICKSTAD, M. J., JUN, Y., LI, X., AND JUN, S. Invariance of Initiation Mass and Predictability of Cell Size in Escherichia coli, may 2017.

[185] SIGAL, A., MILO, R., COHEN, A., GEVA-ZATORSKY, N., KLEIN, Y., LIRON, Y., ROSENFELD, N., DANON, T., PERZOV, N., AND ALON, U. Variability and memory of protein levels in human cells. *Nature 444*, 7119 (nov 2006), 643–646.

[186] SILANDER, O. K., NIKOLIC, N., ZASLAVER, A., BREN, A., KIKOIN, I., ALON, U., AND ACKERMANN, M. A genome-wide analysis of promoter-mediated phenotypic noise in Escherichia coli. *PLoS Genetics 8*, 1 (jan 2012), e1002443.

[187] SLAGER, J., AND VEENING, J.-W. Hard-Wired Control of Bacterial Processes by Chromosomal Gene Location. *Trends in Microbiology* (2016).

[188] SLAVOV, N., AIROLDI, E. M., VAN OUDENAARDEN, A., AND BOTSTEIN, D. A conserved cell growth cycle can account for the environmental stress responses of divergent eukaryotes. *Molecular biology of the cell 23*, 10 (may 2012), 1986–97.

[189] SMITS, W. K., KUIPERS, O. P., AND VEENING, J.-W. Phenotypic variation in bacteria: the role of feedback regulation. *Nature Rev. Microbiol 4*, 4 (apr 2006), 259–271.

[190] SOLOPOVA, A., VAN GESTEL, J., WEISSING, F. J., BACHMANN, H., TEUSINK, B., KOK, J., AND KUIPERS, O. P. Bet-hedging during bacterial diauxic shift. *Proceedings of the National Academy of Sciences of the United States of America 111*, 20 (may 2014), 1–6.

[191] SOMPAYRAC, L., AND MAALØE, O. Autorepressor Model for Control of DNA Replication. *Nature 241*, 109 (1973), 133–135.

[192] STEWART, E. J., MADDEN, R., PAUL, G., AND TADDEI, F. Aging and death in an organism that reproduces by morphologically symmetric division. *PLoS biology 3*, 2 (feb 2005), e45.

[193] STOCKWELL, S. R., LANDRY, C. R., AND RIFKIN, S. A. The yeast galactose network as a quantitative model for cellular memory. *Molecular bioSystems 11*, 1 (jan 2015), 28–37.

[194] SWAIN, P. S., ELOWITZ, M. B., AND SIGGIA, E. D. Intrinsic and extrinsic contributions to stochasticity in gene expression. *Proceedings of the National Academy of Sciences of the United States of America 99*, 20 (2002), 12795–800.

[195] TAHERI-ARAGHI, S., BRADDE, S., SAULS, J. T., HILL, N. S., LEVIN, P. A., PAULSSON, J., VERGASSOLA, M., AND JUN, S. Cell-size control and homeostasis in bacteria. *Current biology : CB 25*, 3 (feb 2015), 385–91.

[196] TANIGUCHI, Y., CHOI, P. J., LI, G.-W., CHEN, H., BABU, M., HEARN, J., EMILI, A., AND XIE, X. S. Quantifying E. coli proteome and transcriptome with single-molecule sensitivity in single cells. *Science (New York, N.Y.) 329*, 5991 (jul 2010), 533–8.

[197] TENG, S.-W., MUKHERJI, S., MOFFITT, J. R., DE BUYL, S., O'SHEA, E. K., HARMER, S. L., PANDA, S., KAY, S. A., DUNLAP, J. C., MIHALCESCU, I., HSING, W. H., LEIBLER, S., AMDAOUD, M., VALLADE, M., WEISS-SCHABER, C., MIHALCESCU, I., TOMITA, J., NAKAJIMA, M., KONDO, T., IWASAKI, H., RUST, M. J., MARKSON, J. S., LANE, W. S., FISHER, D. S., O'SHEA, E. K., MARKSON, J. S., O'SHEA, E. K., QIN, X. M., BYRNE, M., XU, Y., MORI, T., JOHNSON, C. H., ISHIURA, M., NAKAHIRA, Y., YOUNG, M. W., KAY, S. A., GALLEGO, M., VIRSHUP, D. M., KITAYAMA, Y., NISHIWAKI, T., TERAUCHI, K., KONDO, T., O'NEILL, J. S., REDDY, A. B., O'NEILL, J. S., NAKAJIMA, M., ZWICKER, D., LUBENSKY, D. K., TEN WOLDE, P. R., HOSOKAWA, N., XU, Y., MORI, T., JOHNSON, C. H., CHABOT, J. R., PEDRAZA, J. M., LUITEL, P., VAN OUDENAARDEN, A., YANG, Q., PANDO, B. F., DONG, G., GOLDEN, S. S., VAN OUDENAARDEN, A., MOFFITT, J. R., LEE, J. B., CLUZEL, P., TASS, P., GONZE, D., HALLOY, J., GOLDBETER, A., AND GILLESPIE, D. T. Robust circadian oscillations in growing cyanobacteria require transcriptional feedback. *Science (New York, N.Y.) 340*, 6133 (2013), 737–40.

[198] TO, T.-L., AND MAHESHRI, N. Noise Can Induce Bimodality in positive transcriptional feedback loops without bistability. *Science 1142*, February (2010), 1142.

[199] TORO, E., AND SHAPIRO, L. Bacterial chromosome organization and segregation. *Cold Spring Harbor perspectives in biology 2*, 2 (Feb. 2010), a000349.

[200] TSURU, S., YASUDA, N., MURAKAMI, Y., USHIODA, J., KASHIWAGI, A., SUZUKI, S., MORI, K., YING, B.-W., AND YOMO, T. Adaptation by stochastic switching of a monostable genetic circuit in escherichia coli. *Molecular systems biology 7*, 1 (2011), 493.

[201] TU, B. P., KUDLICKI, A., ROWICKA, M., AND MCKNIGHT, S. L. Logic of the yeast metabolic cycle: temporal compartmentalization of cellular processes. *Science (New York, N.Y.) 310*, 5751 (nov 2005), 1152–8.

[202] TYPAS, A., BANZHAF, M., GROSS, C. A., AND VOLLMER, W. From the regulation of peptidoglycan synthesis to bacterial growth and morphology. *Nature Reviews Microbiology 10*, 2 (dec 2011), 123–36.

[203] TANASE-NICOLA, S., AND TEN WOLDE, P. R. Regulatory control and the costs and benefits of biochemical noise. *PLoS Computational Biology 4*, 8 (aug 2008), e1000125.

[204] VAN BOXTEL, C., VAN HEERDEN, J. H., NORDHOLT, N., SCHMIDT, P., AND BRUGGEMAN, F. J. Taking chances and making mistakes: non-genetic phenotypic heterogeneity and its consequences for surviving in dynamic environments. *Journal of The Royal Society Interface 14*, 132 (2017).

[205] VAN HEERDEN, J. H., WORTEL, M. T., BRUGGEMAN, F. J., HEIJNEN, J. J., BOLLEN, Y. J. M., PLANQUÉ, R., HULSHOF, J., O'TOOLE, T. G., WAHL, S. A., TEUSINK, B., PLANQUE, R., HULSHOF, J., O'TOOLE, T. G., WAHL, S. A., TEUSINK, B., PLANQUÉ, R., HULSHOF, J., O'TOOLE, T. G., WAHL, S. A., TEUSINK, B., PLANQUE, R., HULSHOF, J., O'TOOLE, T. G., WAHL, S. A., AND TEUSINK, B. Lost in Transition: Startup of Glycolysis Yields Subpopulations of Nongrowing Cells. *Science 343*, February (feb 2014), 1245114–1245114.

[206] VAN HOEK, M., AND HOGEWEG, P. The effect of stochasticity on the lac operon: an evolutionary perspective. *PLoS computational biology 3*, 6 (jun 2007), e111.

[207] VEENING, J. W., KUIPERS, O. P., BRUL, S., HELLINGWERF, K. J., AND KORT, R. Effects of phosphorelay perturbations on architecture, sporulation, and spore resistance in biofilms of Bacillus subtilis. *Journal of Bacteriology 188*, 8 (apr 2006), 3099–3109.

[208] VENTURELLI, O. S., ZULETA, I., MURRAY, R. M., AND EL-SAMAD, H. Population diversification in a yeast metabolic program promotes anticipation of environmental shifts. *PLoS biology 13*, 1 (jan 2015), e1002042.

[209] VERSTRAETEN, N., KNAPEN, W., FAUVART, M., AND MICHIELS, J. A historical perspective on bacterial persistence. *Bacterial Persistence: Methods and Protocols* (2016), 3–13.

[210] VOLKMER, B., AND HEINEMANN, M. Condition-dependent cell volume and concentration of Escherichia coli to facilitate data conversion for systems biology modeling. *PloS one 6*, 7 (jan 2011), e23126.

[211] VOORN, W. J., AND KOPPES, L. J. Skew or third moment of bacterial generation times. *Archives of Microbiology 169*, 1 (dec 1997), 43–51.

[212] WAITE, A. J., FRANKEL, N. W., DUFOUR, Y. S., JOHNSTON, J. F., LONG, J., AND EMONET, T. Non-genetic diversity modulates population performance. *Molecular Systems Biology 12*, 12 (2016), 895.

[213] WAKAMOTO, Y., DHAR, N., CHAIT, R., SCHNEIDER, K., SIGNORINO-GELO, F., LEIBLER, S., AND MCKINNEY, J. D. Dynamic Persistence of Antibiotic-Stressed Mycobacteria. *Science 339*, 6115 (2013).

[214] WALKER, N., NGHE, P., AND TANS, S. J. Generation and filtering of gene expression noise by the bacterial cell cycle. *BMC biology 14*, 1 (jan 2016), 11.

[215] WALLDEN, M., FANGE, D., LUNDIUS, E. G., BALTEKIN, Ö., AND ELF, J. The Synchronization of Replication and Division Cycles in Individual E. coli Cells. *Cell 166*, 3 (jul 2016), 729–739.

[216] WANG, P., ROBERT, L., PELLETIER, J., DANG, W. L., TADDEI, F., WRIGHT, A., AND JUN, S. Robust growth of escherichia coli. *Current Biology 20*, 12 (jun 2010), 1099–1103.

[217] WANG, X., MONTERO LLOPIS, P., AND RUDNER, D. Z. Bacillus subtilis chromosome organization oscillates between two distinct patterns. *Proceedings of the National Academy of Sciences of the United States of America 111*, 35 (sep 2014), 12877–82.

[218] WANG, Z., AND ZHANG, J. Impact of gene expression noise on organismal fitness and the efficacy of natural selection. *Proceedings of the National Academy of Sciences of the United States of America 108*, 16 (apr 2011), E67–76.

[219] WEISSE, A. Y., OYARZÚN, D. A., DANOS, V., AND SWAIN, P. S. Mechanistic links between cellular trade-offs, gene expression, and growth. *Proceedings of the National Academy of Sciences 112*, 9 (2015), E1038–E1047.

[220] WIENTJES, F. B., AND NANNINGA, N. Rate and topography of peptidoglycan synthesis during cell division in Escherichia coli: Concept of a leading edge. *Journal of Bacteriology 171*, 6 (jun 1989), 3412–3419.

[221] WOLDRINGH, C. L., HULS, P., PAS, E., BRAKENHOFF, G. J., AND NANNINGA, N. Topography of Peptidoglycan Synthesis during Elongation and Polar Cap Formation in a Cell Division Mutant of Escherichia coli MC4100. *Microbiology 133*, 3 (mar 1987), 575–586.

[222] WOLF, L., SILANDER, O. K., AND VAN NIMWEGEN, E. Expression noise facilitates the evolution of gene regulation. *eLife 4* (2015), e05856.

[223] YANG, J., MCCORMICK, M. A., ZHENG, J., XIE, Z., TSUCHIYA, M., TSUCHIYAMA, S., EL-SAMAD, H., OUYANG, Q., KAEBERLEIN, M., KENNEDY, B. K., AND LI, H. Systematic analysis of asymmetric partitioning of yeast proteome between mother and daughter cells reveals “aging factors” and mechanism of lifespan asymmetry. *Proceedings of the National Academy of Sciences 112*, 38 (sep 2015), 11977–11982.

[224] YANG, S., KIM, S., RIM LIM, Y., KIM, C., AN, H. J., KIM, J.-H., SUNG, J., AND LEE, N. K. Contribution of RNA polymerase concentration variation to protein expression noise. *Nature communications 5* (sep 2014), 4761.

[225] YANSURA, D. G., AND HENNERT, D. J. Use of the Escherichia coli lac repressor and operator to control gene expression in Bacillus subtilis (hybrid promoter/isopropyl 13-D-thiogalactoside induction). *Biochemistry 81*, 2 (jan 1984), 439–443.

[226] YVERT, G. How does evolution tune biological noise? *Frontiers in genetics 5* (2014), 374.

[227] ZENKLUSEN, D., LARSON, D. R., AND SINGER, R. H. Single-RNA counting reveals alternative modes of gene expression in yeast. TL - 15. *Nature structural & molecular biology 15 VN - r*, 12 (dec 2008), 1263–1271.

[228] ZOPF, C. J., QUINN, K., ZEIDMAN, J., AND MAHESHRI, N. Cell-Cycle Dependence of Transcription Dominates Noise in Gene Expression. *PLoS Computational Biology 9*, 7 (jul 2013), e1003161.

List of publications

List of publications

APPELHAGEN, I., THIEDIG, K., **NORDHOLT, N.**, SCHMIDT, N., HUEP, G., SAGASSER, M., AND WEISSHAAR, B. Update on transparent testa mutants from Arabidopsis thaliana: characterisation of new alleles from an isogenic collection. *Planta 240*, 5 (2014), 955–70.

APPELHAGEN, I., **NORDHOLT, N.**, SEIDEL, T., SPELT, K., KOES, R., QUATTROCHIO, F., SAGASSER, M., AND WEISSHAAR, B. TRANSPARENT TESTA 13 is a tonoplast P3A -ATPase required for vacuolar deposition of proanthocyanidins in Arabidopsis thaliana seeds. *The Plant journal : for cell and molecular biology 82*, 5 (2015), 840–9.

RABBERS, I., VAN HEERDEN, J. H., **NORDHOLT, N.**, BACHMANN, H., TEUSINK, B., AND BRUGGEMAN, F. J. Metabolism at evolutionary optimal States. *Metabolites 5*, 2 (2015), 311–43.

VAN BOXTEL, C.*, VAN HEERDEN, J. H.*, **NORDHOLT, N.***, SCHMIDT, P.*, AND BRUGGEMAN, F. J. Taking chances and making mistakes: non-genetic phenotypic heterogeneity and its consequences for surviving in dynamic environments. *Journal of The Royal Society Interface 14*, 132 (2017).

NORDHOLT, N., VAN HEERDEN, J. H., KORT, R., AND BRUGGEMAN, F. J. Effects of growth rate and promoter activity on single-cell protein expression. *Scientific Reports 7*, 1 (2017), 6299.

Unpublished

VAN HEERDEN, J. H.*, KEMPE, H.*, DOERR, A., MAARLEVELD, T. R., **NORDHOLT, N.**, AND BRUGGEMAN, F. J. Statistics and simulation of growth of single bacterial cells: illustrations with *B. subtilis* and *E. coli*. *Under review.*

NORDHOLT, N., VAN HEERDEN, J. H., AND BRUGGEMAN, F. J. Single *Bacillus subtilis* cells display systematic deviations from exponential growth and biphasic growth behaviour along their cell cycle. *In preparation.*

* Contributed equally to this work

Summary

Summary

Bacterial cells that divide by binary fission double their size and molecular content from birth to division. What sounds like a simple procedure is actually the result of the coordination of countless complex molecular processes that are involved in cell growth and gene expression. With this in mind, it is not surprising that even clonal cells that grow under constant conditions exhibit substantial intercellular differences in their sizes, growth rates and gene expression levels. These phenotypic differences can simply be a consequence of asynchronous growth, i.e. cells having different sizes depending on the time that has elapsed since their birth (their age). They can also arise from the stochastic nature of biochemical processes, i.e. cells having different sizes or molecular compositions at the same age. But despite the complexity of cell growth and gene expression and the randomness that affects them, bacteria are able to maintain homeostasis in cell size and expression levels under constant conditions. This indicates the existence of compensation mechanisms that steer the properties of individual cells, such as size or gene expression levels, towards a condition dependent (optimal) value. The nature of these mechanisms, and the principle cellular properties that they monitor and steer, are not well understood yet. In this thesis, we explore the interrelation and coordination of growth and gene expression in individual bacterial cells by combining theoretical approaches (modelling, microbial growth theory, variance decomposition) with single cell observation techniques (flow cytometry, time-lapse microscopy), using the gram-positive model bacterium *Bacillus subtilis*.

Chapter 1 provides a brief overview of the history of single cell measurements and introduces key concepts that recur throughout this thesis. In **chapter 2** we extensively review the available literature on the topic of non-genetic heterogeneity in microorganisms and its influence on the ability of a microbial population to survive in and to adapt to dynamic environments.

Chapter 3 and **chapter 4** constitute the experimental part of this thesis. In **chapter 3** we use flow cytometry to measure the expression levels and variability of a fluorescent protein in individual *B. subtilis* cells under different environmental conditions. We then use theory to decompose and quantify the overall expression variation into variation that arises from different cellular processes. We find that the expression level of the fluorescent protein is the main determinant for the magnitude of expression variability across individual cells and that protein production rate and environmental conditions only have indirect effects on variability, by acting on the expression level. The findings from **chapter 3** can help us in the rational design of genetic circuits that could be of use for production strains in industrial settings. Our results underline the importance of condition dependence for the intended function of a genetic design.

In **chapter 4** we quantify the relationship between growth and gene expression by means of studying the cell cycles of thousands of individual cells, using time-lapse microscopy. We discover systematic and structured deviations from exponential growth along the cell cycle under three independent environmental conditions. We observe a qualitative change in growth behaviour at a fairly constant time to division. Despite the substantial fluctuations that we observe in the growth rates during the life time of each individual cell, we find that gene expression levels stay nearly constant, suggesting that cells compensate these systematic fluctuations. We discuss potential cellular processes that could underlie the observed growth deviations. The results from **chapter 4** might help us to find the mechanisms that decide when cells divide, which leads to cell size homeostasis and allows a bacterial population to reach a state of balanced growth.

Finally, I discuss our experimental findings in the context of recent literature in **chapter 5**. I reflect on the usefulness of phenomenological 'principles' and 'laws' that are used to describe how bacteria are able to maintain cell size homeostasis across many generations. Furthermore, I discuss the question of the evolutionary costs and benefits of non-genetic heterogeneity and gene expression noise. To conclude, I propose experimental approaches that can help us to fill remaining gaps in our

understanding of growth and gene expression in bacterial cells.

Samenvatting

Samenvatting

vertaald door Iraes Rabbers

Bacteriële cellen die delen middels binaire splijting, verdubbelen tussen hun geboorte en deling in grootte en moleculaire inhoud. Wat als een simpele procedure klinkt, is in werkelijkheid het resultaat van coördinatie tussen ontelbare complexe moleculaire processen die betrokken zijn bij celgroei en genexpressie. Dit in gedachte houdend, is het niet verwonderlijk dat zelfs klonale cellen die onder constante condities groeien, substantiële intercellulaire verschillen vertonen in hun afmetingen, groeisnelheden en genexpressie niveaus. Deze fenotypische verschillen kunnen simpelweg een consequentie zijn van asynchrone groei, oftewel cellen die verschillende afmetingen hebben afhankelijk van de tijd die verstreken is sinds hun geboorte (hun leeftijd). Ze kunnen ook veroorzaakt worden door de stochastische aard van biochemische processen, ofwel cellen die verschillende afmetingen of moleculaire samenstellingen hebben op dezelfde leeftijd. Maar ondanks de complexiteit van celgroei en genexpressie en de willekeur die hen beïnvloedt, zijn bacteriën in staat om homeostase in celgrootte en expressie niveaus in stand te houden onder constant condities. Dit is een indicatie voor compensatie mechanismen die de eigenschappen, zoals grootte of genexpressie niveaus, van individuele cellen sturen richting een omstandigheids-afhankelijk niveau. De aard van deze mechanismen en de voornaamste cellulaire eigenschappen die ze monitoren en sturen, zijn nog niet goed begrepen. In dit proefschrift verkennen we de interrelatie en coördinatie van groei en genexpressie in individuele bacteriële cellen, door een theoretische aanpak (modelleren, microbiële groei theorie, variantie decompositie) te combineren met enkele cel observatie technieken (flow cytometrie, time-lapse microscopie), waarbij we de gram-positieve model bacterie *Bacillus subtilis* gebruiken.

Hoofdstuk 1 geeft een kort overzicht van de geschiedenis van enkele cel metingen, en introduceert sleutel concepten die terugkomen in de rest van het proefschrift. In **hoofdstuk 2** bespreken we de beschikbare literatuur betreffende niet-genetische heterogeniteit in micro-organismen, en diens invloed op het vermogen van een microbiële populatie om te overleven in en zich aan te passen aan een dynamische omgeving.

Hoofdstuk 3 en **hoofdstuk 4** vormen het experimentele gedeelte van dit proefschrift. In **hoofdstuk 3** gebruiken we flow cytometrie om de expressie niveaus en variabiliteit van een fluorescent eiwit te meten in individuele *B. subtilis* cellen, onder verschillende omgevings omstandigheden. Vervolgens gebruiken we de theorie om de totale expressie variatie te decomposeren en kwantificeren, in variaties die uit verschillende cellulaire processen voortkomen. We vinden dat het expressie niveau van het fluorescente eiwit de voornaamste determinant is voor de grootte van expressie-variabiliteit tussen individuele cellen, en dat eiwit productiesnelheid en omgevings omstandigheden alleen indirecte effecten hebben op variabiliteit, door het expressie niveau te beïnvloeden. De bevindingen uit hoofdstuk 3 kunnen ons helpen in het rationale ontwerp van genetische circuits die gebruikt kunnen worden voor productie stammen in industriële omgevingen. Onze resultaten onderschijven het belang van omstandigheids-afhankelijkheid voor de bedoelde functie van een genetisch ontwerp.

In **hoofdstuk 4** kwantificeren we de relatie tussen groei en genexpressie door de cel cycli van duizenden individuele cellen te bestuderen met time-lapse microscopie. We ontdekken systematische en gestructureerde afwijkingen van exponentiële groei gedurende de cel cyclus, onder drie onafhankelijke omgevings omstandigheden. We observeren een kwalitatieve verandering in groei gedrag bij een redelijk constante tijd-tot-deling. Ondanks de substantiële fluctuaties die we observeren in de groeisnelheden gedurende de levensduur van elke individuele cel, vinden we dat genexpressie niveaus nagenoeg gelijk blijven, wat suggereert dat cellen deze systematische fluctuaties compenseren. We bediscussiëren potentiële cellulaire processen die ten grondslag liggen aan de geobserveerde groei afwijkingen. De resultaten van **hoofdstuk 4** zouden ons kunnen helpen met het vinden van mechanismen die beslissen wanneer cellen delen, wat leidt tot celgrootte

homeostase en bacteriële populaties toestaat om een staat van gebalanceerde groei te bereiken.

Tot slot bediscussieer ik onze experimentele bevindingen in de context van recente literatuur in **hoofdstuk 5**. Ik reflecteer op het nut van fenomenologische 'principes' en 'wetten' die gebruikt worden om te beschrijven hoe bacteriën in staat zijn celgrootte homeostase gedurende vele generaties in stand te houden. Verder bespreek ik de vraag van de evolutionaire kosten en voordelen van niet-genetische heterogeniteit en genexpressie ruis. Om af te sluiten stel ik experimentele benaderingen voor, die ons kunnen helpen om de overblijvende gaten in onze kennis over groei en genexpressie in bacteriële cellen op te vullen.

Acknowledgements

Acknowledgements

The last paragraphs of this thesis are reserved for the people that helped me complete this thesis, be it through scientific guidance, (emotional) support or beer. Thank you!
Frank, thank you for giving me the opportunity to work with you and for teaching me so many things, first and foremost your way of thinking about scientific problems. You were always there when I had a problem in the lab, with theory or Mathematica. Thank you for your patience, the freedom you granted me in pursuing my work and the guidance that you provided when it was necessary. I think we got along great and it was always fun to have you around!
Remco, thank you for the opportunity to pursue my work, even after we had to make decisions that changed the direction of the project.
Johan, thank you for your invaluable guidance in the lab and teaching me the art of 'mierenneuken'. I think you are a great scientist and I could not have wished for a better teacher! An even bigger thank you for your friendship and the good times outside the lab, and your (emotional) support during the writing of my thesis. You were always the voice of reason that made the seemingly impossible appear doable. I can not say how happy I am that you (re)joined the lab in my time there!
My paranimphs, Iraes and Phillipp, I thank you for your paranimph duties and for fond memories from sharing the office in N229-A. Good times were had! Iraes, thank you for showing me around when I just started, for gezelligheid and for your help with the translation of the summary. Phillipp, thank you for your punny humour (one could call it pun-gent, even), your positive attitude and our many evenings in Amsterdam. I'm sure those were not the last, although we might meet more often in Berlin now.
Next, I would like to thank all members of the Systems Bioinformatics and Molecular Cell Physiology groups at the VU Amsterdam. Thank you Bas for forming such an awesome group and letting me be part of it. No lab in the world would be able to function without technicians, and ours is not an exception to this rule. Thank you Marijke, Vera, Martin for keeping things running. Thank you Jacqueline and Jeannet for taking care of all the administrative things of which I have no clue whatsoever. Lucas F., Lucas P., Joost, Mark, thank you for our stelling nights. Mark, thank you also for insisting on a double bed every time we shared a room during a conference. Anne, Susanne, Evert, Timo, Joost B., Meike, Coco, Daria, Esther, Chrats, rooie Ronnie, Dennis, Savakis, Qing, Daan, Tim, Hans, Herwig, Douwe, Fred, Brett, Willi, Jurgen, Ulisses, Paul, Daan, Filipe, Pinar, thank you all for making my time in Amsterdam as pleasant as it was.
I would also like to thank Leendert Hamoen and all members of his lab for the time that I spent in their group at the UvA, especially Terrens, Laura, Edward, Michaela.
Thank you, AMBERani, for the good times during the workshops in Newcastle, Paris and Amsterdam.
Thorsten Schüttmann, ich bin dir sehr dankbar dafür, dass du mir ein Büro und nette Kollegen zur Verfügung gestellt hast! Das hat mir in der schwierigsten Phase meiner Arbeit die ein oder andere willkommene Abwechslung bereitet. Danke Marco, Franzi, Abdullah, Marlon, Jenny, (und natürlich Yoshi). Ohne euch wäre ich wahrscheinlich noch immer nicht fertig, außer mit den Nerven!
Natürlich möchte ich auch euch danken, Mama, Papa, Nadja und Max (und Cleo), für eure Liebe, eure Unterstützung und euer Vertrauen über all die Jahre. Danke Oma, Inge & Holger, Horst & Hanna.
Zu guter Letzt, danke Britta & Wilma. Britta, du hast mich immer bedingungslos unterstützt und mir alle Freiheiten gelassen, die nötig waren um diese Arbeit fertigzustellen. Wilma, du kamst in der wahrscheinlich stressigsten Zeit meines Lebens auf die Welt und es hätte keinen besseren Zeitpunkt geben können. Wann immer es mir unmöglich erschien diese Arbeit jemals zu vollenden und ich das Gefühl hatte, alles bricht über mir zusammen, habt ihr beide mich daran erinnert, was wirklich wichtig ist. Ich liebe Euch.

Niclas

im Dezember 2017